MOLECULAR BIOMECHANICS OF SEED GERMINATION IN *ARABIDOPSIS THALIANA* AND *LEPIDIUM SATIVUM*

MELANIA GEORGETA GHITA

BSc (Hons), MSc

A thesis submitted to The University of Nottingham for the degree of Doctor of Philosophy

June 2014

Abstract

Seed germination is a key process in world agriculture. For this reason, the capacity of a seed to germinate with minimum input from farmers is highly desirable, keeping the production costs as low as possible. The physiological mechanism of germination is well known, involving the rupture of the endosperm and testa envelope by the expanding embryo, but the molecular and biomechanical changes underlying this process are poorly understood. In order to answer the question of how the plant developmentally regulates changes in cell wall stiffness associated with germination, an innovative molecular biomechanics approach was developed. It combines biophysical, engineering and molecular biology approaches. A comparative approach was taken using the related species *Arabidopsis thaliana* and *Lepidium sativum*, the former due to the wealth of genomic resources, and the latter due to larger size and ease of use in biomechanics experiments.

Environmental scanning electron microscopy imaging revealed that the endosperm structure is intact after protrusion of the radicle, confirming the fact that rupture occurs between individual cells. Germination is a process that requires targeted cell separation or/ and cell wall remodeling. For this reason, following the predictions of the gene network SeedNet, containing the endosperm-specific sub-network cluster 19 (Bassel et al., 2011), endosperm specific genes were studied.

In order to localize their expression, *promoter::GUS* constructs were used for the genes *DELTA-VPE*, *SCPL51* and *DOF2.1*, and different mutant alleles of four transcription factors from cluster 19 (*athb23*, *bhlh-115*, *bee2* and *dof2.1*) were screened to identify changes in germination behaviour.

DELTA-VPE and *SCPL51* were proven to be endosperm specific and ABA insensitive. *DELTA-VPE* was GA insensitive and *SCPL51* expression required GA. Also, *DELTA-VPE* expression could be observed after 15 minutes of imbibition in the whole endosperm, while *SCPL51* showed a temporal expression requiring 18 hours of imbibition before being observed in all endosperm cells. The analysed T-DNA lines showed an epistatic relationship

between *ATHB23* and *DOF 2.1* and a decreased sensitivity to stress factors like osmotic and salt stresses, than the wild type.

Using nanoindentation, a differentiation between different regions of endosperm was attempted, but the methodology was not sensitive enough. However, different elastic modulus values for imbibed and dry Lepidium seeds were registered. To image the internal changes in seed structure during germination, micro-CT was used, estimating values for endosperm thickness from dry state to germinated one.

This work enforces the knowledge of the molecular biology and biomechanical properties of the endosperm.

Acknowledgements

I would like to thank to my supervisors Dr. Nicola Everitt and Prof. Michael Holdsworth, for their support, encouragement and guidance through my PhD.

I would like to thank Holdsworth lab members who have assisted me in my project but also making a familiar and enjoyable place to work: Dr. Cristina Sousa Correia, Julietta Marquez, Geeta Prasad, Sophie Berckhan, Dr. Guillermina Mendiondo, Dr. Jorge Vicente Conde, Daniel Rooney, Dr. Daniel Gibbs and many others unmentioned here.

I would like to thank to my family who supported me all these years, and to my best friend Mileva Jarcov for her continuous support. *NIHIL SINE DEO*

List of Figures

LIST OF TABLES

LIST OF ABBREVIATIONS

3-AT	3-Amino-1, 2, 4-triazole
ABA	Abscisic acid
AFM	Atomic force microscopy
BR	Brassinosteroids
COT	Cotyledons
CRWEs	Cell wall remodeling enzymes
DIC	Digital image correlation
dNTPs	Deoxynucleotide triphosphates
DRY	Whole dry seeds
E	Establishment
E_r	Elastic modulus
eSEM	Environmental scanning electron microscopy
G	Germination
GA	Gibberellic acid
GFP	Green fluorescence protein
GO	Genome ontology
GPa	GigaPascal
GUS	β-glucuronidase
H	Hardness
HIS	Histidine
IAA	Indol-3-acetic acid (auxin)
IKI	Iodine potassium iodide
Leu	Leucine
MCE	Micropylar and chalazal endosperm
MD	Morphophysiological dormancy
Micro-CT	Micro x–ray computed tomography
PAC	Paclobutrazol
PD	Physiological dormancy
PE	Peripheral endosperm
PEG	Polyethylene glycol
PMEs	Pectin metylesterases
PY	Physical dormancy
PY+ PD	Combinational dormancy
RAD	Radicle
TR	Testa rupture
TRs	Transcription factors
W	Tryptophan

1. Literature review

1.1 The importance of seeds

Seeds are a vital component of the world`s diet. Also, with seeds the next generation of plants begins. The seed contains the embryo as a new plant in miniature and is physiologically equipped for its role of food supplier for the seedling, until it becomes a plant.

1.2 Engineering seed germination

Seeds studies are performed either for understanding the plant evolution and biodiversity, competition with other plants, adaptation to adverse environmental conditions or tolerance to drought, salts, heavy metals, etc. or just for the scientific knowledge. Seeds remain an important factor of the world food security as major nutritional source for humans and livestock.

Crop yields depend largely on germination quality. For this reason understanding germination helps to improve seed priming (regulated germination) and the co-existence with other crops, but also to minimize seed dispersal in crop plants and to generate yield increase (Liljegren et al., 2000).

The development of proteins markers for seed vigour contributed significantly to seed longevity (Ogé et al., 2008) improving crop seed quality further used as food, feed or green chemistry (increased content of vitamins A and E in crops (DellaPenna, 2005) and usage of plant oils for the production of chemicals and biofuels (Damude & Kinney, 2007; Ruiz-López et al., 2009)).

In order to engineer seed germination the principles behind it must be first understood and described. How the protective layers of the embryo are physically arresting the radicle protrusion, but also what genetic background is involved in germination, are questions still to be answered.

To improve the resistance of seeds to mechanical harvesting, transportation and storage, the physical properties of the covering layers must be known, in

order to avoid the deterioration or viability loss of seeds (Khodabakhshian, 2012).

Biomechanical analysis of seed germination aims to elucidate the physics and also the mechanics of this physiological process. How the physical properties of endosperm change through the germination process is still unclear for Arabidopsis, although for Lepidium was proven that it is weakening in the micropylar region (the 0.5 mm long, cone-shaped, region of the endosperm enclosing the radicle tip) prior radicle protrusion (Müller et al., 2006).

1.3 Seed structure

In angiosperms the double fertilisation process leads to three genetically distinct seed tissues: the seed coat (maternal origin), the triploid endosperm (two maternal sets of chromosomes and one paternal) and the diploid embryo (Berger et al., 2006).

The most outer layer of the seed is called testa, consisting of dead tissue in mature Arabidopsis and Lepidium seed accumulates mucilage or flavonoids (Figure 1.2). Testa confers seed coat imposed dormancy (Debeaujon & Koornneef, 2000).

1.4 Seed dormancy and germination

1.4.1 Seed dormancy

Dormancy is an adaptive trait that optimizes the distribution of germination over time in a population of seeds (Bewley, 1997). A broad definition of dormancy was proposed by Baskin & Baskin, in 2004: a dormant seed does not have the capacity to germinate in a specified period of time under any combination of normal physical environmental factors that are otherwise favourable for its germination (Baskin & Baskin, 2004).

Although dormancy can be measured only by the absence of germination, it is rather a characteristic of the seed that determines the conditions required for germination (Vleeshouwers, 1995; Fenner & Thompson, 2005). Baskin & Baskin (2004), have proposed a comprehensive classification system, based on the devised dormancy classification system developed by Nikolaeva in 1967, which considers both morphological and physiological properties of the seed (Nikolaeva, 2004). This system includes five classes of seed dormancy: physiological (PD), morphological (MD), morphophysiological (MPD), physical (PY) and combinational (PY+ PD).

Physiological dormancy is the most common dormancy class and it is found in seeds of gymnosperms and all major angiosperm clades. The system proposed by Baskin & Baskin (2004) divides physiological dormancy into three levels: deep, intermediate and nondeep. In the first level, the embryos excised from the seeds either do not grow or will produce abnormal seedlings. Treatment with gibberellic acid does not break dormancy, and stratification (subjecting seeds to cold and moist conditions, simulating winter conditions) is required before germination can take place (Baskin & Baskin, 2004).

The great majority of seeds, including those of *Arabidopsis thaliana*, have nondeep PD (Baskin & Baskin, 2004). Excised embryos from these seeds produce normal seedlings. Gibberellic acid (GA), scarification (physical alteration of the seed coat) and stratification can break this type of dormancy.

Morphological dormancy appears in seeds with undeveloped but differentiated embryos. These embryos are not dormant, but simply need time to grow and germinate, e.g. *Apium graveolens* (Jacobsen & Pressman, 1979).

Morphophysiological dormancy is also evident in seeds with undeveloped embryos, but in addition they have a physiological component to their dormancy. These seeds require a dormancy-breaking treatment (Baskin & Baskin, 2004).

Physical dormancy is caused by impermeability of the seed or fruit coat, which prevents water-uptake by seed. This type of dormancy can be broken by mechanical or chemical scarification (Baskin, 2003).

Combinational dormancy is evident in seeds with water-impermeable coats combined with physiological embryo dormancy (Baskin & Baskin, 2004).

1.4.2 Seed germination

Seed germination consists of those events that commence with water uptake by the quiescent dry seed and terminate with the elongation of the embryonic axis (Bewley & Black, 1994).

Uptake of water by a mature dry seed is triphasic (Figure 1.1), with a rapid initial uptake followed by a plateau phase. A further increase in water uptake occurs only after germination is completed, as the embryonic axis elongates (Bewley, 1997).

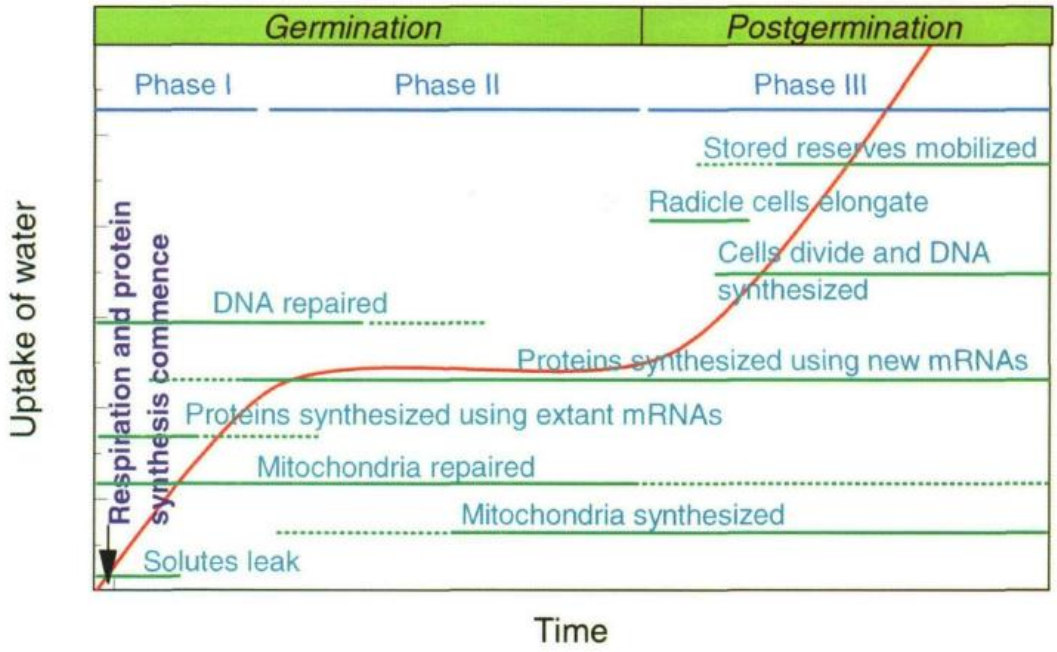

Figure 1.1 Time course of major events associated with germination and subsequent postgerminative growth (Taken from Bewley, 1997).

Upon imbibition, the seed rapidly resumes metabolic activity. The structures and enzymes necessary for this initial resumption of metabolic activity are generally assumed to be present within the dry seed, having survived the desiccation phase that terminates seed maturation (Bewley, 1997).

The embryo-covering layers can confer mechanical constraint that must be overcome by the growth potential of the embryo (Kucera et al., 2005). Two forms of mechanical constrains and release mechanisms can be distinguished: (1) living seed-covering layers, where a regulated tissue weakening occurs before germination and the tissue itself can produce enzymes for this process (e.g. endosperm or inner testa) and (2) mostly dead seed-covering layers where predetermined breaking points facilitate tissue rips before germination (e.g. outer testa, pericarp). Enzymes facilitating testa rupture might be released by the endosperm and/ or the radicle (Morris et al., 2011; Lee et al., 2012).

1.5 Plant hormones involved in seed germination

Among the most important functions of plant hormones are controlling and coordinating cell division, growth and differentiation (Hooley, 1994). The phytohormones: abscisic acid (ABA), ethylene, gibberellins (GA), auxin (IAA), cytokinins, and brassinosteroids are biochemical substances controlling many physiological and biochemical processes in the plant. These vital molecules are produced by plants and also by soil microbes (Jiménez, 2005; Santner et al., 2009).

Plant hormones can affect different seed physiological processes including dormancy and germination (Graeber et al., 2010). The major hormones influencing germination and dormancy are discussed below.

1.5.1 ABA

Recent studies have elucidated the core of ABA signaling pathway. PYRABACTIN RESISTANCE 1 (PYR1) was identified as an ABA receptor

through a chemical genetics approach (Park et al., 2009). The Arabidopsis genome encodes 13 genes similar to PYR1, which were named as PYR1 LIKE1-13 (PYL1-13). Ma et al., 2009, named them RCARs (REGULATORY COMPONENTS OF ABA RECEPTOR (Ma et al., 2009). All PYR1/PYL1-PYL13/RCARs belong to the same gene family in Arabidopsis (Park et al., 2009; Ma et al., 2009).

Protein phosphatase 2C (PP2C) was proven to be acting as a negative regulator in ABA signaling (Rodriguez et al., 1998). *ABSCISIC ACID INSENSITIVE1, 2 (ABI1, ABI2),* identified based on their insensitivity to ABA have been shown to encode paralogous of PP2Cs (Meyer et al., 1994; Leung et al., 1997).

HOMOLOGY TO ABI1 (HAB1 and HAB2) are also two other ABA signaling regulators (Saez et al. 2004). Another PP2Cs important for the ABA response of germination, are *ABA-HYPERSENSITIVE GERMINATION1* and *3 (AHG1* and *AHG3)*; AHG1 function is specific to seed germination and early post-germinative growth, whereas AHG3 is involved in later stages of growth (Nishimura et al., 2007).

ABA induction of *ABI*1 and *ABI*2, negative regulators of ABA signaling, is inhibited by the transcription factor ABI3 in a feed-forward pathway (Suzuki et al., 2003). In another feed-forward pathway, ABI3 activates the transcription factor ABI5, a positive regulator of ABA signaling (Lopez-Molina et al., 2002).

ABI5 is important in determining ABA responsiveness during embryogenesis, seed maturation and regulating the transition after germination to vegetative growth (Finkelstein & Lynch, 2000). ABI5 promoter activity was observed in the whole embryo and specifically in the micropylar endosperm in the presence of high ABA concentration (Penfield et al., 2006), confirming its role in arresting the germination potential (Bewley, 1997).

Other positive regulators of ABA signaling have been identified as SNF-1 related protein kinases 2 (SnRK2s) (Nambara et al., 2010). In Arabidopsis, 10

SnRK protein kinases were identified and divided into 3 subclasses. Only three of them: SRK2D/SnRK2.2, SRK2I/SnKR2.3 and SRKD2E/SnRK2.6/OST1 are involved in seed germination, being strongly controlled by ABA (Nakashima et al., 2009).

The proposed model of ABA signal transduction begins with ABA binding to the PYR/PYL/RCAR. This binding inhibits PP2C activity, thus the phosphorylated state of SnRK2s. PP2Cs normally de-phosphorylate SnRK2s, keeping them inactive. De-repression of SnRK2s protein kinase activates downstream signaling targets by phosphorylation such as ABI5 and other transcription factors (Nambara et al., 2010).

ABA deficiency during seed development is associated with the absence of primary dormancy of the mature seed (Koornneef & van der Veen, 1980; Kucera et al., 2005). ABA production can have dual origins: the embryo or maternal tissues, but only the ABA of embryonic origin is necessary to impose dormancy (Nambara & Marion-Poll, 2003). ABA deficient mutants not only exhibit the appearance of nondormant seeds but also show seed vivipary (precocious germination on mother plant).

In Arabidopsis, the inhibitory effects of ABA on germination is through delaying the radicle expansion and weakening of the endosperm, as well as the enhanced expression of transcription factors, which may adversely affect the process of seed germination (Graeber et al., 2010; Müller et al., 2006).

Upon seed imbibition, within the first 12 hours, the ABA level in dormant and nondormant seeds drops 10 fold (Piskurewicz et al., 2008). Dormant seeds have the capacity to synthesize *de novo* ABA; however the mechanism by which this happens is still unknown (Lee et al., 2010).

The Arabidopsis *abi* have been identified by selecting the seeds capable of germination on high ABA concentrations media, inhibitive for the wild type (Koornneef & Karssen, 1994).

The *abi1* mutant seed phenotype was described as having reduced dormancy, easily broken by chilling or dry storage, reduced ABA sensitivity of germination and no precocious germination (Beaudoin et al., 2000).

The *abi3* and *4* showed reduced seed longevity and reduced chlorophyll breakdown, which might be due to the reduced seed dormancy (Clerkx et al., 2003).

1.5.2 Ethylene

Compared with the other plant hormones, ethylene has the simplest biochemical structure (C_2H_4). However, it influences a wide range of plant processes, e.g. flowering, fruit ripening, aging, dormancy inhibition and seed germination (Matilla, 2000; Matilla & Matilla-Vázquez, 2008; Arteca & Arteca, 2008).

It is not yet understood how ethylene influences seed germination. There are different ideas regarding seed germination. According to several studies, ethylene is produced as a result of seed germination, while others claim that ethylene is a prerequisite condition for seed germination (Matilla, 2000; Petruzzelli et al., 2000; Petruzzelli et al., 2003).

The amount of ethylene increases during the germination of many plant seeds including wheat, corn, soybean and rice, affecting the rate of seed germination (Pennazio & Roggero, 1991). Ethylene production is higher in non-dormant seeds than in dormant seeds (Matilla, 2000).

The primary action of ethylene could be the promotion of radial cell expansion in the embryonic hypocotyl, increased seed respiration or water potential (Kucera et al., 2005). High-level induction of ABA-sensitive class I β-1,3-glucanase gene expression in the micropylar endosperm of tobacco seeds requires endogenous ethylene and promotes endosperm rupture (Leubner-Metzger et al., 1998).

Brassinosteroids and auxin are able to stimulate the production of ethylene (Arteca & Arteca, 2008). Gibberellins, ethylene and BR can induce seed germination by promoting the rupture of testa and endosperm, while antagonistically interacting with the inhibitory effects of ABA on seed germination (Finch-Savage & Leubner-Metzger, 2006; Holdsworth et al., 2008).

Ethylene is perceived by a family of receptors related to Arabidopsis ETR1 (ETHYLENE RESPONSE1), the first cloned plant hormone receptor, and its binding inhibits the signaling activities of this receptors family (Stepanova & Alonso, 2005).

In the absence of ethylene, the ETR1 activates CTR1, CONSTITUTIVE TRIPLE RESPONSE1, which is a negative regulator of downstream signaling components. CTR1 is inactive in the presence of ethylene (Schaller et al., 1995; Stepanova & Alonso, 2005). Also, ETHYLENE-INSENSITIVE2 (EIN2) is a downstream signaling component, which in the absence of ethylene is down-regulated by CTR1 (Kendrick & Chang, 2008).

ctr1 and *ein2* have been recovered as receptors and suppressor mutants, respectively, of *abi1* (Beaudoin et al., 2000). Also, *era3 enhanced response to ABA3* was showing an increased sensitivity of the seeds to ABA by overaccumulating of ABA (Ghassemian et al., 2000). Ethylene has been shown to interact with ABA in its role in the promotion of germination (Linkies et al., 2009; Linkies & Leubner-Metzger, 2012).

1.5.3 Gibberellins

The most active endogenous gibberellin in Arabidopsis is GA_4; its expression increases with seed imbibition and reaches its peak just before radicle protrusion (Ogawa et al., 2003), underlying the importance of the novo GA biosynthesis for the radicle protrusion control, in Arabidopsis seeds.

Severe mutants defective in GA biosynthesis like *ga1-3* (null allele), *GA1* gene is deleted, defective in *ent*-copalyl diphosphate synthase (a step in GA biosynthesis pathway (Sun & Kamiya, 1994), fail to germinate displaying dwarfism, reduced fertility and delayed flowering (Richards et al., 2001).

Positive regulators of GA signaling pathway in Arabidopsis, are *SLY1 (SLEEPY1)* and *PKL (PICKLE)*, while the negative regulators include *SHI*, *SPY*, *RGA*, *GAI*, *RGL1* and *RGL2* (McGinnis et al., 2003). *SLY1* encodes an F-box component of the SCF E3 ubiquitin ligase. This component mediates the GA-induced degradation of the DELLA proteins GAI, RGA, RGL2, removing their negative regulatory action and allowing the promotion of the GA-induced response (Tyler et al., 2004).

DELLA proteins are conserved growth repressors that modulate all aspects of GA responses. These GA-signalling repressors are nuclear localized and likely function as transcription associated regulators. Recent studies demonstrated that GA, upon binding to its receptor, depresses its signalling pathway by binding directly to DELLA proteins and targeting them for rapid degradation via the ubiquitin-proteasome pathway (Zentella et al., 2007).

DELLA proteins play two important roles in GA signaling: (1) they help establish GA homeostasis by direct feedback regulation on the expression of GA biosynthetic and GA receptor genes, and (2) they promote the expression of downstream negative components that are putative transcription factors/regulators or ubiquitin E2/E3 enzymes (Zentella et al., 2007).

During seed germination five DELLAs are involved: *REPRESSOR OF GA1-3* (*RGA*), *GA-INSENSITIVE* (*GAI*), *RGL1*, *RGL2* and *RGL3* (Tyler et al., 2004). RGL2 is key to repressing seed germination: *rgl2* can germinate on low GA concentrations (Lee et al., 2002).

RGL2 has a conserved DELLA motif essential for its proteasome-mediated destruction (Lee et al., 2002). GA binds to Arabidopsis GIBERELLIN-INSENSITIVE DWARF1 (GID1)-like receptors (*GID1a*, *GID1b*, and *GID1c*) (Griffiths et al., 2006; Voegele et al., 2011) and

enhances RGL2 interaction with the F-box protein SLEEPY 1 (SLY1), facilitating RGL2 ubiquitination and degradation, subsequently (Feng et al., 2008).

In addition, one of the putative DELLA targets, XERICO, promotes accumulation of ABA that antagonizes GA effects. Therefore, DELLA may restrict GA-promoted processes by modulating both GA and ABA pathways (Zentella et al., 2007).

Although GAI and RGA also play a role in germination, RGL2 is considered to be the main DELLA factor repressing germination (Lee et al., 2002; Tyler et al., 2004). Overaccumulation of RGA may stimulates ABA synthesis (Zentella et al., 2007).

The weakening of the endosperm is produced by GA activation of genes encoding cell wall remodeling enzymes (Voegele et al., 2011), while ABA prevents its weakening (Müller et al., 2006; Linkies et al., 2009).

In seeds, gibberellins stimulate the synthesis and production of hydrolases, especially α-amylase, proteases and β- glucanases (Yamaguchi, 2008).

1.5.4 Auxin

Auxin regulates many aspects of plant growth and development through the Transport inhibitor response1 (TIR1)/Additional F box protein (AFB)-Aux/indole-3-acetic acid (IAA) - AUXIN RESPONSE FACTOR (ARF) signalling system (Chapman & Estelle, 2009). ARFs regulate the expression of a large set of auxin-responsive genes by binding to auxin response elements (AuxREs) in their promoters (Mockaitis & Estelle, 2008).

Auxin is a plant hormone, which plays a key role in regulating cell cycling, growth and development (He et al., 2005), formation of vascular tissues (Davies, 1995) and pollen development (Ni et al., 2002). The growth and development of different plant organs, including the embryos, leaves and

roots is believed to be controlled by auxin transport (Rashotte et al., 2000; Popko et al., 2010).

Auxin by itself is not a necessary hormone for seed germination. However, according to the available data, auxin is present in the seed radicle tip during and after seed germination (Liu et al., 2007). Although indole-3-acetic acid (IAA), the major auxin, may not be necessary for seed germination, it is necessary for the development of young seedlings (Hentrich et al., 2013). The accumulated IAA in the seed cotyledons is the major source of IAA for the seedlings. In legumes, saturated fatty acids are the major source of IAA in mature seeds (Bialek & Cohen, 1989).

Auxin enhances ABA-mediated seed dormancy through the recruitment of *ARF10/16* to maintain *ABI3* expression during seed imbibition (Liu et al., 2013) and regulates the GA pathway by modulating the effect of GA on the levels of DELLA proteins (Fu & Harberd, 2003).

Although IAA by itself may not be important for seed germination, its interactions and cross talk with gibberellins and ethylene may influence the processes of seed germination and seedlings establishment (Fu & Harberd, 2003).

1.5.5 Cytokinins

Cytokinins are derived from adenine molecules. They were first discovered in 1950, based on their ability to enhance cell division (Miller & Skoog, 1955). They are present in developing seeds, localized in the endosperms (Mok & Mok, 2001), it is assumed that they are required for embryo cell divisions (Kucera et al., 2005).

The cytokinin receptors *CRE1/AHK4*, *AHK2* and *AHK3* are able to regulate different functions related to the development and physiology of *Arabidopsis thaliana*, such as: embryo development by affecting the cellular division, seed size, seed production and germination, hypocotyls and shoot

growth, senescence of leaf, roots growth, nutrients uptake, handling and surviving stress agents (Riefler et al., 2006; Heyl et al., 2012).

1.5.6 Brassinosteroids

Brassinosteroids have been identified as positive regulators of germination and counteract the inhibitory effects of ABA during seed germination. Playing a major role in cell elongation, cell division and skotomorphogenesis, BRs mutants did not show any phenotype in germination (Steber & McCourt, 2001).

When used as external add, they rescued the *ga1-3* (GA deficient mutant) and *sly1* (GA insensitive mutant) germination phenotypes, suggesting their role in normal germination (Steber & McCourt, 2001).

The BR mutants share a common phenotype with GA mutants, such as male sterility and dwarfism. *DET2* encodes a steroid 5 α-reductase which is required for BR biosynthesis (Li et al., 1997). A good candidate as BR receptor is *BRI1* (BRASSINOSTEROID INSENSITIVE1) a leucine-rich repeat receptor-like kinase (Noguchi et al., 1999).

The BR biosynthetic *det2-1* mutant and the BR insensitive *bri1-1* mutant were more affected by the ABA than the wild type, suggesting that a BR signal is required to overcome the inhibitive effect of ABA on germination (Steber & McCourt, 2001).

BRs, gibberellic acid and ethylene are able to increase the ability of embryos to develop into new plants by facilitating endosperm`s rupture and antagonistically interacting with ABA (Finch-Savage & Leubner-Metzger, 2006).

1.6 The function of endosperm in germination

The endosperm acts as a mechanical barrier to germination of angiosperms seeds (Finch-Savage & Leubner-Metzger, 2006). During seed germination there is a prerequisite condition for radical protrusion: the weakening of the micropylar endosperm for species like *Arabidopsis thaliana*, species from *Asteraceae*, *Solanaceae* and *Rubiaceae* (Kucera et al., 2005).

Endosperm weakening can be promoted by GA and inhibited by ABA (Müller et al., 2006). It has been proposed that the endosperm-weakening mechanism is part of the germination process of nondormant seeds and is not part of a dormancy release process *per se* (Baskin & Baskin, 2004).

Within a dormant seed population, for all seeds, there is a distribution of forces required to puncture the endosperm layer covering the radicle, which moves to lower puncture forces during stratification, suggesting that these changes begin to occur while the seed is still dormant (Finch-Savage & Leubner-Metzger, 2006).

The endosperm structure differs between species. For example, *Arabidopsis thaliana* has a single-cell layer throughout the endosperm, while *Lepidium sativum* has multicellular layers in the micropylar region (Figure 1.2).

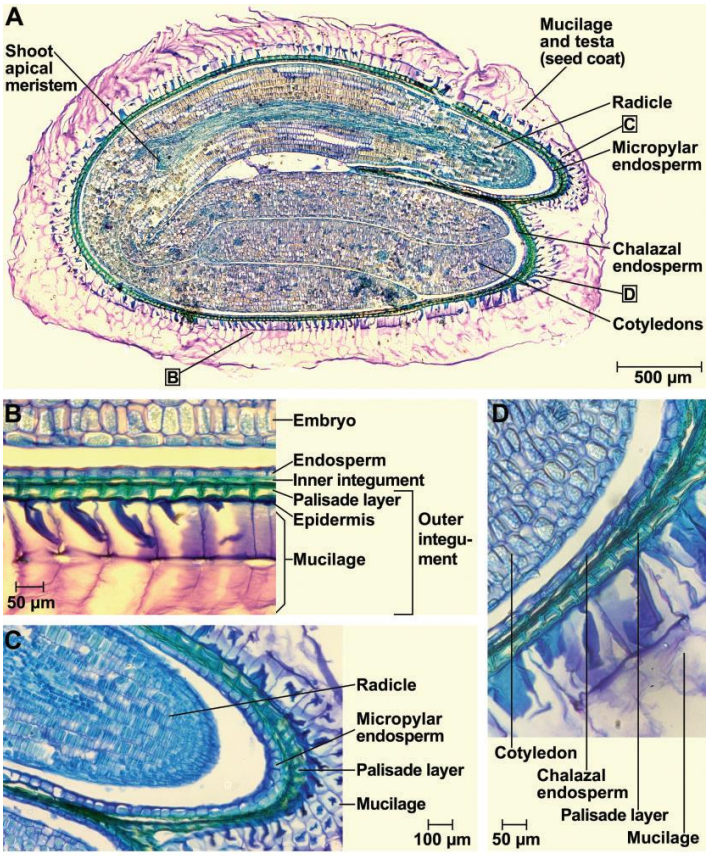

Figure 1.2 (A) Structure of a mature seed of *Lepidium sativum*. (B) Endosperm, a single cell layer; and testa (inner and outer integument). The outer testa develops mucilage upon imbibition. (C) Structure of the micropylar endosperm (1-2 cell layers) covering the radicle tip. (D) Structure of the chalazal seed region. (Taken from Müller et al., 2006)

1.6.1 Endosperm development and structure

During female gametophyte development, a haploid megaspore undergoes three rounds of mitosis without cellularization to produce an eight-nucleate structure. Cellularization results in three antipodal cells at the chalazal pole, one egg cell and two synergid cells at the micropylar pole, and a central cell in the center, which inherits two nuclei.

In Arabidopsis these nuclei fuse to form the diploid central cell nucleus and the antipodal cells degenerate before fertilization. Thus, in the mature female gametophyte of Arabidopsis, the central cell occupies most of the volume of the embryo sac being located at the chalazal pole.

The central cell has three regions that become distinct as the seed grows: the embryo-surrounding region or micropylar endosperm (MCE), the peripheral endosperm (PEN) in the central chamber, and the chalazal endosperm (CZE) (Brown et al., 1999; Boisnard-Lorig, 2001; Sorensen, 2002).

In members of *Brassicaceae* family, the endosperm consists of three domains: micropylar, central and chalazal (Brown et al., 1999; Sørensen et al., 2001). The chalazal domain is assumed to play an important role in loading the storage compounds into developing seeds (Nguyen et al., 2000; Nguyen et al., 2001).

Arabidopsis thaliana and *Lepidium sativum* belong to the same family, *Brassicaceae*, and although their seeds have similar anatomies and similar germination physiology, they differ by size, significantly. For biomechanical approaches, Lepidium seeds have a size which allows methods such as puncture force or nanoindentation (Figure 1.3).

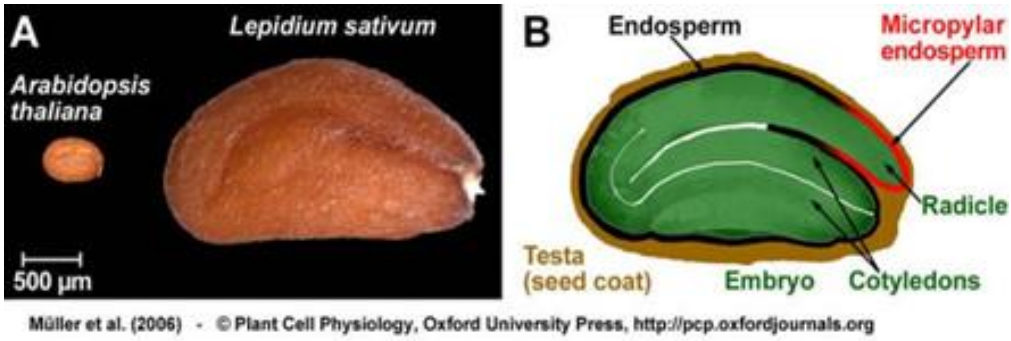

Figure 1.3 Arabidopsis and Lepidium seeds: (A) The larger size of Lepidium seeds allows the use of methodologies, for which Arabidopsis seeds are too small; (B) Drawing of a mature Lepidium seed: the embryo is enclosed by the endosperm and the surrounding testa (Taken from Müller et al., 2006)

1.6.2 Testa rupture and endosperm weakening during germination

Testa rupture and endosperm rupture are temporally separate events during the germination of many seeds (Leubner-Metzger, 2003; Petruzzelli et al.,

2003). These events are also mechanistically distinct processes, because the testa is dead and the endosperm alive.

The current findings (Finch-Savage & Leubner-Metzger, 2006) support the view that germination control by seed-covering layers is achieved through the combined or successive actions of several cell-wall-modifying proteins.

In several species endosperm weakening has been associated with the GA-induction of cell wall remodeling enzymes, e.g. in tomato seeds such as: endo-β-mannanases (Nonogaki et al., 2000), β-1,3-glucanase and chitinases (Wu et al., 2001) and xyloglucan endotransglycosylase (Chen et al., 2001). In Arabidopsis, an extensin-like gene (*AtEPR1*) was shown to be expressed in the micropylar endosperm (Dubreucq et al., 2000).

Analysis of transcriptome expression data sets derived from isolated embryo and endosperm tissues could be used to reveal which cell-wall related genes were endosperm-specific (Penfield et al., 2006). In one analysis, the majority of the 51 cell wall-associated genes (as defined by the Genome Ontology (GO) cellular component "cell wall") showed higher expression in the endosperm than embryo, encoding endotransglycosylase-related proteins, pectin metylesterases and expansins (Holdsworth et al., 2008).

Concerning the hormones orchestrating the processes of germination, ABA has an inhibitive effect on the endosperm rupture but not on the testa rupture. This inhibitory effect of ABA is counteracted by GA supporting the view that endosperm rupture is under the control of an ABA-GA antagonism (Koornneef et al., 2002; Yamaguchi & Kamiya, 2000; Leubner-Metzger, 2003; Kucera et al., 2005).

The hypothesis that GA is an embryo signal for the induction of the endosperm weakening is consistent with published work on GA biosynthesis and response during Arabidopsis seed germination (Yamaguchi et al., 2001; Yamaguchi & Kamiya, 2000; Yamauchi et al., 2004; Ogawa, 2003).

1.7 The correlation gene network

Using a total of 138 samples representing three ecotypes and eight mutants, 73 nongerminating and 65 germinating samples, Bassel et al., 2011, generated SeedNet. A condition-dependent network model of transcriptional interactions associated with dormant and germinating seeds, it highlights the interactions between the germination and dormancy regulators, making predictions of regulators interactions with 50% accuracy (Bassel et al., 2011).

This network subdivided the seed in 3 regions (Figure 1.4). Genes (nodes) associated with dormancy were exclusively located in region 1 of the network, while the ones associated with germination were located in region 3. Transcripts induced by the dormancy breaking after-ripening were associated with region 3, whilst those down-regulated by after-ripening were associated with region 1.

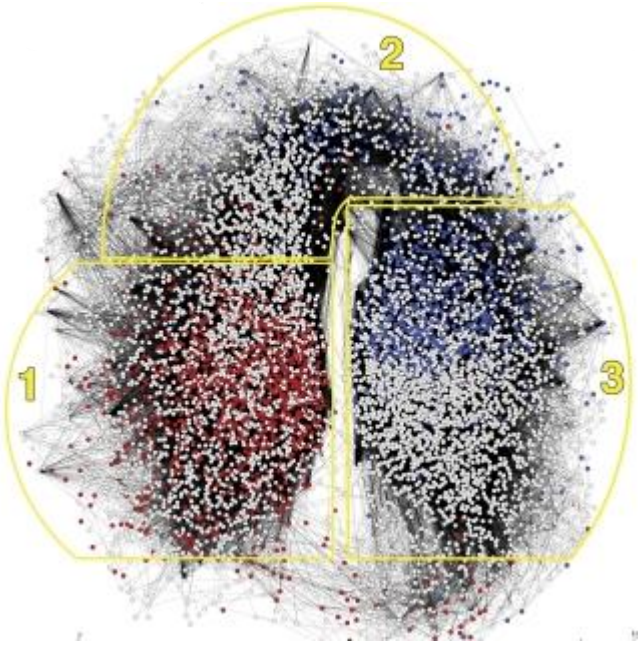

Figure 1.4 SeedNet-Coexpression network in Arabidopsis seeds (Bassel et al., 2011). Region 1 (red dots) - genes associated with dormancy, ABA-up and after-ripening down regulated; Region 3 (blue dots) - genes associated with germination, ABA down and GA up-regulated; Region 2- genes associated with the transition between region 1 and region 3.

Also, according to hormonal response, the genes up-regulated by ABA were predominantly located in region 1 of the network, although many were present in region 3. ABA-down-regulated genes were associated with region 3. Conversely, the genes up-regulated by GA were exclusively located in region 3 of the network, while the down-regulated ones in region 1.

In addition, genes up-regulated by ABA- regulated vegetative abiotic stresses as drought, were associated with region 1, whilst the ones regulated by non-ABA stresses, such as hypoxia, were not. Region 1 of SeedNet is associated with non-germination and transcripts induced by ABA-mediated abiotic stresses in plants.

Using a Molecular Complex Detection algorithm, there were defined 136 modules, or clusters of significantly interacting genes. These modules were associated either with dormancy and ABA, or germination and GA, or with genes with no developmental or hormonal control. For example, module 2 was associated with germination and GA, comprises genes associated with cell expansion, CWREs, protein translation, cytoskeleton or water channels. Within the modules associated with dormancy and ABA, an abundance of key regulators to complete the germination was found.

In this study, module 19 was chosen for analyzying the endosperm-specific gene interactions during germination (Figure 1.5), being the only cluster comprising the endosperm genes. The representative gene for this cluster was chosen to be At5g05290, *EXPA2 (ARABIDOPSIS THALIANA EXPANSIN A2)* one of the CWREs.

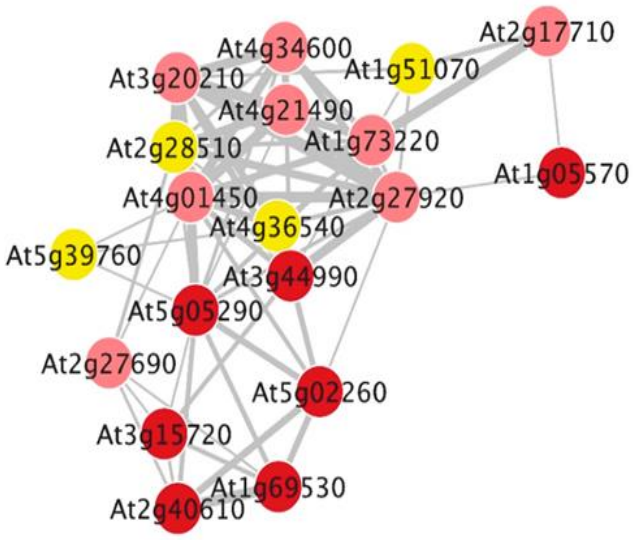

At3g15720glycoside hydrolase family 28 protein / polygalacturonase (pectinase) family protein
At1g69530ATEXPA1 (*ARABIDOPSIS THALIANA* EXPANSIN A1)
At4g36540BEE2 (BR ENHANCED EXPRESSION 2); DNA binding / transcription factor bHLH
At4g21490NDB3; NADH dehydrogenase
At5g05290ATEXPA2 (*ARABIDOPSIS THALIANA* EXPANSIN A2)
At5g39760ATHB23 (*ARABIDOPSIS THALIANA* HOMEOBOX PROTEIN 23); DNA binding / transcription factor
At1g73220ATOCT1 (*ARABIDOPSIS THALIANA* ORGANIC CATION/CARNITINE TRANSPORTER1);
At2g27690CYP94C1 (cytochrome P450, family 94, subfamily C, polypeptide 1); oxygen binding
At4g34600similar to unknown protein [*Arabidopsis thaliana*] (TAIR:AT2G16385.1)
At3g44990XTR8 (xyloglucan:xyloglucosyltransferase 8); hydrolase, acting on glycosyl bonds
At2g17710similar to unnamed protein product [Vitisvinifera] (GB:CAO42932.1)
At4g01450nodulin MtN21 family protein
At5g02260ATEXPA9 (*ARABIDOPSIS THALIANA* EXPANSIN A9)
At1g51070 basic helix-loop-helix (bHLH) family protein
At3g20210 DELTA-VPE (delta vacuolar processing enzyme); cysteine-type endopeptidase
At1g05570CALS1 (CALLOSE SYNTHASE 1); transferase, transferring glycosyl groups
At2g28510Dof-type zinc finger domain-containing protein
At2g40610ATEXPA8 (*ARABIDOPSIS THALIANA* EXPANSIN A8)

Figure 1.5 Cluster 19 of the SeedNet positive correlation network reveals expression interactions between endosperm-specific components. Circles- genes: pink- others; red- CRWEs; yellow- transcription factors. Lines- significant transcriptional interactions between genes. Increased node size corresponds to higher degree of interaction and edge width to interaction strength (Bassel et al., 2011).

EXPA2 was shown to be exclusively expressed in germinating seeds and the mutant (Salk_117075) showed delayed germination, suggesting that *EXPA2* is involved in controlling seed germination (Yan et al., 2014). Also, it was proven that *EXPA2* expression is controlled mainly by *RGL1* and that its overexpression confers a higher tolerance to stress factors (Ogawa et al., 2003; Yan et al., 2014).

1.8 Plant biomechanics

Although growth and morphogenesis are controlled by genetics, physical shape change in plant tissue results from a balance between cell wall loosening and intracellular pressure. Despite recent work demonstrating a role for mechanical signals in morphogenesis, precise measurement of mechanical properties at the individual cell level remains a technical challenge (Routier-Kierzkowska et al., 2012).

Plant cells are surrounded by cell walls that contain considerable turgor pressure within (Schopfer, 2006). Although morphogenesis occurs at the tissue level (Coen et al., 2004), wall mechanical properties are controlled at the cellular level through the deposition and chemical modification of cell wall material (Köhler & Spatz, 2002; Baskin, 2005; Burgert, 2006; Cosgrove, 2005; Schopfer, 2006). For this reason, the mechanical properties of the cell walls have to be studied *in planta*, at the cellular and subcellular scales (Geitmann, 2006; Mirabet et al., 2011).

In 1965, Lockhart provided the first model to answer the question of growth limitation at cellular level. For a cell to expand there are two prerequisite conditions: the cell wall must increase its surface area and water must enter the cell to increase its volume, concomitantly (Lockhart, 1965). Cell extension depends on a balance of antagonizing wall-loosening and wall-stiffening processes that can be independently regulated by different growth factors such as hormones and light (Schopfer, 2006).

As plant shape is defined by cells number and cell size, it is important to understand growth at cellular level. It is valid for seeds too, considering their importance in human life, but also to explain and understand physiological processes definitive in plants life.

Plant growth occurs when the cell wall expands, due to the differences in turgor pressure between the cell and extracellular space, and it is possible due to the cell wall elasticity and extensibility, physical properties given by the cell wall components (Ray et al., 1972).

The cell wall is a viscoelastic complex which undergoes plastic deformation when the turgor pressure is higher than the yield threshold. The yield threshold describes the energy that the cell wall components can store elastically before being irreversible deformed. This irreversible wall extensibility is called cell wall stiffness (Braidwood et al., 2013).

In single cells, stiffness can be investigated in situ using micro and nanoindentation methods (Geitmann, 2006). A thin probe indents the cell surface, while both the applied load and the probe displacement are monitored. Stiffness values are extracted by computing the slope of the force-displacement curve at maximal indentation depth. The stiffness obtained reflects not only cell wall elastic properties but also turgor pressure (Wang et al., 2004), cell and indenter geometry (Bolduc et al., 2006) and mechanical stresses prior to indentation (Zamir & Taber, 2004).

Although there are still debates on what generates growth, it is the negative water potential or the alteration of the cell wall composition, it seems that the growth direction is established by the components of the cell wall (Winship et al., 2011).

1.8.1 Biomechanics of seed germination

Only in the last decade, the study of seed germination became an interdisciplinary effort including methods and approaches from engineering, mathematical, and computer sciences. These interdisciplinary approaches have added a new dimension to our understanding of plant biology in general and seed germination in particular (Geitmann & Ortega, 2009; Moulia, 2013; Schopfer, 2006).

When dry seeds come in contact with water, water uptake is driven by the low water potential in the dry seed. The seed cells continue to swell until the osmotic forces are balanced by the tensile forces from viscoelastic stretching of the cell wall, and any other forces transmitted from the surrounding cells. If the

cell wall flexibility is increased by cell wall restructuring then the same tensile force will produce a larger change in size (Schopfer, 2006).

Measurements of the temporal increase of the fresh weight of seeds through water uptake shows a triphasic water uptake profile for many species (Bewley, 1997; Weitbrecht et al., 2011).

In a first phase rapid water uptake can be observed, concomitant with an increase in seed volume or swelling. In a second phase, the fresh weight remains constant for some time as the seed undergoes metabolic preparations for the termination of germination and subsequent seedling growth. Finally, in phase three, the embryo elongates due to more water uptake and breaks through the covering tissue layers, marking the end of germination.

The force required for the testa rupture is given by the difference between the embryo expansion potential and the constraint generated by its surrounding layers. In an orthodox seed, a seed which will survive drying and/or freezing during ex-situ conservation (Hahm et al., 2009), the embryo expansion potential must be positive, otherwise the seed does not germinate remaining in a dormant state (Schopfer, 2006). There are environmental factors which can change the germination potential level, thus the dormancy can be broken by light, hormones, low temperatures, etc. (Baskin, 2003).

One might assume that the embryo first breaks through the adjacent layer covering it. In *Arabidopsis thaliana* and *Lepidium sativum*, this layer is the endosperm. Interestingly, however, the outer surrounding seed coat, ruptures first (Liu et al., 2005; Müller et al., 2006). In several crop species such as tobacco (Manz et al., 2005) the same germination pattern is followed: first the testa ruptures followed by endosperm rupture and radicle protrusion, while in tomato testa and endosperm rupture in the same time (Groot & Karssen, 1987).

All shape and size changes of tissues in germinating seeds are the result of cell growth, as no cell division can be observed during germination (Sliwinska et al., 2009).

To quantify the force needed for the radicle to break the endosperm, physical measurements have been carried out using isolated endosperms from different species: tomato (Groot & Karssen, 1987), coffee (da Silva et al., 2004) and cress (Müller et al., 2006). The mutual conclusion from these puncture force experiments was that the micropylar region of the endosperm is weakened prior endosperm rupture. Endosperm rupture together with the embryo`s growth potential are inhibited by ABA and stimulated by GA (Müller et al., 2006).

1.9 Seed cell wall structure

Although the investigations on cell growth mechanics started more than a century ago, with Sachs in 1887 (Sachs, 1887) and de Vries in 1877, the mechanism is not yet fully understood.

The conventionally accepted model for plant cell walls implies a complex composite of polysaccharides with low protein content. The polysaccharides consist mainly in cellulose and a range of non-cellulosic polysaccharides, such as pectic polysaccharides (galacturonic acid) and hemicelluloses (xyloglucans, heteroxylans, heteromannans) (Burton et al., 2010).

The biosynthesis of cell wall components is taking place in the Golgi complex (the matrix polysaccharides) and in the plasma membrane (cellulose, up to 36 complexes of cellulose synthases) (Burton et al., 2010).

The cellulose is grouped in microfibrils (Somerville, 2006), while the pectic polysaccharides form complex hydrated gels, cross-linked by covalent and ionic bonds with other cell wall components (Caffall & Mohnen, 2009).

The pectins confer strength and flexibility to the cell wall, while hemicellulose is reinforcing the cell wall by cross-linking cellulose microfibrils (Scheller & Ulvskov, 2010).

In 2011, a new cell wall structure was suggested by Dick-Perez et al., consisting of a single network of polysaccharides featuring interactions between cellulose, xyloglucans and pectin (Dick-Pérez et al., 2011).

Cell expansion in meristematic tissue is a major and irreversible cell process requiring the remodeling of the cell wall. This growth is not only caused by the water uptake, driven by the osmotic pressure, but it also involves processes of hydrolysis, rearrangement or disassembly of structural polymers (Rodríguez-Gacio et al., 2012). All the processes are dependent on enzymatic activity: hydrolases, expansins, transglycosylases or reactive oxygen species (Schopfer, 2006; Burton et al., 2010).

1.9.1 New cell wall remodeling proteins

Although it is still unclear what initiates growth, it is clear that cell wall modification is required to direct growth (Braidwood et al., 2013). A softening of the cell wall is not taking place only in the meristematic tissues, or in fruit ripening, programmed cell death but also in endosperm rupture upon germination (Weitbrecht et al., 2011).

For the completion of germination, the cell wall must thus be remodelled in the embryo to allow the cell elongation, and/or in the endosperm to lower its resistance to the radicle expansion (Cosgrove, 2001). As expression and activity of a number of cell wall modifying enzymes change in both embryo and endosperm (Lee et al., 2012; Morris et al., 2011), it can be assumed that both change their biophysical properties.

Cell walls are modifying their physical properties by altering the composition or/and interaction of the cell wall components, enabling a rapid structure modification. The most common proteins released by plants to alter their cell wall promoting growth, are the glycosyltransferases, expansins and pectin methylesterases (PMEs) (Peaucelle et al., 2011).

1.9.2 Cell wall expansins

There are known 4 families of expansins in Arabidopsis, two families contain members that have the ability to extend cell walls (EXPA or α-expansin, and EXPB or β-expansin), whereas the functions of the other two related families (EXLA and EXLB, for expansin-like family A and B) are still not clear (Cosgrove, 2005).

Cell-wall enlargement begins with wall stress relaxation, which allows the cells to take up water and physically enlarge. Expansins are a group of non-enzymatic wall proteins that induce wall stress relaxation and extension. They mediate the disrupting of non-covalent linkages that hold microfibrils in place. The mechanism by which the cell wall is loosened is not fully understood. There might be an enzymatic release of xyloglucans, resulting in increasing the cell wall extensibility and cell growth or a non-enzymatic action of hydroxyl radicals which cuts the polysaccharides (Cosgrove, 2005).

The pH of the cell wall of growing cells is typically between 4.5 and 6, which is the range in which acidification activates expansin activity. This is biologically important because a number of agents alter cell growth, by inducing the cell to alter its wall, e.g. stem and root tropisms (bending toward or away from a stimulus), hormone-induced growth, light-induced stimulation of leaf expansion and inhibition of stem elongation, responses of shoots, roots and leaves to water deficits and salt stresses and early outgrowth of root hairs (Cosgrove, 2005).

1.10 Methods to study plant biomechanics

1.10.1 Atomic force microscopy

Atomic force microscopy (AFM) enables the collection of force-indentation curves at various cell surface points. Each curve comprises the approach and retraction of the cantilever, considered as a small elastic beam, from the surface while recording its deformation.

The cantilever has a calibrated stiffness constant so that the attractive/ repulsive forces between the tip and the sample surface can be measured, and mechanical properties such as adhesion and elasticity can be quantified (Goldsbury & Scheuring, 2002).

For almost two decades AFM has been used to image the surface of living animal cells in a non-destructive manner. In plants, very few studies have used this technology (Milani et al., 2013). Among these, observations have been done on extracted or isolated cell walls from various tissues and species in order to examine cell-wall structure and texture (Well et al., 1996; Davies & Harris, 2003).

In plants, AFM was first used to study the mechanical properties of fiber walls in wood (Clair et al., 2003). Using AFM, Marga et al., 2005, have visualized and characterized the effect of expansin on cellulose microfibrils network, demonstrating that it acts selectively on the cross-linking polymers between parallel microfibrils, rather than more generally on the wall matrix (Marga *et al.*, 2005).

In 2011, Milani et al., used AFM to measure cell wall properties of the shoot apical meristem epidermis. They found a difference in elasticity of the tip compared with the peripheral region of the apical meristem; the cell walls were less elastic in the meristematic tip (5 ± 2 MPa) than in the flanks of the meristem (1.5 ± 0.7 MPa) (Milani et al., 2011).

Using a similar method, in 2012 Fernandes et al., performed AFM on Arabidopsis roots. The plasticity of root cell walls was revealed by the

difference in the approach and retraction curves. This study did not reveal any spatial differences in plastic or viscoelastic behaviour along the root (Fernandes et al., 2012).

In 2013, Braybrook and Peaucele, using AFM demonstrated that auxin increases the cell wall elasticity in the shoot apex prior to organ emergence, in Arabidopsis (Braybrook & Peaucelle, 2013).

1.10.2 Nanoindentation of biological materials

Nanoindentation is a technique which uses the recorded depth of penetration of an indenter into the specimen along with the measured applied load to determine the area of contact and hence the hardness of the tested specimen. Many other mechanical properties can also be obtained from the experimental load-displacement curve, the most straight-forward being the reduced modulus, but properties such as the strain-hardening index, fracture toughness, yield strength and residual stress can also be obtained in some circumstances (Fischer-Cripps, 2005).

With a typical working force range of 1 μN to 500 mN and displacement range of 1 nm to 20 μm, this technique bridges the gap between AFM and macroscale mechanical testing (Ebenstein & Pruitt, 2006).

Load and displacement are monitored continuously during the indentation process, resulting in a load-displacement curve, as shown in Fig. 1.6a. The interaction between the tip and the sample during the indentation process is illustrated in Fig. 1.6b.

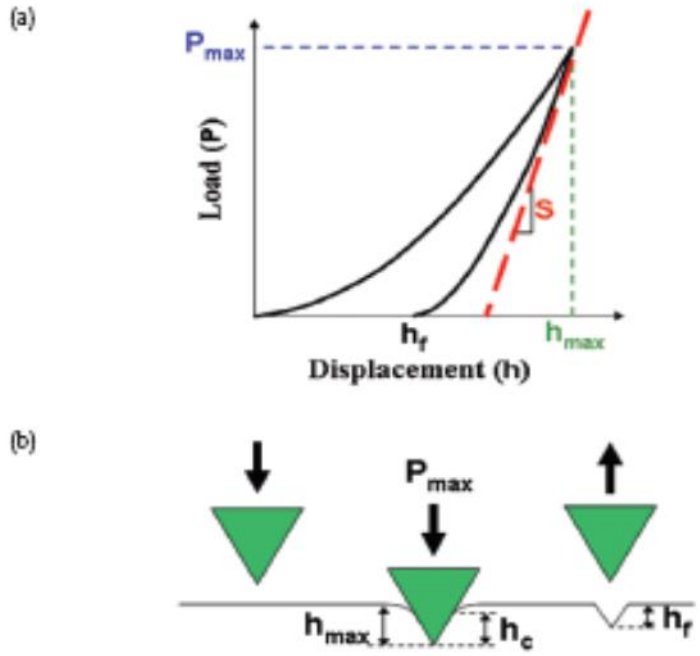

Figure 1.6 Schematic of (a) a typical load-displacement curve; (b) the indentation process P_{max} = maximum load applied; h_{max} = penetration depth; h_c = contact depth (the height of the contact between the tip and the sample); h_f = final depth; S= unloading stiffness (Taken from Ebenstein & Pruitt, 2006).

In plants, nanoindentation has been used to evaluate the properties of fibres (which are reinforcement materials), such as cotton stalk (*Gossypium herbaceu*), soybean stalk (*Glycine max*), cassava stalk (*Manihot esculent*), rice straw (*Oryza sativa* L.) and wheat straw (*Triticum aestivum* L.) (Wu et al., 2010).

The elastic modulus of wheat straw was found to be 20.8 GPa, which was the highest value for straws, while the highest hardness was observed in cotton stalk at 0.85 GPa (Wu et al., 2010).

1.10.2.1 Principle of the method

The analysis used to determine the hardness (H) and elastic modulus (E_r), is an extension of the method proposed by Doerner and Nix (2011), that

accounts for the fact that unloading curves are distinctly curved in a manner that cannot be accounted for by the flat punch approximation. In the flat punch approximation used by Doerner and Nix, the contact area remains constant as the indenter is withdrawn, and the resulting unloading curve is linear. In contrast, experiments have shown that unloading curves are distinctly curved and usually well approximated by the power law relation:

$$P = \alpha (h_{\max} - h_f)^m,$$

where α and m are power law fitting constants (Oliver & Pharr, 1992).

Oliver and Pharr (Oliver & Pharr, 1992) further generalized their approach, resulting in the widely used compliance method for indentation analysis. Letting $F(d)$ be an "area function" that describes the projected (or cross sectional) area of the indenter at a distance d back from its tip, the contact area A is then

$$A = f(h_c).$$

Once the contact area is determined, the hardness is estimated from:

$$H = \frac{P_{\max}}{A}.$$

This definition of hardness is based on the contact area under load; it may deviate from the traditional hardness measured from the area of the residual hardness impression if there is significant elastic recovery during unloading (Oliver & Pharr, 2004).

Measurement of the elastic modulus follows from its relationship to contact area and the measured unloading stiffness through the relation:

$$S = \beta \frac{2}{\sqrt{\pi}} E_{eff} \sqrt{A},$$

Where E_{eff} is the effective elastic modulus defined by

$$\frac{1}{E_{eff}} = \frac{1-\nu^2}{E} + \frac{1-\nu_i^2}{E_i} \ .$$

The effective elastic modulus takes into account the fact that elastic displacement occurs in both the specimen, with Young`s modulus *E* and Poisson`s ratio *v*, and the indenter, with elastic constants E_i and ν_i (Oliver & Pharr, 2004). The indenter material properties are usually known (E_I = 1141 GPa, ν_i = 0.07 for diamond, a common tip material), so the Young`s modulus of a material can be calculated from the reduced modulus if the Poisson`s ratio of the sample material is known. If the Poisson`s ratio of the sample is not known, the plane strain modulus

$$E` = \frac{E}{(1-\nu^2)}$$

can be reported.

1.10.2.2 Adaptation for indentation of polymeric biomaterials and tissues

Polymeric biomaterials and tissues often exhibit viscoelastic or time-dependent behaviour (Fung, 1993) and may be subject to adhesive interactions between the tip and the sample. The compliance method is based on assumption of elastic, isotropic materials and negligible adhesion (Oliver & Pharr, 2004).

Creep is the most observed effect of viscoelasticity or the tip is sinking into the sample under a constant load. To avoid its appearance Briscoe et al., incorporated a 10 s hold period at peak load in order to allow the material to approach equilibrium prior to unloading (Briscoe et al., 1998). An appropriate hold time should be selected based on the creep and unloading rates used in experiments (Wu et al., 2011).

Adhesion between the tip of the indenter and the sample can interfere with measurements of modulus using the compliance method in soft tissue samples. The compliance method overestimates the modulus when there is a significant tip-sample adhesion (Carrillo et al., 2011).

1.10.2.3 Indenter shape and size

Indenter tips are usually made out of very stiff materials, such as diamond and sapphire, so that the compliance of the tip is much lower than the sample compliance.

The three sided pyramid Berkovich indenter is the most popular geometry for nanoindentation testing, and is used for metals, ceramics, glassy polymers or mineralized tissues. Also, there is a four-sided Vickers pyramid indenter, but it is much easier to grind the faces of the indenter to meet at a single point than a line, so the Berkovich indenter is preferred.

For soft tissues a spherical tip is commonly used to minimize plastic deformation and stress concentrations, but also to avoid damage to the sample. For viscoelastic materials the cylindrical flat punch is used; it has the advantage of a constant, known contact area as a function of depth, but has high stress concentration at the contact perimeter.

The dimension of the tip is also important. If the goal is to measure tissue-level properties in a soft tissue, a large diameter spherical tip will be necessary so that the contact area will be much greater than the diameter of an individual cell or fiber (Ebenstein & Pruitt, 2006).

1.10.2.4 Corrections to recorded data

The most common and necessary corrections are the initial penetration, the instrument frame compliance and the indenter area function.

Initial penetration

The determination of the initial contact between the indenter and the specimen is important because the contact point determines the datum of the displacement measurement. The initial contact force is set by the user and once it is achieved the depth sensor set to zero and the loading then proceeds.

The significance of initial penetration correction depends upon magnitude of the maximum load applied to the indenter relative to the magnitude of the initial contact force. The lowest force that can be detected or set in atypical initial penetration is in the order of 2-5 μm and the initial penetration is a few nanometers (Fischer-Cripps, 2006).

Frame compliance

The compliance correction is dependent on the load and is not a constant (as the initial penetration correction). It becomes particularly important when testing very stiff materials. Its correction requires knowledge of the value of the compliance of the instrument, often measured by the manufacturer and set within the software.

The best way to measure and verify the value of the instrument compliance is to conduct a series of tests at different loads on a fairly stiff specimen (sapphire). A common mistake in operating or calibrating a nanoindenter is to determine the compliance using only one reference standard. For best results, the compliance should be determined on a variety of standard specimens (fused silica, silicon and sapphire). The resulting values should be consistent for each of the specimens (Fischer-Cripps, 2006).

Area function

The area function of the indenter is a function or a table of values that provides the best estimate of the area of contact as a function of the contact depth for the indenter being used. It is common to test a material of known modulus or hardness using the following equation (Fischer-Cripps, 2006):

$$A = C_1 h_c^2 + C_2 h_c + C_3 h_c^{1/2} + C_4 h_c^{1/4} + \ldots$$

Where h is the plastic (or contact) depth and C_1 is usually a number close to 24.5 and the remaining fitting constants account for the tip rounding and other departures from the ideal shape.

Thermal drift

Thermal drift refers to changes in dimension of the indenter, specimen and the instrument, resulting from a temperature change during the test. It is measured in nm/s.

Thermal drift can introduce large errors into the load-displacements curves causing the measured hardness and elastic modulus to be in error. The most common situation is at the contact between the indenter and the specimen (Fischer-Cripps, 2006). There are two ways to correct it:

(1) Reduce the temperature variations at the specimen to an absolute minimum. The machine should be enclosed into an isolated cabin and located into a controlled environment (just above room temperature).

(2) Correct the data for thermal drift. The correction is made by accumulating depth readings while holding the load constant (5-10 s). The preferred option is the hold data at 10% of unloading curve, since the creep of the specimen is minimized.

1.10.2.5 Material-related effects

There are various materials-related effects which can cause errors in the estimation of elastic modulus and hardness of the specimen. The most significant is piling-up. It is the most unresolved issue in nanoindentation testing. There are two ways to approach the problem: perform an area function calibration on a reference specimen which has a similar ratio of elastic modulus/hardness as the test specimen or as ISO 14577 recommends, ignore the effect and treat the resulting values as comparative values (Fischer-Cripps, 2006).

1.10.3 Micro x–ray computed tomography

The imaging process in computed tomography is based on the differential attenuation of x-rays in relation to specific density of the tissue (i.e. the beam passes more easily through low-density, whereas dense objects absorb or reflect the beam) (Pajor et al., 2013).

Evolving primarily from medical sciences it is now considered as an established tool for non-invasive, non-destructive, precise visualization and quantification of the internal structures of materials in 3D (Pajor et al., 2013).

The first attempt of scanning Arabidopsis seeds was done in 2006, by Cloetens et al., using synchrotron facilities to investigate the structure and spatial distribution of intracellular voids (Cloetens et al., 2006).

In 2008, another attempt was done by Kaminuma et al., using a commercially available CT scanner to obtain datasets of Arabidopsis leaves and seeds. Although level of detail was sufficient to reveal the spatial distribution of trichomes in leaves, the scans of seeds were extremely noisy (Kaminuma et al., 2008).

In recent years, x-ray CT has been widely utilized in rhizosphere studies, mainly focusing on the study of soil structure (Mooney, 2006), interactions between soil and microbes (Pajor et al., 2013), and *in vivo* imaging of plant roots, root development and architecture (Tracy et al., 2012).

1.10.4 Digital image correlation (DIC)

Digital image correlation (DIC) is a non-contacting method that analyzes the full-field shape, deformation and motion by applying related algorithm to the acquired images data of the subject. The application of DIC has contributed greatly to the research fields that cover material sciences and experimental mechanics (Pan et al., 2009).

With the development of DIC, there are mainly two important assumptions involved that convert image information into experimental measurement and

analysis of the strains and displacements on objects. One is the motion of points from both image and object directly corresponding to each other. According to this assumption, the displacement of points on target object can be quantified by determining the image motions. Consequently, such kind of assumption can provide a uniform (one to one) correspondence between points on image and points on object in a 2-D vision.

Another assumption is based on the contrast at each sub-region of the object, so that accurate matching can be performed to show up the movements/deformations (Sutton, 2008). A sufficient contrast can be achieved by applying a pattern on the specimen. Usually, grids, lines or dots are preferred and they can be easily obtained by painting, adhering or surface machining (Bornert et al., 2008).

Generally, there are three steps involved in 2-D DIC implementation:

1) Experimental setup and specimen preparation;

2) Capturing images;

3) Determine the displacement and strain by processing the obtained images using a specific software (Istra 4D) (Pan et al., 2009).

1.11 Recent work in seed germination mechanics

Changes in the properties of the endosperm significantly affect the timing of radicle emergence in non-dormant seeds. The mechanical resistance of micropylar endosperm is mainly due to the thick and rigid cell walls in this tissue, therefore its weakening is due to cell wall modification (Bewley et al., 2013).

Bassel et al., (2014), following the mathematical theory assuming that growth depends on the abundance of cell-wall remodeling agents and the amount of stress/strain in the wall itself, developed a mechanical model using finite-element method.

According to the model described by Bassel et al. (2014), cell size and arrangement of cells in tissue affect the stress on cell wall, as well as the cell ability to expand in response to turgor pressure. It is not only the cell wall remodeling activity but also the amount of stretch in the cell wall that leads to tissue weakening and rupture.

However, a new hypothesis stands for a "mechanosensing" wound response, provided by embryo pressure directed on micropylar cells, rather than chemical molecules for endosperm weakening (Dekkers et al., 2013; Martínez-Andújar et al., 2012). Pathogen-response genes were identified as micropylar endosperm enriched genes in tomato seeds (Martínez-Andújar et al., 2012) suggesting the fact that testa rupture triggers a wound response thus activation of genes expression in the tissue.

Together with testa rupture, genes known to be induced by touch or thigmotropism are activated (2.5% of Arabidopsis genes encoding calcium-binding, cell wall modifying, defense, transcription factor and kinase proteins are rapidly up-regulated in touch-stimulated plants) (Braam 2005).

Also, Dekkers et al., (2013) observed that gene expression associated with jasmonate biosynthesis was activated upon testa rupture in the micropylar endosperm; recently shown to be a key regulator of plant morphogenesis and enhanced pest resistance upon touch (Chehab et al., 2012).

1.12 Aims and objectives of the project

The aim of this study was to correlate gene expression with physical property changes, in the endosperm of *Arabidopsis thaliana* and *Lepidium sativum* seeds during germination.

The objectives of this thesis were:

• To generate/estimate values of endosperm stiffness, hardness, or changes in structure and shape using imaging and mechanical approaches.

The hypothesis tested was that the endosperm stretches during germination, becoming thinner. Another assumption to be confirmed was that endosperm physical properties are changing through germination, weakening in the micropylar region in order to allow radicle protrusion.

Another objective was to detect differences in stiffness of Arabidopsis mutants with known biochemical alteration of the cell wall composition, using nanoindentation. The methodologies used to visualize and detect changes in seeds shape and structure were: AFM, Micro-CT and nanoindentation.

• To reveal the tissue specificity (spatial and temporal distribution) of the genes from cluster 19 (cluster comprising endosperm specific genes) confirming the predictions of SeedNet

The hypothesis tested was based on SeedNet predictions, that cluster 19 comprises genes specifically expressed in the endosperm during germination. The expression of several gene promoters (*EXPA2*, *DELTA-VPE*, *SCPL51* and *DOF2.1*) was monitored using GUS staining technique, to reveal their spatial distribution in the endosperm, during germination. Also, the effect of ABA/GA and the embryonic signal required for their expression was observed.

To reveal the interactions between the transcription factors from cluster 19, the behaviour of germination of their mutants was studied: *ATHB23*, *BEE2*, *bHLH115*, *DOF2.1*. To analyse the transcription factors (T-DNA lines) mutants, and their putative interactions with *EXPA2* promoter fragments, using yeast one hybrid system.

2. Materials and Methods

2.1 Seeds and plants

2.1.1 Seed material

Mutants of Arabidopsis were kindly provided, by Dr. Bas Dekkers, Utrecht University and by Dr. Kieran Lee, Leeds University. The wild type Arabidopsis (Col-0) was obtained from members of the Holdsworth research group.

2.1.1.1 Seed sterilization and plating

Seed sterilization was carried out in the laminar air flow chamber. Seeds were aliquoted into micro centrifuge tubes (1.5 ml) and were surface sterilized using freshly diluted 5% (v/v) bleach (Parazone, UK) for 5 minutes. Seeds were then washed three times with sterile water. Seeds were plated onto media using an Ultipipette tip. Plates were sealed using micropore tape (3M, Bracknell, UK).

2.1.1.2 Germination media

Germination media contained 0.7% (w/v) agar supplemented with half-strength Murashige & Skoog salts (DuchefaBiochemie B.V., Haarlem, Netherlands, Murashige & Skoog 1962). The pH of the media was adjusted to 6.2 before autoclaving. All media were stored at 4°C and allowed to warm for at least 20 minutes before use.

2.1.1.3 Seed germination conditions

Seeds on media plates were incubated at 22°C in continuous light (light intensity 60 μmols m^{-2} s^{-1}) in a controlled environment growth chamber. Germination was achieved when the radicle protruded through the endosperm. Seedlings were transplanted into soil when the first true leaves had appeared.

2.1.2 Plant growth conditions

Plants were grown in controlled environment chambers at 22°C in continuous light conditions (light intensity 60 μmols m^{-2} s^{-1}). The soil contained four parts of compost (LevingtonM3, Scotts, Godalming, UK), two parts of vermiculite (medium grade, 2.0-2.5 mm, Sinclair, Lincoln, UK) and one part perlite (standard grade, 2.0-2.5 mm, Lincoln, Sinclair, Lincoln, UK).

2.1.3 Statistical treatment

All germination assays were conducted with four replicates of at least 50 seeds per line. Biological replicates were seed lots collected from different plants that were grown at the same time. Data are presented as the mean +/- the standard error. The formula used to calculate standard error was: Standard error = standard deviation/ $\sqrt{n}$, where n is the sample size; Standard deviation = $\pm\sqrt{\Sigma}$ $(x-\bar{x})^2$/ n-1, where x = sample value, $\bar{x}$= mean.

2.1.4 Cross pollination of Arabidopsis plants

All flowers showing petals and all opened buds were removed from the recipient (female) inflorescence. Remaining floral buds were emasculated using forceps. All siliques were removed. A mature flower was selected and removed from the donor line (male) with forceps. This was then brushed onto the emasculated stigma of the recipient plant until pollen stuck on to the recipient stigma surface. Siliques of cross pollinated stigmas were collected in a 1.5 ml Eppendorf tube after the siliques began to turn yellow.

2.2 RNA Manipulation

2.2.1 Borate isolation of RNA

For RNA extraction the Protocol from Cotton Genome Center, UC Davis (http://cottongenomeceter.ucdavis.edu/protocols/RNA), was modified, as follows:

The Borate extraction buffer was made up in DEPC-treated water: 0.2 M $Na_2B_4O_7 \cdot 10H_2O$, 30 mM EGTA, 1% (w/v) SDS and 1% (w/v) sodium deoxycholate. After prepared fresh, were added: 2% (w/v) PVP, 10 mM DTT, 1% Nonidet-40, 25 mg/ml proteinase K, 2 M KCl and 8 M LiCl.

2.2.2 QiagenRNeasy RNA extraction kit

Frozen tissue (100 g) was ground to a fine powder in a mortar and pestle cooled with liquid nitrogen. 0.7 ml borate buffer, chilled on ice, was added for each 100 mg tissue. The samples were grinded until the liquid nitrogen thawed and transferred to chilled Eppendorf tubes. 0.35 mg of proteinase K was added in each tube. The tubes were incubated in a water bath, at 42°C, for one hour and 30 minutes. After adding 56 µl 2 M KCl, the samples were placed on ice for 1 hour. To remove the debris, the tubes were centrifugated for 12 minutes at 4°C at 12 000 g. The supernatant was transferred to new Eppendorf tubes, and LiCl was added to a final concentration of 2M, and incubated at 4°C, overnight. The second day, the precipitated RNA was collected after a cold centrifugation at 12 000 g, for 20 minutes. The formed pellet was resuspended in 100 µl DEPC water, by vortexing, and manipulated further according with manufacturer protocol (Qiagen, Ltd., Manchester, UK).

2.2.3 QiagenRNeasy Plant Mini Kit – RNA Clean Up Protocol

Samples were manipulated according with the manufacturer instructions (Qiagen Ltd., Manchester, UK). Concentration was checked using Nanodrop ND1000 spectrophotometer (Nanodrop, Wilmington, USA).

2.2.4 RNA Gel electrophoresis

Samples were run in an electrophoresis 1.2% (w/v) agarose gel (0.48 g agarose, 4 ml of 10x MOPS Buffer (section **3.2.4.1**), 36 ml of water, 720 µl 37% (v/v) formaldehyde and 0.4 µl of 10 mg/ml Ethidium bromide). Before loading on the gel, each sample was mixed with 5x RNA loading buffer (section **3.2.4.2**). The running buffer used, was containing 200mM MOPS (free acid), 50 mM Sodium acetate (pH 7.5), 10 mM EDTA (pH 8.0). The pH was corrected to 7.0 with NaOH. The RNA loading buffer was prepared in aliquots, stable for 3-4 months kept at 4°C, using: 16 µl saturated bromophenol blue, 80 µl 500 mM EDTA pH 8.0, 720 µl 37% (v/v) formaldehyde, 2 ml 100% (v/v) glycerol, 3084 µl formamide solution, 4 ml 10 x MOPS buffer and RNase-free water.

2.2.4.1 1xMOPS gel buffer (300ml)

30 ml 10 x MOPS Buffer
6 ml 37% Formaldehyde
264 ml water

2.2.4.2 5 x RNA loading buffer

16 µl saturated bromophenol blue
80 µl 500 mM EDTA pH 8.0
720 µl 37% formaldehyde
2 ml 100% glycerol
3084 µl formamide
4 ml 10 x MOPS buffer
+ RNase-free water to 10 ml.

2.2.5 First strand cDNA synthesis

For a final volume of 20 µl volume reaction, 1 µl of $(dT)_{20}$ oligo (50 µM), 50-250 ng of random primer or 2 pmol of gene-specific primer, 10 pg-5 µg total RNA 500 ng/µl and 1µl 10 mM dNTPs Mix, were mixed with distilled water to 13 µl. The mixture was heated at 65°C for 5 min and cooled on ice for

at least 1 min. After a short centrifugation, 4 µl 5xFirst-Strand Buffer, 1 µl 0.1M DTT, 1 µl RNase OUT Recombinant RNase Inhibitor and 1 µl Super Script III RT (200 u/µl) (Invitrogen, Paisley, UK), were added. Everything was incubated for 60 min at 55°C. To inactivate the reaction, the tube was heated at 70°C for 15 min.

2.3 DNA Manipulation

2.3.1 PCR reaction

Using DNA (genomic DNA or cDNA) as template, PCR was performed to amplify specific genes, using gene-specific primers. For a volume of 50 µl, the next protocol was followed: 5 µl of 10 x PCR Buffer [200 mM Tris-HCl, pH 8.4, 500 mM KCl], 1 µl of dNTPs, 1 µl of 10 µM sense primer, 1 µl of 10 µM antisense primer, 0.4 µl of Taq-DNA polymerase (5 U/µl) (Phusion High-Fidelity DNA Polymerase, Thermo Scientific, Fisher Scientific - UK Ltd) and 2 µl of DNA template were mixed with autoclaved distilled water to the final volume of 50 µl. The PCR machines used here were GeneAmp PCR System 9700; PE Applied Biosystem.

98°C - 5 minutes
98°C - 30 seconds
57°C - 30 seconds
72°C -2 minutes } 30-40 cycles
72°C - 7 minutes

The primers used for different amplifications are shown in Table 2.1.

Gene name	Sequence
At3g20210	pDELTA-VPE f GGGGACAAGTTTGTACAAAAAAGCAGGCTGAAATGGAGTGAGACCATTGTTA
	pDELTA-VPE r GGGGACCACTTTGTACAAGAAAGCTGGGTCTTGAATCTGATTCTTGTGAGAA
At2g27920	pSCPL51_f GGGGACAAGTTTGTACAAAAAAGCAGGCTTTGTAGTGTCAATTGTAAAATTG
	pSCPL51_r GGGGACCACTTTGTACAAGAAAGCTGGGTTCAGACGATTCTTTGTGGATCAAT
At5g39760	ATHB23_1st_f ATTACAAACAAGTGTAACTATG
	ATHB23_1st_r GAATAAGCTTACTCTAAGCTTC
	ATHB23_2nd_f GGGGACAAGTTTGTACAAAAAAGCAGGCTGCTTCGAACCCAATCATTTTGAG

	ATHB23_2nd _r GGGGACCACTTTGTACAAGAAAGCTGGGTACGACGACGATGATCCGTTAAC
At2g28510	Dof 1st f TAATAGCAAGCTCGCTCATTTCG
	Dof 1st r GTGGTGTACAAACATGTGATGAC
	Dof 2nd f GGGGACAAGTTTGTACAAAAAAGCAGGCTCATTGCAATCATATCTTTAATAG
	Dof 2nd r GGGGACCACTTTGTACAAGAAAGCTGGGTAGACCAAAGGAGTGTTGAGTAAA
At3g20210	pDELTA-VPE_f ACATTTCAAGGCAGTTAATTC
At2g27920	SCPL51_f CAGTAAGAATTTAGCTGACATTC
At2g28510	DOF_f CAATTTGAATTATAAATAAAAATC
At2g28510 (GK_668G12)	dof2.1 f AAGGAAAAGTAGGATCCATTGC
	dof2.1 ATGTGCAGGAAATCTCAAACG
At5g39760 (SALK_059288)	athb23 f AATCTTTTTGTTTCTTCATCCG
	athb23 r CTCTCAAATGTGCTGCTTGTG
At1g51070 (SALK_053219)	bhlh115-1 f CGCTGAGGTAATTCCTCTTCC
	bhlh115-1 r CAGAGGAACGTAAGCAAAACG
At4g36540 (SAIL_388_C01)	bee2 f TCATGTTAGGGCTAGACGAGG
	bee2 r TTTTGGCTCTCTGTTTGTTGG
At1g51070 (SALK_104253)	bhlh115-2 f AAGACTTGGGATTTTTGATTGG
	bhlh115-2 r AAGCCATCCACTTCAACACTG
At4g36540	Bee2_f GGGGACAAGTTTGTACAAAAAAGCAGGCTTCATGGACTTGTCTGTACTTGATAG
	Bee2_r GGGGACCACTTTGTACAAGAAAGCTGGGTCTTACTTGAGGCTGAAGAAATTGG
At5g39760	Athb23_f GGGGACAAGTTTGTACAAAAAAGCAGGCTTCATGATGGATATGACTCCTACAAT
	Athb23_r GGGGACCACTTTGTACAAGAAAGCTGGGTCTCACGACGACGATGATCCGTTAA
At1g51070	BHLH_fGGGGACAAGTTTGTACAAAAAAGCAGGCTTCATGGTGTCTCCGGAGAATACGAA
	BHLH_rGGGGACCACTTTGTACAAGAAAGCTGGGTCTTAAGCAACTGGAGGACGAAGGA
At2g28510	Dof_fGGGGACAAGTTTGTACAAAAAAGCAGGCTTCATGGATCCTGAACAGGAAATCTC
	Dof_rGGGGACCACTTTGTACAAGAAAGCTGGGTCCTAGACCAAAGGAGTGTTGAGTA
At5g05290	EXPA2_0_-4_f GGGGACAAGTTTGTACAAAAAAGCAGGCTGTTTCTCATGACTGATGA
	EXPA2_0_-4_r GGGGACCACTTTGTACAAGAAAGCTGGGTGAAGTTGGTAATTCGTT
	EXPA2_-3_-7_f GGGGACAAGTTTGTACAAAAAAGCAGGCTATGACTATAGACTATAGTCTA
	EXPA2_-3_-7_rGGGGACCACTTTGTACAAGAAAGCTGGGTACAGATTCACATGTCATTTGA
	EXPA2_-6_-10_f GGGGACAAGTTTGTACAAAAAAGCAGGCTGAATGTGTCAAGTTACAT
	EXPA2_-6_-10_r GGGGACCACTTTGTACAAGAAAGCTGGGTACATATAAGTGAAGTTCG
	EXPA2_-9_-12_f GGGGACAAGTTTGTACAAAAAAGCAGGCTGTAAGTCTAAGTTTGTTA
	EXPA2_-9_-12_r GGGGACCACTTTGTACAAGAAAGCTGGGTATGTATGCTTACATATCA
At5g05290 (SALK_137972C)	expa2_2 LP_ GCCACTGATCTGTCTTTGAGC
	expa2_2 RP_TCCACGTGGCATAAAAGTAGG

Table 2.1 Primers used for different amplifications: Gateway cloning: GUS primers (violet) + gene specific primers (black); genotyping the T-DNA lines (blue).

2.3.2 Promoter cloning through Gateway cloning system

Gateway cloning (Invitrogen, Paisley, UK) technology is a DNA recombinant technology that uses specific enzyme to mediate the cloning procedure without depending on the traditional restriction enzyme based

cloning limitations and enabling to use practically any expression system, bacteria or yeast cells.

2.3.2.1 BP Clonase reaction

Gateway BP Clonase II enzyme mix catalyses the *in vitro* recombination of PCR products (containing *att*B sites) and a donor vector (containing *att*P sites) to generate entry clones. The donor vectors used here were pDONR221/pDONRZeo. These vectors are part of the Gateway system which uses a specific enzyme for cloning. The cloning procedure follows the principle of specific adaptor flanking at the 5` of the primer with specific enzyme reaction. Two steps of recombination were needed in order to produce the final construct before *Agrobacterium*-mediated Arabidopsis transformation. The PCR primers used in the first cloning step were designed with a special adapter at the 5` end named as attB1 (forward primer) and attB2 (reverse primer).

The amplicon derived from PCR was then cloned into intermediate vectors, pDONR221 and pDONRZeo to produce an entry clone (subclone) for the next recombinant reaction. These vectors have two adaptors, named attP1 and attP2. A recombination reaction mediated by the BP Clonase II enzyme produced the entry clone, forming new adaptors (attL1 and attL2). These vectors were also designed with *ccdB* gene which helps the screening of positive clones. The *ccdB* gene is a lethal gene that targets DNA gyrase. This principle is useful for ensuring that the plasmid containing it cannot be propagated in standard *E. coli* strains (for cloning purposes). The *ccdB* positive-selection marker acts by killing the background of cells with no cloned DNA, only cells containing a recombinant DNA giving rise to viable clones.

For cloning of PCR products, fragments were amplified using Finnzymes Phusion High-Fidelity Polymerase (NEB, Hitchin, UK). PCR was carried out in 50 µl reactions, with 0.1 U Phusion Polymerase, 1x Phusion HF Buffer, 200 µM each dNTP, 0.5 pMol each primer.

BP cloning was performed using Gateway BP Clonase II enzyme mix from Invitrogen as followed:

*att*B- PCR product (15-150 ng)	1-7 µl
Donor vector (pDONR221/pDONRZeo- 150 ng/µl)	1 µl
TE buffer; pH 8.0	to 8 µl

2 µl BP clonase enzymes was added to the solution and incubated at 25°C for 1 hour. 1 µl of Proteinase K was added to the sample and incubated at 37°C for 10 minutes to terminate the reaction. NEB 5-α competent cells from NEB England Biolabs were thawed on ice, then 1 µl of the cloning reaction was added to the cells and they were incubated on ice for 20 minutes. They were then heat shocked at 42°C for 45 seconds, incubated on ice for 2 minutes, then 250 µl pre-warmed LB media was added, and the cells recovered at 37°C in a shaking incubator for 1 hour. 50 µl or 200 µl were plated onto LB-agar plates containing 50 µg/ml Kanamycin or Zeocin 30 µg/ml (Sigma Aldrich, Gillingham, UK), and the plates were incubated overnight at 37°C.

Colonies were picked using a sterile micropipette tips and PCR was carried out with the same primers that were designed for BP clonase reaction. This PCR was used to check for the presence of the desired fragment. Overnight cultures (16 hours incubated at 37°C) were grown from the positive colonies which were proven by PCR and DNA minipreps were carried out to extract plasmid DNA from the cultures using the Qiagenminiprep kit following the manufacturer's protocol (Qiagen, Ltd., Manchester, UK). Plasmids DNA (represent the Entry clones) were then sent for DNA sequencing with M13 forward and reverse primers to confirm the sequence of the cloned fragment and to ensure it was inserted correctly and in frame, to Source Biosciences Labs, Nottingham, UK.

2.3.2.2 LR Clonase reaction

The positive entry clones (from BP reaction) which were shown to be correctly cloned by the sequencing results were used for the LR recombinant

reaction. Gateway LR Clonase II enzyme mix catalyses the in vitro recombination of subcloning DNA segments from clones (containing *attL* sites) and a destination vector (containing *attR* sites) to generate final clones. The destination vectors used in these experiments were pKAN, pGWB433, pDEST22 and pHISLEU2GW.

To generate final clone for promoter studies, LR cloning was performed using Gateway LR Clonase II enzyme mix from Invitrogen. Entry clone from previous BP clonase reaction was used in this reaction with the LR Clonase II enzyme mix from Invitrogen as followed:

Entry clone (50-150 ng)	1-7 µl
Destination vector (150 ng/µl)	1 µl
TE buffer; pH 8.0	to 8 µl

2 µl LR clonase enzymes was added to the solution and incubated at 25°C for 1 hour. 1 µl of Proteinase K was added to the sample and incubated at 37°C for 10 minutes to terminate the reaction. NEB 5-α competent cells from NEB England Biolabs were thawed on ice, then 1 µl of the cloning reaction was added to the cells and they were incubated on ice for 20 minutes. They were then heat shocked at 42°C for 45 seconds, incubated on ice for 2 minutes, then 250 µl pre-warmed LB media (section **2.3.2.2.1**) was added, and the cells recovered at 37°C in a shaking incubator for 1 hour. 50 µl and 200 µl of the cells were plated onto LB-agar plates with 100 µg/ml Spectinomycin for pKAN and pGWB433, 100 µg/ml Ampicillin for pDEST22 and 50 µg/ml of Kanamycin for pHISLEU2GW (Sigma Aldrich, Gillingham, UK), and the plates were incubated overnight at 37°C.

Colonies produced on the respective antibiotic agar plates for bacterial selection were used for plasmid extraction and the isolated plasmids were sent for sequencing to Source Biosciences Labs, Nottingham, UK.

Overnight cultures (16 hours incubated at 37°C) from positive clones were grown, and minipreps were carried out to extract plasmids DNA from the cultures using the Qiagenminiprep kit following the manufacturer's protocol

(Qiagen, Ltd., Manchester, UK). Positive clones were transformed into *Agrobacterium tumefaciens*.

2.3.2.2.1 LB media- Luria-Bertani

10 g/L Tryptone
5 g/L Yeast extract
10 g/L NaCl
+ 1.5-2% (w/v) agar for solid media plates.

2.3.3 Transformation of recombinant clones from LR reaction into competent *Agrobacterium tumefaciens* GV3101 PMP90

Agrobacterium tumefaciens strain GV3101 PMP90 competent cells were thawed on ice, then 1 µl of the LR cloning reaction was added to the cells and they were incubated on ice for 20 minutes. Cells were then electro pulse using a BioRad electroporator which the programme was set as transformation via *Agrobacterium*. 900 µl pre-warmed LB media was added, and the cells recovered at 28°C in a shaking incubator for 4 hour. Cells were recovered by centrifugation for 2 minutes at 3040 x g, and then resuspended in 250 µl LB media. 50 µl and 200 µl of the cells were plated onto LB-agar plates with 100 µg/ml Spectinomycin, 25 µg/ml Gentamycin, 50 µg/ml Rifampicin (Sigma Aldrich, Gillingham, UK), to select for the construct and for the correct bacterial resistance. Plates were incubated for 2 days at 28°C.

Individual colonies from selection plates were picked using sterile micropipette tips; PCR was used to check for the presence of the desired fragment using the same primers used for colonies PCR of LR recombinant selection and PCR condition as described below:

94°C – 5 minutes

94°C – 30 seconds
57°C – 30 seconds
72°C – 2 minutes
} 30-40 cycles

72°C– 7 minutes

Plant transformation was then performed using the *Agrobacterium* strain containing the correct constructs.

2.3.3.1 *Agrobacterium*-mediated Arabidopsis plant transformation

Arabidopsis plants were grown with 8 plants per 9 cm pot. They were allowed to flower, the first bolts were removed when they had reached approximately 10 cm in height. Roughly 5 days later the plants were ready for use in transformation experiments.

A 4 ml of *Agrobacterium* inoculated culture containing the construct for transformation was grown for 24 hours at 28ºC with shaking at 2000 rpm. From this, 2 ml was transferred into 200 ml LB media containing 100 µg/ml Spectinomycin, 25 µg/ml Gentamycin, 50 µg/ml Rifampicin (Sigma Aldrich, Gillingham, UK) and was grown for 24 hours. This culture was centrifuged at 3040 x g, 4°C for 10 minutes to pellet the cells, which were resuspended in 5% (w/v) sucrose solution. Before dipping into plant, 26 µl of Silwet L-77 surfactant was added into 250 ml sucrose solution containing the resuspended cells pellet. This Silwet L-77 surfactant was added to aid transformation by reducing surface tension of the sucrose solution containing the resuspended cells pellet and increase the wetting performance. The plants were then covered in a sealed plastic sleeve for 24 hours, then left to grow and form seeds.

2.3.3.1.1 Selection of transformed plants

To identify transformed plants more quickly and more easily, seeds were sterilized and plated on agar plates containing specific antibiotic as usual and

stratify for 2 days. The plates were transferred to growth room and exposed to light for 4-6 h, then covered and kept in the dark for 48 h. After a further 24 h in light, resistant seedlings could be easily identified as darker green (on 50 µg/ ml kanamycin) and with longer hypocotyls than non-resistant seedlings.

2.4 β-glucuronidase (GUS) staining

GUS is successfully used to identify tissue-specific gene expression in many plant organs. In mature Arabidopsis seeds, the testa is no longer a living tissue, a fact that makes the seeds impermeable to the GUS substrate. Therefore, all staining procedures involved prior separation of embryo from testa and endosperm.

2.4.1 Preparing the GUS stain

The GUS stain solution contains: 100 mM sodium phosphate buffer; 0.1% (v/v) Triton X-100; 2 mM X-Gluc; with pH 7.0.

To make a 10 ml phosphate buffer with a pH of 7.0, two stock solutions were mixed: 1 M Sodium Monophosphate (A) and 1 M Sodium Diphosphate (B). The two solutions were mixed at a ratio of 39:61 (390 µl of A and 610 µl of B). The result was 1 ml phosphate buffer with pH 7.0. 9 ml of water was added to dilute the 1M Phosphate Buffer and 100 mM Buffer pH 7.0, was obtained. 10.44 mg of X-Gluc substrate was added to the buffer solution, vortexed until dissolved, completely. Then, Triton X-100 was added by pipetting up and down, until the whole amount was incorporated.

2.4.2 Performing GUS staining

Before being used, two different cyanide solutions were added fresh into the GUS staining solution (above). Two stock solutions of 100X concentrated cyanide were prepared: 100 mM Potassium Ferri-cyanide and 100 mM Potassium Ferro-cyanide. For each of 10 ml GUS solution (1 mM), 0.1 ml of each 100 mM Potassium Ferri-cyanide and Potassium Ferro-cyanide were

added. Tissues were covered in GUS staining solution. After seeds were dissected separating the endosperm/testa from the embryo, each tissue was incubated in 20 µl GUS stain solution, using 0.5 ml tubes, at 37 °C, for 24 hours.

Subsequent to staining, the tissues were placed in 450 ml of fixative (3:1 Ethanol: Acetic Acid + 1% Tween v/v). Stained and fixed samples were mounted on microscope slides and imaged, using a LEICA DIC microscope (Leica DFC 420C).

Seed testa being dark-brown coloured makes impossible the visualisation of the endosperms underneath, so for this reason, the endosperm plus the covering testa were bleached. After 30 minutes in 25% (v/v) Parazone solution, the testa became transparent. The separated embryos and endosperms were resuspended in 450 µl of distilled water. This treatment had no effect on GUS stain.

2.4.3 Mounting embryos and endosperms

Each embryo and endosperm was mounted in Hoyer's solution (30 g Arabic gum, 200 g chloral hydrate, 20 g glycerol, 50 ml water). The embryo or endosperm were pipetted onto microscope slides using a 200 µl pipette set to 150 µl and using a yellow tip with the end cut off (to create a large opening at the end). The excess water was removed before the Hoyer`s solution was added on the microscope slides. The cover slips were placed on top of the samples.

2.5 Nanoindentation

2.5.1 Initial System Evaluation

Before indentations on plant tissue were carried out, the system performance was checked using 100 mN and 300 mN indentations on a reference sample of fused silica (FS) with the ~12.5 µm radius sphero-cone

indenter which was to be employed. On this very stiff specimen (with no time-dependent properties) a random array of 10 indentations produced closely bunched repeatable curves with properties in the right area. However it should be noted that this does not count as a full and proper calibration and the physical property values quoted in results section, should be viewed as comparative rather than absolute.

2.5.2 Indentation conditions

A MML Nanotest NTX instrument (Wrexham, UK), running Platform 2 software, was used (Fig 2.2).

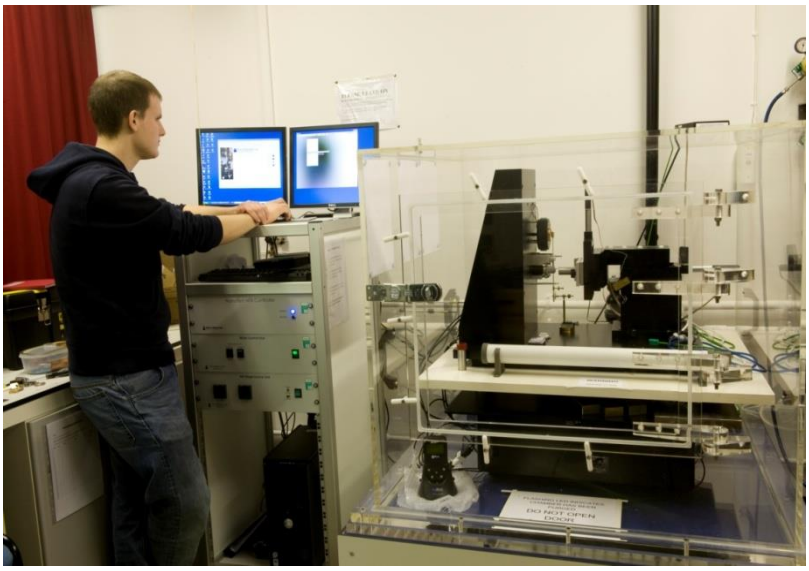

Figure 2.2 MML Nanotest NTX Instrument

Leaves: a 12.5 µm radius spherical nanoindenter tip was used, and the load applied was between 0.1-0.5 mN. The samples were fixed on a metallic stub with acrylic glue or mounted on double sided tape, on a glass slide. 9 leaves of Arabidopsis wild type Col-0 were cut in half, one half being used on adaxial side and the other half on abaxial side. When Arabidopsis mutants were compared with the correspondent wild type, 4 leaves for each were tested. A 10

indentations cycle required 2 hours, after this time, the sample dehydrates. The indented areas were chosen randomly, avoiding main veins, when leaves or stem or used as samples. The temperature inside the cabin was 22°C.

Seeds: Dry whole *Lepidium sativum* seeds (10 seeds) or imbibed seeds (6 seeds) with the testa removed were glued with Loctite 454 onto a metallic stub. Five to twenty indentations were performed on each seed with a 12.5 µm spherical indenter radius in a temperature regulated cabin at 22°C.

Maximum load applied was between 1- 5 mN. The loading and unloading time was 20 s, while the dwell period was 60 s. The surface was detected by the system measuring a load of 0.05 mN. The unloading cycle was interrupted for 60 s at 10% of max load for collection of thermal drift data.

The indented area was chosen approximatively in the same position for the subjected samples, e.g. smooth area for leaves (between veins) and the region above the radicle for seeds, closer to the micropylar end.

2.5.3 Statistical analyses of nanoindentation results

The significance of nanoindentation results was analysed using Minitab two-tail t-test, comparing the mean values for elastic modulus of seeds in different stages of imbibition (dry and 1 or 16 hours imbibed seeds) or the elastic modulus values for leaves of Arabidopsis mutants (altered cell wall composition) and wild types (Col-0 and QRT).

2.6 Micro X–ray Computed Tomography

X-ray computed tomography is a minimally-invasive structural imaging method that allows 3-D reconstruction of scanned objects. It involves the acquisition of a series of x-ray projection images at a known number of angular positions through 360 degrees.

Lepidium seeds (imbibed for 1, 3, 8, and 16 hours) were fixed for 16 h at 4 °C in neutral-buffered formalin (3.7% formaldehyde in 0.1 M phosphate buffer, pH 7.0). Fixed as well as unfixed seeds sampled at the same time points

were stained for 16 h in a solution containing 0.1% (w/v) iodine and 0.2% (w/v) potassium iodide in water, washed in water and dehydrated in 70% ethanol (3 washes for 10 minutes each) (Metscher, 2009). The staining was performed with a contrast agent (staining the starch) to improve the x-ray attenuation. The samples were scanned in 70% ethanol in 0.2 ml PCR tubes, (Extragene).

Eight replicate Lepidium seeds (imbibed or dry) were used for X–ray micro-CT scanning. Each seed was placed in a 0.2 ml micro-centrifuge tube and held in place with a conical-shaped polystyrene bung to minimize movement of the sample during the scan. Each sample was scanned for 40 minutes using a Phoenix Nanotom 180NF x–ray computed tomography system (GE Sensing and Inspection Technologies GmbH, http://www.ge-mcs.com) fitted with a molybdenum transmission target at maximum electron acceleration energy of 60 kV, a current of 140 µA, and 1200 projection images were acquired. The detector size during the scan was 2304 x 2304 pixels, resulting in a spatial resolution of 2.25 µm. Projection images were reconstructed using Datos|rec reconstruction software (GE Sensing and Inspection Technologies GmbH) using a filtered back-projection algorithm. Seed morphology was quantified using the automatic material calibration tool within StudioMax version 2.0 (Volume Graphics, http://www.volumegraphics.com), in which the background (air) and material (seed) are differentiated based on the grey value of individual voxels, which relates to the x–ray attenuation and hence material density of the sample. The intracellular pore space was quantified within a region of interest (created from a mask fitted to the surface of the seed) by summing the voxels defined as air from the calibration.

2.6.1 Statistical analyses of estimated endosperm thickness

In order to detect any significant difference between endosperm thicknesses in the same region or between regions (micropylar, lateral or peripheral), estimated values from micro-CT scans were compared using

GenStat two-way ANOVA statistical test. 30 Lepidium seeds were imaged at different time points of imbibition (1, 3, 8, 16 hours of imbibition), 6 seeds for each time point were analysed.

2.7 Environmental Scanning Electron Microscopy

An environmental scanning electron microscope (eSEM) allows imaging of a specimen in its natural state. eSEM images of Arabidopsis were taken in collaboration with Niki Weston (University of Nottingham). All images were taken with a Philips XL30 scanning electron microscope. An accelerating voltage of 10 kV was used for all images, the stage was cooled to ~ 3°C for all samples and a disk of wetted filter paper was used to keep samples hydrated. 80- 100% relative humidity was used during imaging.

2.8 Atomic Force Microscopy

The instrument used for the experiments was a D3000 (Veeco, Santa Barbara, CA) with a liquid cell for imbibed seeds. All measurements were conducted using triangular SiN4 cantilever tips (NP-Veeco) and were done at room temperature. The spring constant of the cantilevers was 0.58 N/m. Force curves were recorded with a velocity of 0.5 μm/s. Seeds of Arabidopsis wild type were studied in dry or 24 hours imbibed state. An online optical microscope was used to align the AFM tip at the appropriate points on the seed surface.

Single measurements were performed at different points along the seed. A reference hard glass surface was used. After the probe is in contact with the surface, any change in the *z* scanner displacement equals the change in cantilever deflection. On a softer surface, to reach the same cantilever deflection, the *z* scanner needs to displace a larger amount because of the indentation into the sample surface. The difference between the hard and soft surface gives the indentation into the sample surface.

2.9 Digital image correlation

To observe and create patterns successfully on Lepidium endosperms for the purpose of strain measuring, the mucilage and testa have been removed. A 20-50 μm chromium powder was used as labelling particles. Then, an optical acquiring system (CMOS camera) was used to obtain the object surface image. After series of images were obtained during the occurrence of the deformation, the performance of image matching was launched by selecting a subset (an n x n pixels multiple pixel region). Istra 4 was used to register images (taking picture every 10 minutes for 2 hours) and also to analyse the results.

In this case, the selected subset was pre-located due to unique grey level (light intensity distribution) in the featured pattern. After deformation, the displacement of the subset based on object surface image, could be exactly located by searching the certain light intensity distribution within subset. Since the subset on the deformed image was located, the displacement of the selected subset (region of interest) could be estimated, as a heat map.

2.10 Yeast1 hybrid screening

Yeast one hybrid system was used to analyse the relationship between *EXPA2* (At5g05290) promoter and the selected transcription factors: *BEE2* (At4g36540); *ATHB23* (At5g39760); *bHLH115* (At1g51070); *DOF2.1* (At2g28510).

2.10.1 Preparation of bait and prey constructs

The transcription factors were fused with GAL4 activation domain (GAL4AD) into a Gateway compatible plasmid (pDEST22, Invitrogen, Paisley, UK), conferring auxotrophy to tryptophan (W). Clones of these constructs were individually introduced into yeast *Saccharomyces cerevisiae* YM4271 (A mating type), creating a yeast library of 96-well plates. As a

negative control, GFP was used (GAL4BD:: prey GFP, Invitrogen, Paisley, UK).

An episomal plasmid to clone bait sequences (*EXPA2* promoter fragments) has been constructed (pTUY1H) (Castrillo et al., under revision). The constructs were introduced into *Saccharomyces cerevisiae* Y187 (α mating type).

Both strains are adenine deficient, so all the used media needed external adenine addition (Sigma Aldrich).

2.10.2 Preparation of bait and control prey constructs inoculum for mating

Fresh colonies from plates with minimal media (DOB) (MP Pharmaceuticals, 4024-012) lacking the respective amino acid: leucine (-L for pTUY1H) or tryptophan (-W), were used to inoculate 2 ml of YPAD medium, a complex medium to inhibit reversion of the *ade1* and *ade2* mutations (3.10.2.1) (10 ml tubes). They were grown at 28°C with shaking for 24 hours.

2.10.2.1 YPAD medium

Yeast extract (1%) 10 g/L

Peptone (2%) 20 g/L

Glucose (2%) 20 g/L

Agar (2%) 20 g/L

Adenine sulphate (0.004%) 40 mg/L

The pH was adjusted to 5.8 with HCl

2.10.3 Mating of yeast strains

200 µl of the bait cultures were mixed with 200 µl of prey cultures, using a 10 ml falcon. They were incubated at 28°C for 48 hours, without shaking.

2.10.4 Enrichment for mated (diploid) cells

From the mated cultures 50 µl were used to inoculate 1 ml of DOB-L-W, into a 10 ml falcon. They were grown at 48°C for 48 hours, with shaking.

2.10.5 3-AT titration of diploid cells

After two days of incubation, diploid enriched cultures were plated on appropriate media to score for diploids and positive bait-prey interactions. 5 µl of each inoculum were plated on the following media:

DOB-L-W;

DOB-L-W-H;

DOB-L-W-H + 1, 5, 10, 15, 30, 60 mM 3-AT (3-Amino-1, 2, 4-triazole, Sigma Aldrich, Gillingham, UK);

The inoculated plates were placed at 28°C for 7 days.

2.10.6 Scoring yeast growth

The yeast growth was scored between day 2 and 7, after plating. In order to know the appropriate media to be used in the real screening, the scoring at day 5 and the lowest 3-AT concentration inhibiting completely the yeast growth, were selected. Leaky expression of the *HIS3* reporter gene was titrated by using diploid cells obtained after mating the two yeast strains. 3-AT is a competitive inhibitor of the product of *HIS3* gene.

3. Results

3.1 Analysis of endosperm specific gene expression in Arabidopsis

3.1.1 Introduction

Bassel et al. (2011), using publically available transcriptome data, developed a network of correlation based interactions between genes expressed in Arabidopsis seeds during either germination or dormancy.

Representing the number of genes, the nodes within SeedNet were separated into 3 regions, associated either with germination (region 3) or dormancy (region 1), or the transition state between them (region 2). The interactions between genes are represented by edges. It was found that genes from regions 1 and 3 were associated with ABA or GA responses.

If Bassel et al. developed a coexpression network (Bassel et al., 2011), in 2013, Dekkers et al. developed two time-based networks comparing the genes expressed in the endosperm and embryo of Arabidopsis seeds: EndoNet and RadNet (Dekkers et al., 2013).

Interactive visualizations of both networks are available online at http://vseed.nottingham.ac.uk.

Using the Molecular Complex Detection (MCODE) algorithm (Bader & Hogue, 2003), Bassel et al. defined 136 modules of significantly interacting genes within SeedNet (Bassel et al., 2011).

In this study, one of these clusters, cluster 19, comprising endosperm specific genes was analysed (Figure 1.5). The most well-known gene of this cluster was *EXPA2* (At5g05290) (Figure 3.2). This gene has been analysed previously, being important in germination, as it encodes an expansin protein involved in endosperm weakening (Yan et al., 2014; Dubreucq et al., 2000; Ogawa et al., 2003; Penfield et al., 2006).

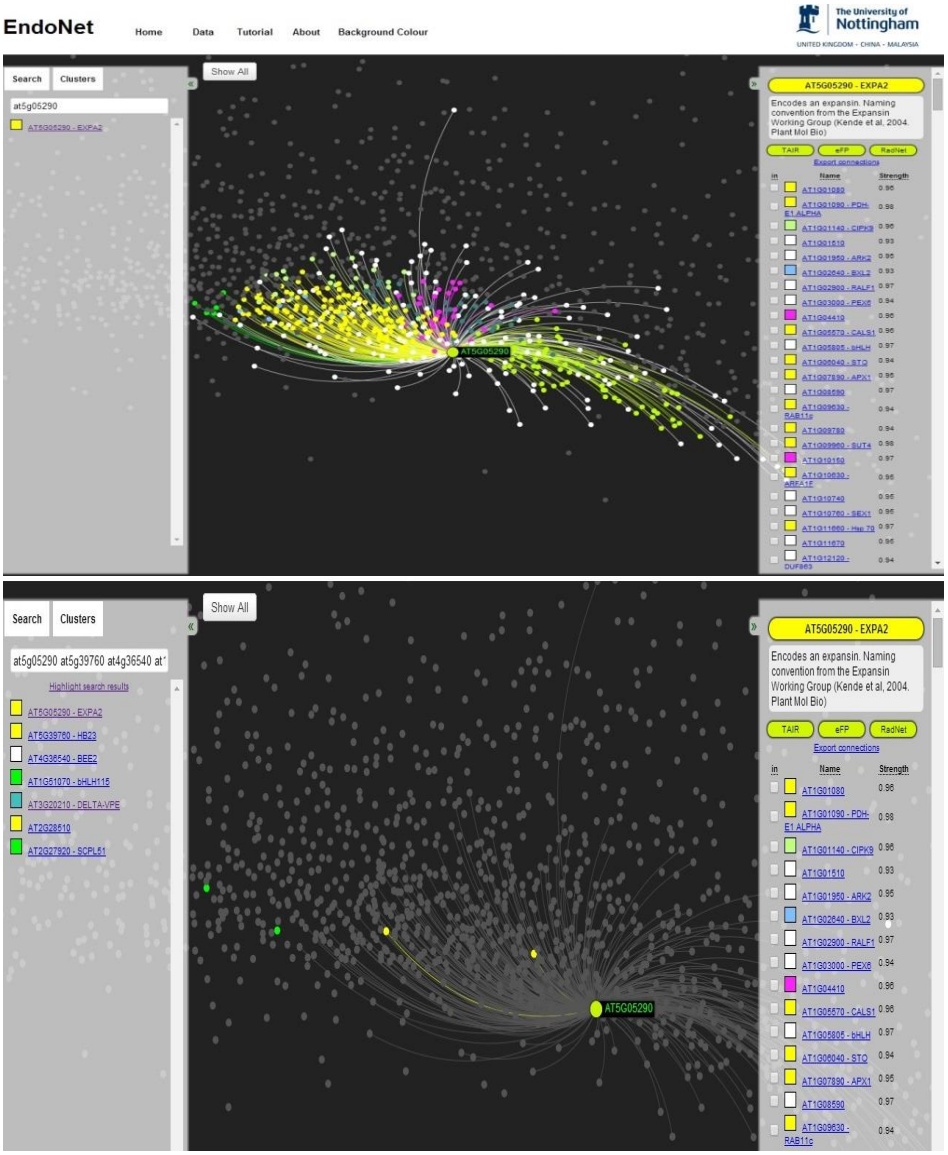

Figure 3.1 EndoNet, gene network, interactions represented by edges. *(A) EXPA2* first neighbours (genes from different clusters; each cluster is represented by a unique colour). *(B)* Genes observed in this study are highlighted.

The hypothesis tested by these analyses, was that the genes from the same cluster are coexpressed in terms of time and spatial distribution, within endosperm during germination. Based on gene networks prediction, it was tested if other genes from cluster 19 were following the same expression pattern as *EXPA2*, and also checked if there are gene interactions during germination between endosperm specific genes.

3.1.2 Analysis of the genetic function of *EXPA2* in germination

Previous work showed that *EXPA2* (Figure 3.2) is involved in the endosperm cell wall remodeling process during germination, that is a GA-inducible and micropylar endosperm specific gene (Ogawa et al., 2003; Yan et al., 2014; Endo et al., 2012).

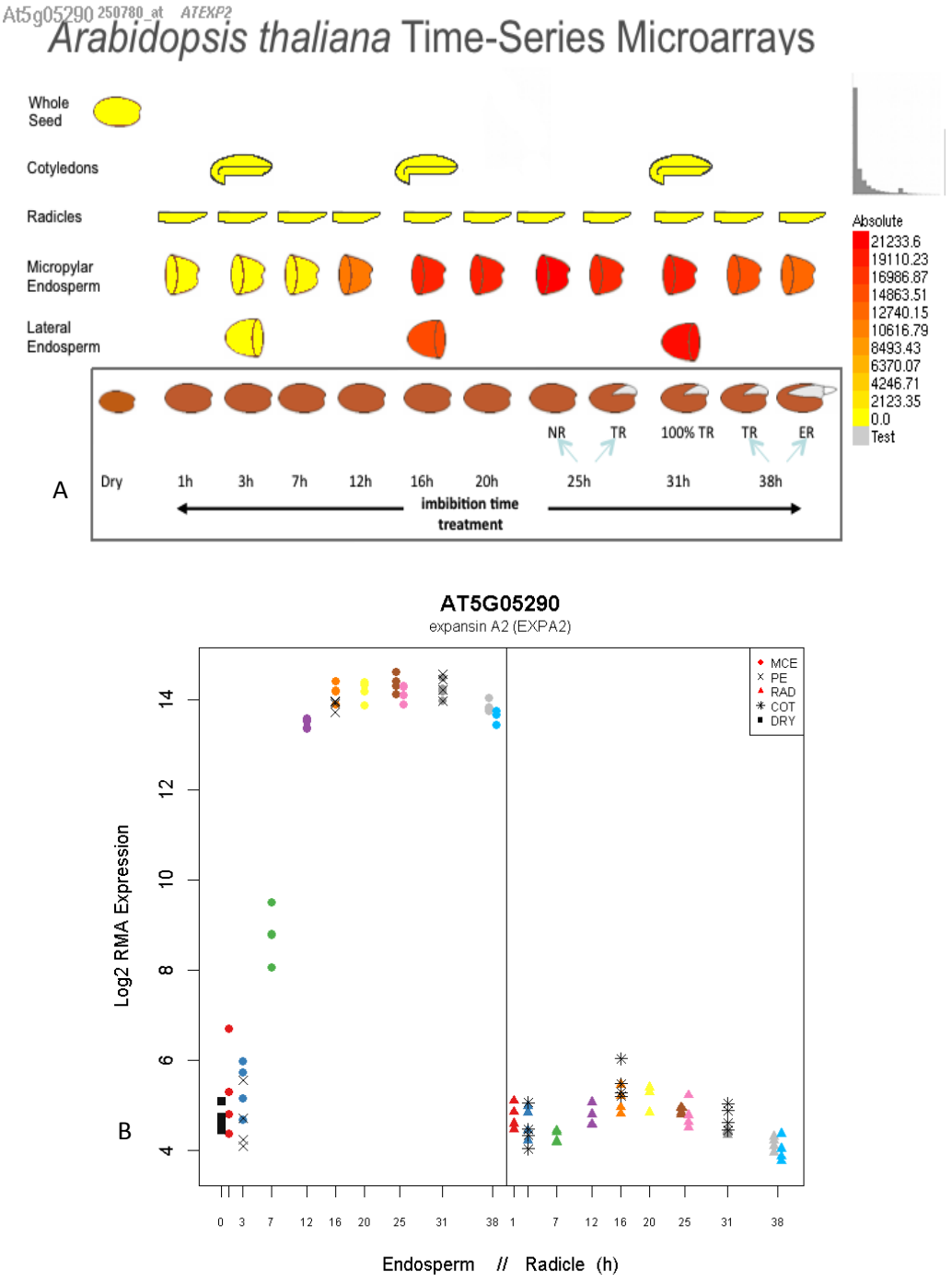

Figure 3.2 *(A) EXPA2* expression in the whole seed using Nottingham Seed eFP Browser. The scale bar indicates the expression of *EXPA2*, the highest expression level represented by red, and the lowest by yellow. (B) Expression of *EXPA2* in vSEED transcriptomic database. The above graphs show (on a log2 scale) the levels of RNA expression in Endosperm and Embryo during germination. MCE = Micropylar and Chalazal Endosperm, RAD = Radicle, PE = Rest of the endosperm, COT = Cotyledons, DRY = Whole dry seeds.

In Arabidopsis, an *expa2-2* mutant, containing a T-DNA insertion in the coding region (Salk_137972C) (Figure 3.3), was grown on media containing paclobutrazol (PAC), an inhibitor of GA biosynthesis. A germination assay was performed, on four different PAC concentrations. Testa rupture (%) was recorded over 7 days of imbibition (Figure 3.4).

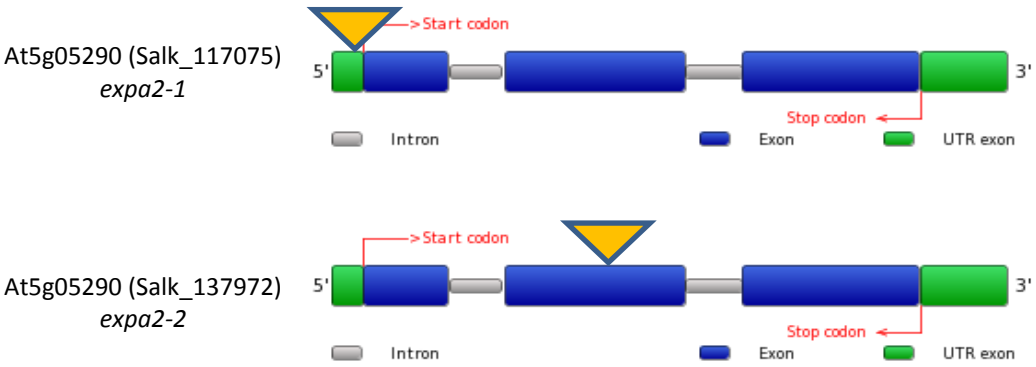

Figure 3.3 T-DNA lines with the insertion positions for *EXPA2* (At5g05290); *expa2-1* (Salk_117075) (Yan et al., 2014) and *expa2-2* (Salk_137972), used in this study.

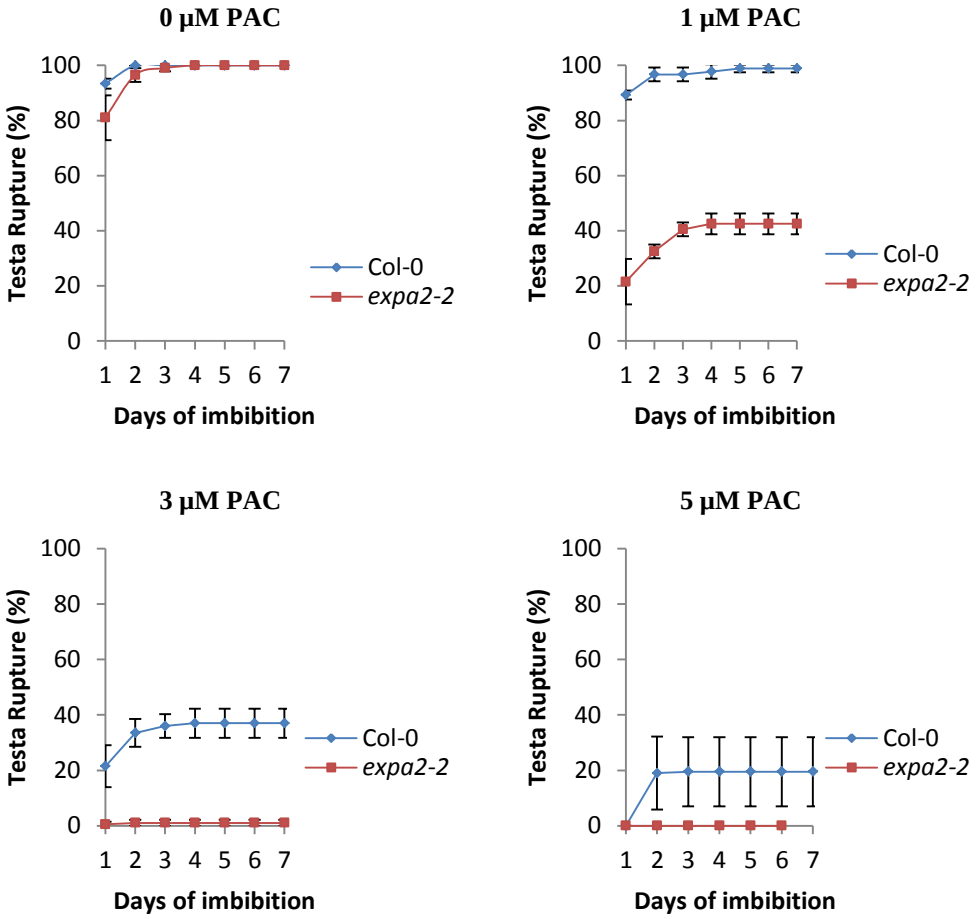

Figure 3.4 Graphs of testa rupture (%) of *expa2-2* in comparison with the wild type (Col-0), on 4 different PAC concentrations: 0, 1, 3, 5 µM. Error bars indicate the standard deviation.

The mutant seeds testa ruptured to a lower final level than the wild type on ½ MS, and as the PAC concentration was increased, the testa rupture of the mutant reduced progressively. The same pattern was followed when germination and establishment were scored, the mutant showing a reduced germination in comparison with the wild type, and a total absence of germination and establishment on higher concentration than 1 µM PAC.

3.1.3 Analysis of promoters of cluster 19 genes

Three first neighbours of *EXPA2* in cluster 19 were examined: one transcription factor *DOF2.1* (At2g28510) (Figure 3.5), *DELTA-VPE* (At3g20210) (Figure 3.6) and *SCPL51* (At2g27920) (Figure 3.7).

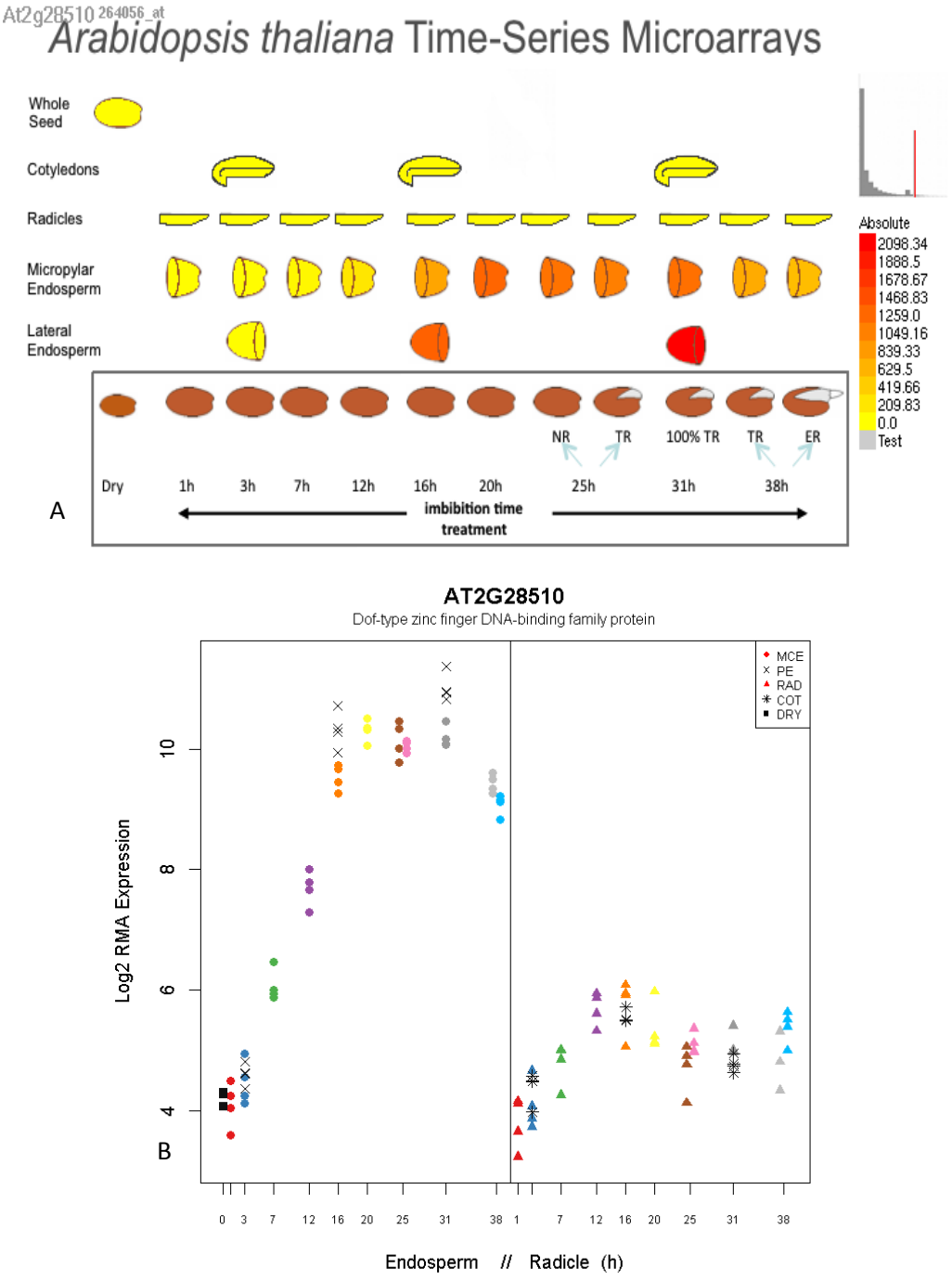

Figure 3.5 *(A) DOF2.1* expression in the whole seed using Nottingham Seed eFP Browser. The scale bar indicates the expression of *DOF2.1*, the highest expression level represented by red, and the lowest by yellow. *(B)* Expression of *DOF2.1* in vSEED transcriptomic database. The above graphs show (on a log2 scale) the levels of RNA expression in Endosperm and Embryo during germination. MCE = Micropylar and Chalazal Endosperm, RAD = Radicle, PE = Rest of the endosperm, COT = Cotyledons, DRY = Whole dry seeds.

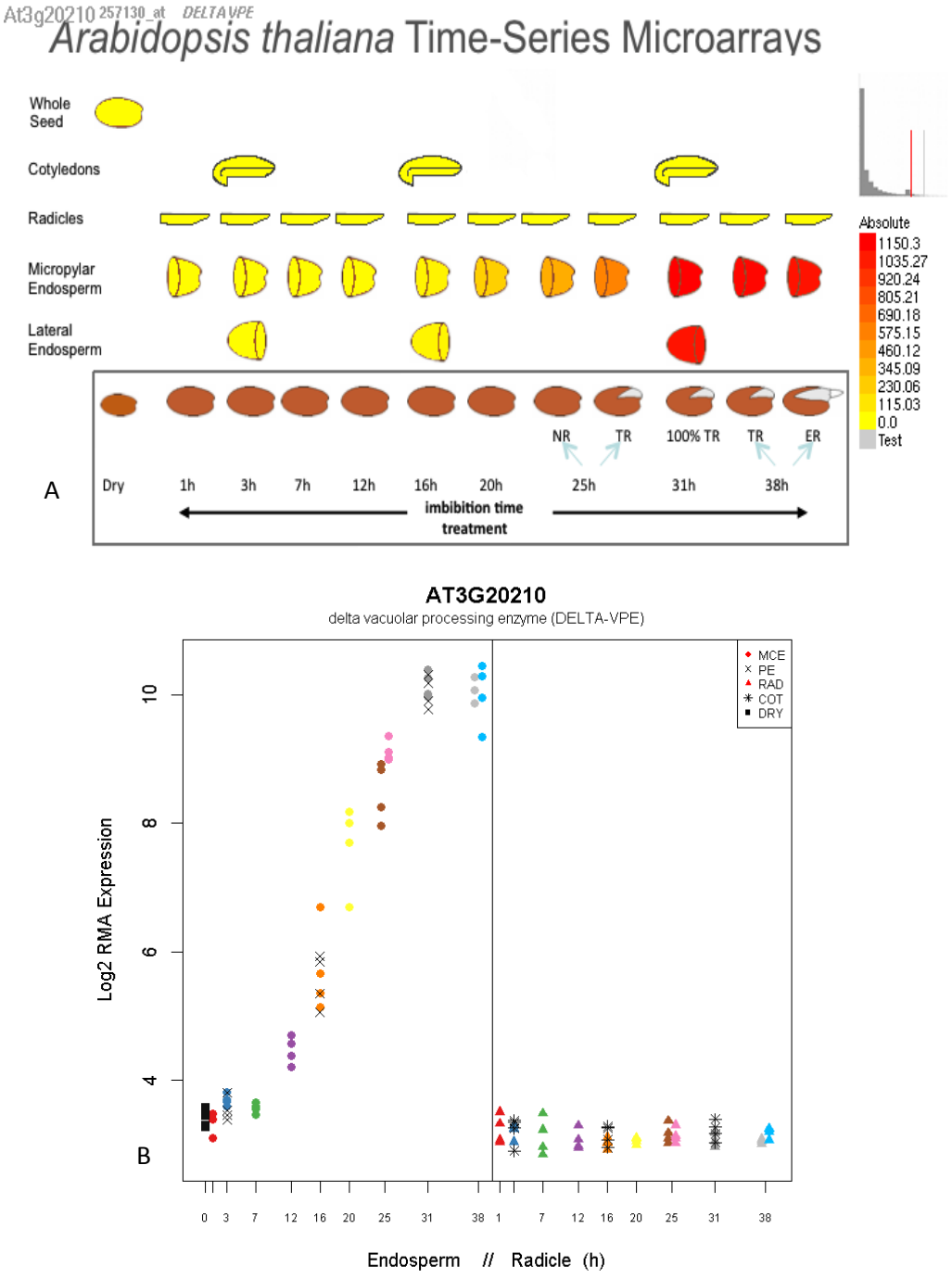

Figure 3.6 *(A) DELTA-VPE* expression in the whole seed according to Nottingham Seed eFP Browser. The scale bar indicates the expression of *DELTA-VPE*, the highest expression level represented by red, and the lowest by yellow. *(B)* Expression of *DELTA-VPE* in vSEED Transcriptomic data base. The above graphs show (on a log2 scale) the levels of RNA expression in Endosperm and Embryo during germination. MCE = Micropylar and Chalazal Endosperm, RAD = Radicle, PE = Rest of the endosperm, COT = Cotyledons, DRY = Whole dry seeds.

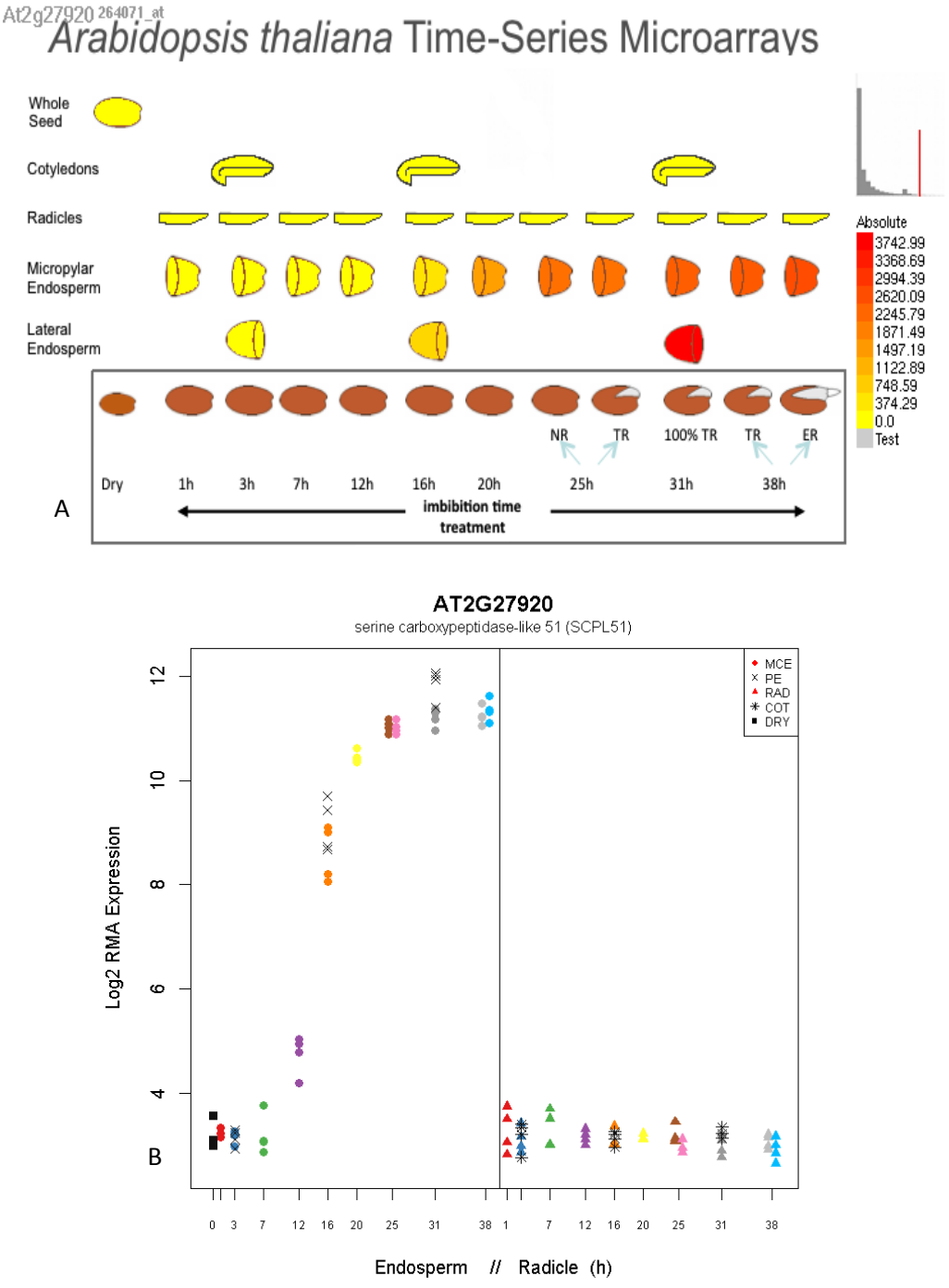

Figure 3.7 *(A) SCPL51* expression in Arabidopsis seed, using Nottingham vSEED eFP Browser. The scale bar indicates the expression of *SCPL51*, the highest expression level represented by red, and the lowest by yellow. *(B) SCPL51* is endosperm specific, according with vSEED transcriptomic database. The above graph shows (on a log2 scale) the levels of RNA expression in Endosperm and Embryo during germination. MCE = Micropylar and Chalazal Endosperm, RAD = Radicle, PE = Rest of the endosperm, COT = Cotyledons, DRY = Whole dry seeds.

GUS constructs were developed containing the promoter region of *DELTA-VPE* and *SCPL51*, consisting of 2000bp, upstream of the ATG, while for *DOF2.1* a translational fusion was performed, including the gene sequence as well. The fragments were amplified using specific GUS primers, into final vectors, using Gateway cloning kit (Figure 3.8).

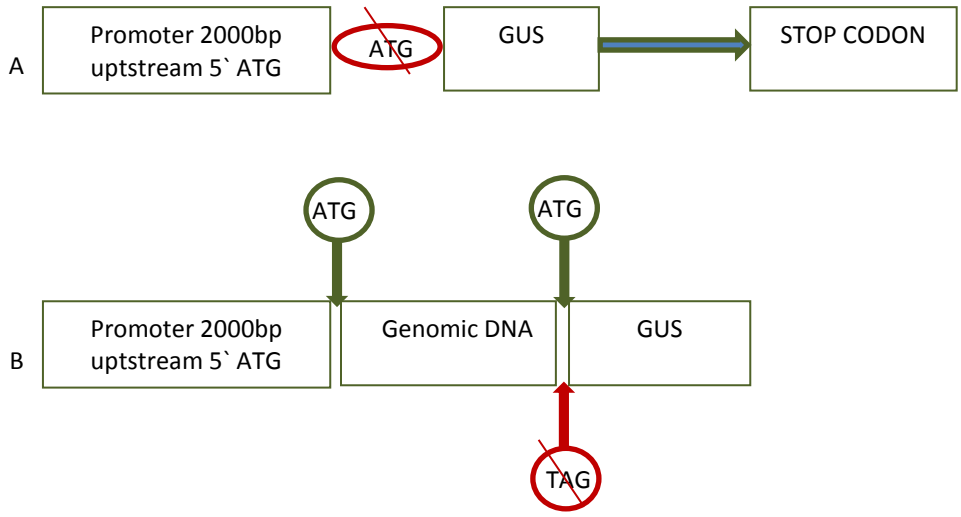

Figure 3.8 *(A)* Promoter fusion construct for *promDELTA-VPE::GUS* and *promSCPL51::GUS*; *(B)* Translation fusion construct for *promDOF2.1::DOF2.1::GUS*, the stop codon was removed to keep the C-terminal GUS protein in frame.

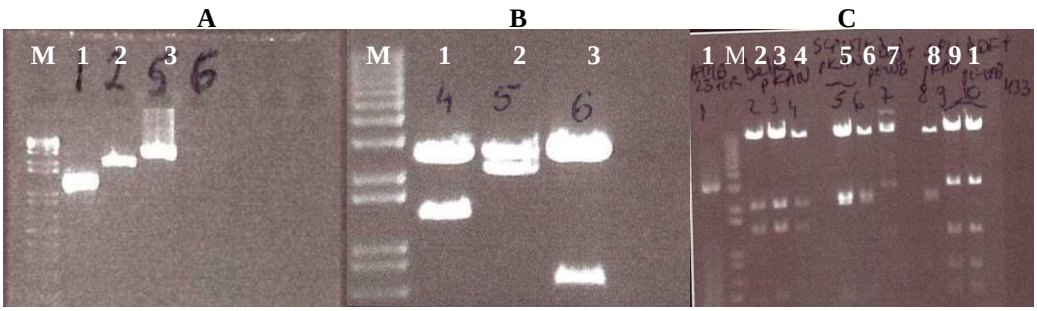

Figure 3.9 *(A)* PCR amplification products of promoters of: (*1*)- *DELTA-VPE* (1.3kb); (*2*)- *SCPL51* (2kb); (*3*)- *DOF2.1* (3.7kb) *(B)* Digestion results with BsrGI of the promoters cloned into donor vector pDONR221 : pDONR221+ *DELTA-VPE (1)*; pDONR221+*SCPL51 (2)*; pDONR221+*DOF2.1 (3) (C)* Digestion products with BsrGI of promoters cloned into final vector pKAN and pGWB433, respectively : *(2)*, (*3*), *(4)* - pKAN+*DELTA-VPE*; (*5*), (*6*), (*8*)- pKAN +*SCPL51*; (*7*), (*9*), (*10*)- pGWB433+*DOF2.1*; M- DNA ladder 1kb+.

The transgenic seeds were used in experiments to confirm the prediction of SeedNet that the selected genes are endosperm specific and to analyse their individual expression characteristics.

3.1.4 Analysis of promoter expression of cluster 19 genes in the endosperm

3.1.4.1 Reporter expression driven by cluster 19 promoters

In order to define the spatial and temporal expression of the promoter of *DELTA-VPE*, *DOF 2.1* and *SCPL51*, a series of experiments were performed. Seeds of *promDELTA-VPE::GUS*, *promDOF2.1::DOF2.1::GUS* and *promSCPL51::GUS* were imbibed on ½ MS for 24 hours and then separated from the embryo and stained overnight. The lines with the most consistent and uniform expression were selected to be used in further experiments.

Four independent transgenic lines for each construct were analysed; fifty seeds per each replicate, with four replicates for each line, counted at 30, 34 and 48 hours of imbibition (Figure 3.10).

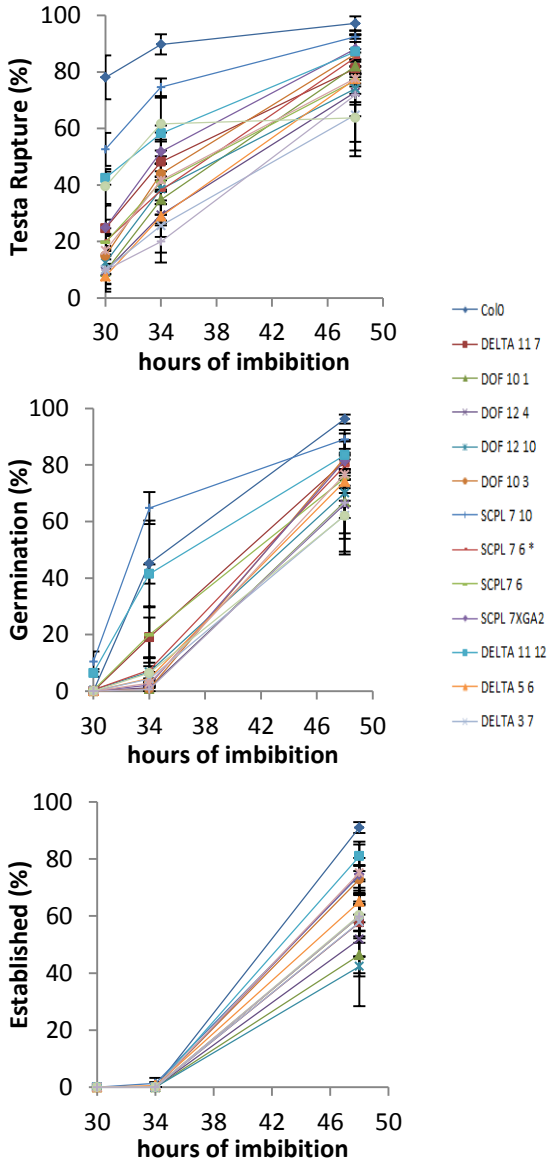

Figure 3.10 Germination assay for the promoter::GUS lines used in the endosperm specific experiments. 4 lines with 4 replicates for each construct were analysed. The germination was scored at 3 different time points: 30, 34 and 48 hours of imbibition. Error bars represent the standard deviation.

The seeds were in the same stage of after-ripening (grown and harvested at the same time) and could therefore be directly compared. The endosperms were dissected after 24 hours of imbibition, and stained overnight, to observe the reporter gene activity (Figure 3.11).

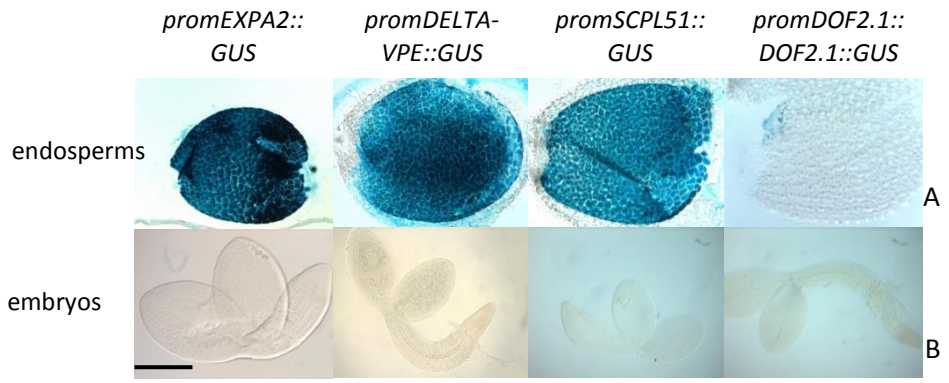

Figure 3.11 Expression properties of the *promEXPA2::GUS*, *promDELTA-VPE::GUS*, *promSCPL51::GUS* and *promDOF2.1::DOF2.1::GUS*. Seeds of transgenic plants were imbibed for 24h, after which seed coat (testa and endosperm *(1)* and embryo *(2)* were separated and assessed for GUS accumulation by staining. The seed coat was bleached to ease visualisation of stain; this treatment did not affect the GUS expression. Scale bar= 25μm.

The expression of GUS driven by all of the promoters could be observed in the endosperm, but not in the embryo. While for *EXPA2*, *DELTA-VPE* and *SCPL51* the expression was visible in the entire endosperm, for the translational fusion of the transcription factor *DOF2.1* an isolated expression could be observed, in the micropylar region.

3.1.4.2 Effect of ABA/GA on expression driven by cluster 19 promoter GUS lines in seeds

To understand the effect of ABA and GA on the expression of promoters of *DELTA-VPE*, *SCPL51* and *DOF2.1*, seeds containing the reporter gene linked to promoters of these genes, were plated on media containing ABA or GA. GA was previously shown to control *EXPA2* activity, its expression being increased by external GA addition, while ABA has no effect on *EXPA2* expression (Ogawa et al., 2003), but nothing is known about the other three genes from cluster 19.

Seeds of *promDELTA-VPE::GUS*, *promDOF2.1::DOF2.1::GUS*, *promSCPL51::GUS* were plated on ½ MS media plus 10 μM ABA, for 5 days, at which point the endosperms were separated from embryos and stained for 24 hours to observe GUS activity (Figure 3.12).

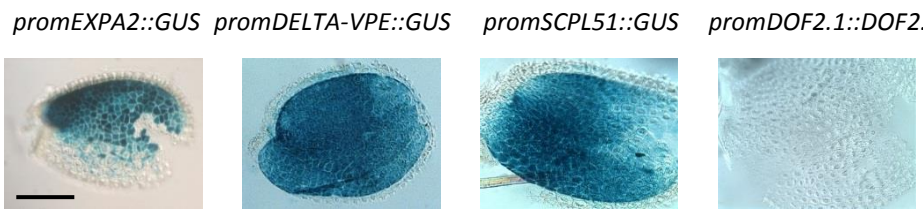

Figure 3.12 GUS expression in the promoters' response to ABA treatment: *promEXPA2::GUS*, *promDELTA-VPE::GUS*, *promSCPL51::GUS*, *promDOF2.1::DOF2.1::GUS*. Seeds were imbibed for 5 days on ½ MS+ 10 μM ABA, dissected at that moment and stained for 24 hours. *promSCPL51::GUS* and *promDELTA-VPE::GUS* were expressed all over the endosperm, but no expression could be detected on *promDOF2.1::DOF2.1::GUS* containing seeds. Image courtesy of Julietta Marquez for *promEXPA2::GUS*. Scale bar= 25μm.

As shown in figure 3.12, the activity of *promEXPA2::GUS*, *promDELTA-VPE::GUS* and *promSCPL51::GUS* was not affected by ABA. The conclusion would be that promoter driven expression of these genes is ABA insensitive. No expression could be observed for *promDOF2.1::DOF2.1::GUS*, either because the expression was at an undetectable level or it was inhibited by ABA presence.

To test the response to GA, after a short imbibition period of 1 hour, half of the dissected endosperms were stained, while the other half was plated on media containing 25 μM GA, for 24 hours before being stained.

The results, shown in figure 3.13, indicate that *promEXPA2::GUS* could be observed in the micropylar endosperm after one hour of imbibition and that when GA was added in the media, its expression spread in the entire endosperm. *promDELTA-VPE::GUS* was expressed in the whole endosperm after 1 hour of imbibition while, and its expression did not require GA, while *promSCPL51::GUS* was expressed only if external GA was added into media. *promDOF2.1::DOF2.1::GUS* expression could not be detected.

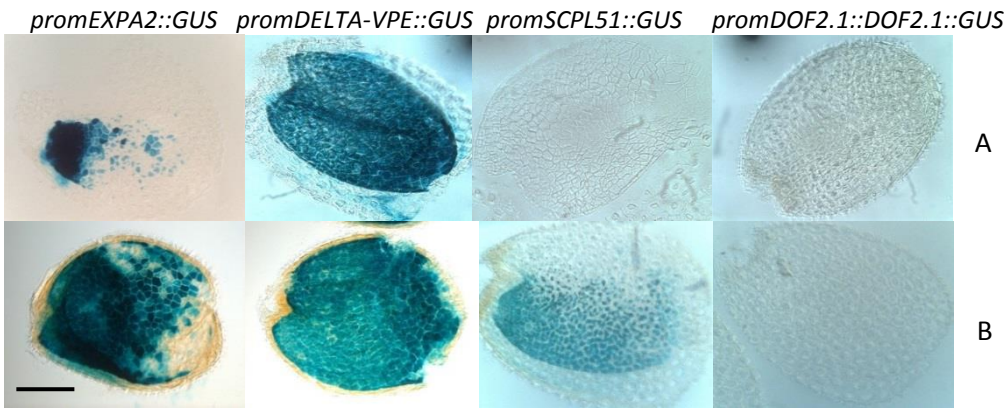

Figure 3.13 GUS expression for *promEXPA2::GUS*, *promDELTA-VPE::GUS*, *promSCPL51::GUS*, *promDOF2.1::DOF2.1::GUS* as a response to GA. Endosperms were separated from embryos after 1 hour of imbibition and placed for 24 hours on ½ MS *(A)* or on ½ MS + 25 µM GA *(B)*. Scale bar= 25µm.

Also, a GA-deficient mutant *ga1-3* was crossed with lines of, *promDELTA-VPE::GUS*, *promDOF2.1::DOF2.1::GUS* and *promSCPL51::GUS*. Homozygous *ga1-3* mutant seeds containing promoter constructs were plated on ½ MS media including an ABA-inhibitor, Norflurazon. The results, represented in figure 3.14, showed a constitutive expression of *promDELTA-VPE::GUS*, and *promSCPL51::GUS* on Norflurazon.

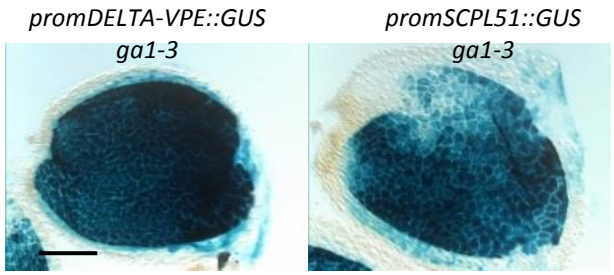

Figure 3.14 Endosperms stained immediately after separation from embryos, after 30 hours of imbibition on 1/2MS + 50 µM Norflurazon. *promDELTA-VPE::GUS ga1-3*; *promSCPL51::GUS ga1-3*. Scale bar= 25 µm

3.1.4.3 Is an embryo signal controlling endosperm gene expression?

In order to answer to the above question, separations of the endosperms from the embryos at different time points were performed. The endosperms were stained straight away or plated for 24 hours on respective media.

The subjected seeds were containing: *promDELTA-VPE::GUS*, *promSCPL51::GUS*, *promEXPA2::GUS* in Col-0 background, or the mutants with GA deficient background: *promDELTA-VPE::GUS ga1-3*, *promSCPL51::GUS ga1-3* and *promEXPA2::GUS ga1-3*.

The first time point, when the separation was possible without destroying the endosperm structure, was between 15-30 minutes of imbibition on ½ MS or ½ MS + 25 μM GA, followed by the separations of the endosperm from embryo. Half of the dissected endosperms were stained immediately after separation from embryos, while the other half was plated on ½ MS media, or ½ MS + 25 μM GA for 24 hours and then stained (Figure 3.15).

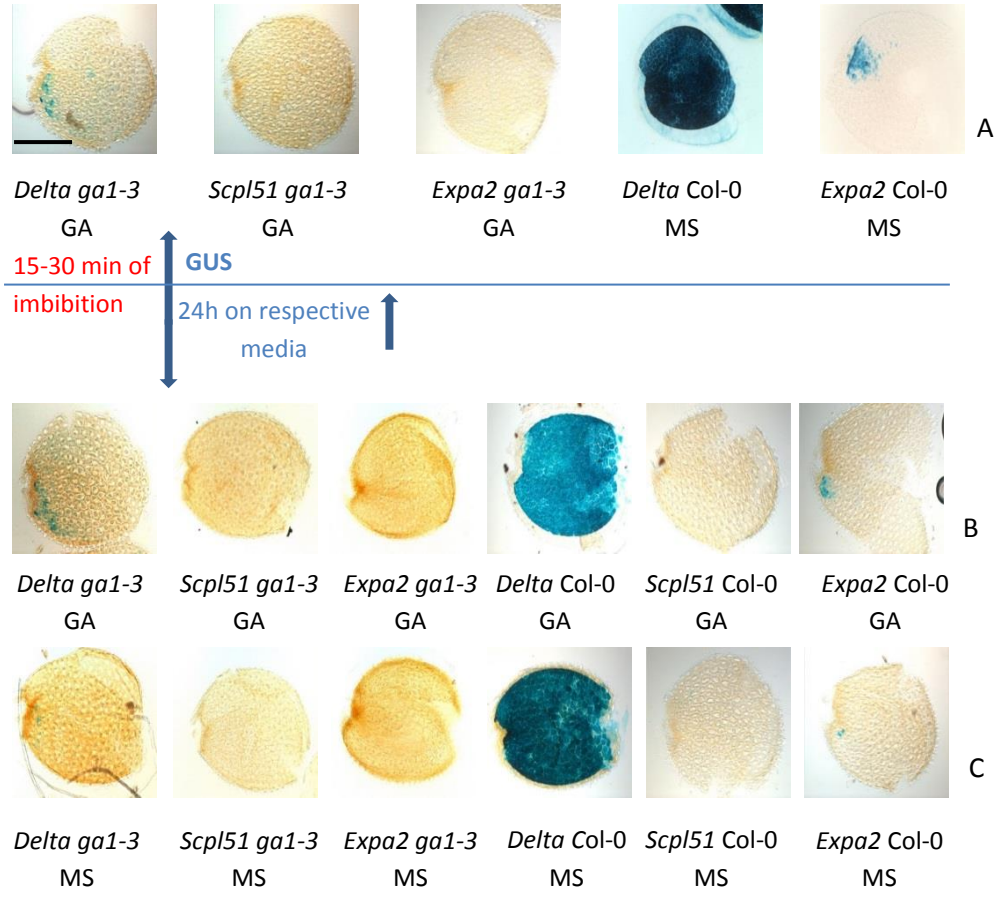

Figure 3.15 GUS expression in endosperm separated after 15-30 minutes of imbition on ½ MS (Col-0 background) or ½ MS+ 25 µM GA (*ga1-3* background). *(A)* Endosperms stained immediately after separation from embryos. *(B)* Separated endosperms were plated on ½ MS + 25 µM GA for 24 hours, then stained. *(C)* Separated endosperms were plated on ½ MS for 24 hours, followed by staining. *Delta ga1-3* represents *promDELTA-VPE::GUS ga1-3*; *Delta* Col-0 is *promDELTA-VPE::GUS* in Col-0 background; *Scpl51 ga1-3* used for *promSCPL51::GUS ga1-3*; *Scpl51* Col-0 is *promSCPL51::GUS* in Col-0 background; *Expa2 ga1-3* represents *promEXPA2::GUS ga1-3*; *Expa2* Col-0 is *promEXPA2::GUS* in Col-0 background. Scale bar= 25 µm

In Col-0 background only the activity of *promDELTA-VPE::GUS* and *promEXPA2::GUS*, could be visible after 15 minutes of imbibition. The promoter expression of *DELTA-VPE*, could be observed in the entire endosperm while, for *EXPA2* only in few cells of the micropylar endosperm.

The expression of *promDELTA-VPE::GUS* in *ga1-3* background after 15-30 minutes of imbibition on media containing GA, could be observed in the micropylar endosperm. Also when the separated endosperms were plated for 24 hours on media with GA a similar expression could be noticed. When there

was no GA in the media, a scarce expression could be observed in few cells of the micropylar endosperm.

No GUS expression could be seen for *promSCPL51::GUS* and *promEXPA2::GUS* in *ga1-3* background, suggesting that their expression might require endogenous GA or an embryonic signal that is developed later than 15-30 minutes of imbibition.

The next time point for endosperm separation from embryo was between 30 and 45 minutes. The results are summarized in the figure 3.16.

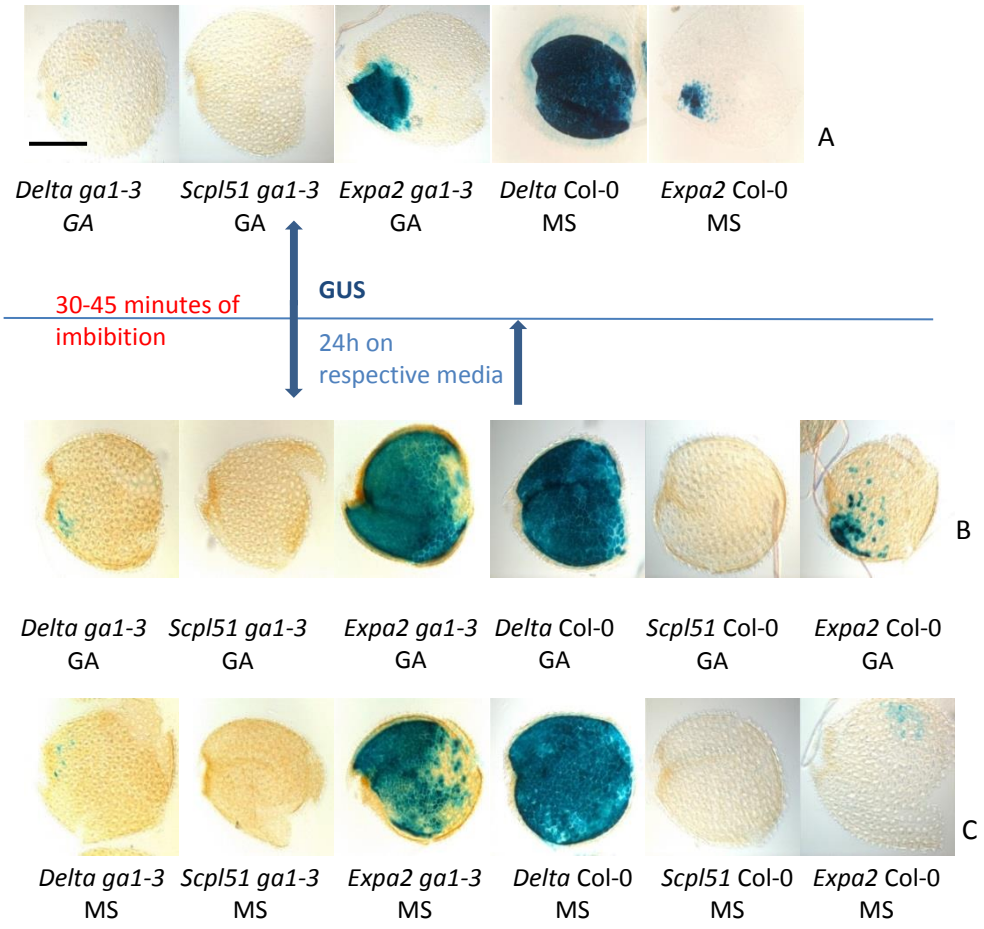

Figure 3.16 GUS expression in endosperm separated after 30-45 minutes of imbition on ½ MS for Col-0 background and ½ MS + 25 µM GA for *ga1-3* background. *(A)* Endosperms stained immediately after separation from embryos. *(B)* Separated endosperms were plated on ½ MS + 25 µM GA for 24 hours, then stained. *(C)* Separated endosperms were plated on ½ MS for 24 hours, followed by staining. *Delta ga1-3* represents *promDELTA-VPE::GUS ga1-3*; *Delta* Col-0 is *promDELTA-VPE::GUS* in Col-0 background; *Scpl51 ga1-3* used for *promSCPL51::GUS ga1-3*; *Scpl51* Col-0 is *promSCPL51::GUS* in Col-0 background; *Expa2 ga1-3* represents *promEXPA2::GUS ga1-3*; *Expa2* Col-0 is *promEXPA2::GUS* in Col-0 background. Scale bar= 25 µm

At 30-45 minutes of imbibition, the expression of *promDELTA-VPE::GUS* in *ga1-3* background could be observed in few cells of the micropylar region either if the endosperms were stained directly after the separation from the embryo, or plated for 24 hours on ½ MS media with or without GA. For *promSCPL51::GUS ga1-3*, no activity was observed.

The GUS expression for *promEXPA2::GUS* in *ga1-3* in the separated endosperms was concentrated in the micropylar region of the endosperm when the endosperms were stained straight after the separation. After 24 hours on ½ MS media with GA, the expression spread all over the endosperm, while laying only on ½ MS the expression was localized everywhere but not in the chalazal endosperm.

For *promDELTA-VPE::GUS* in Col-0 background, GUS expression was seen all over the endosperm cells, regardless if endosperms were stained straight after separations from embryos, or plated on ½ MS with or without GA for 24 hours. For *promEXPA2::GUS* in Col-0, a variation of GUS expression could be seen between endosperm from GA supplemented media, underlying the effect of GA on *EXPA2* activity.

After one 45-60 minutes of imbibition on ½ MS media supplemented with GA, the endosperms were separated and either stained directly for 24 hours, both placed on ½ MS or ½ MS + GA for 24 hours, and then stained (Figure 3.17).

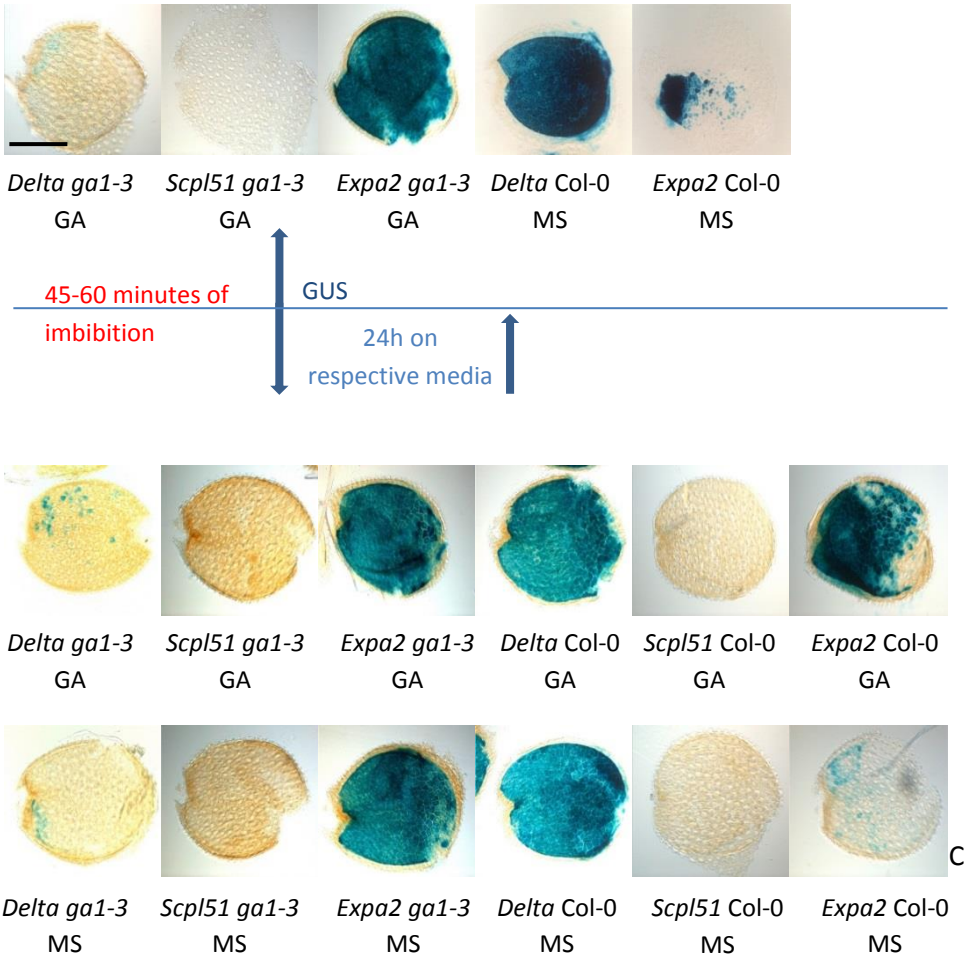

Figure 3.17 GUS expression in endosperm separated after 45-60 minutes of on ½ MS for Col-0 background and ½ MS + 25 µM GA for *ga1-3* background. *(A)* Endosperms stained immediately after separation from embryos. *(B)* Separated endosperms were plated on ½ MS + 25 µM GA for 24 hours, then stained. *(C)* Separated endosperms were plated on ½ MS for 24 hours, followed by staining. *Delta ga1-3* represents *promDELTA-VPE::GUS ga1-3*; *Delta* Col-0 is *promDELTA-VPE::GUS* in Col-0 background; *Scpl51 ga1-3* used for *promSCPL51::GUS ga1-3*; *Scpl51* Col-0 is *promSCPL51::GUS* in Col-0 background; *Expa2 ga1-3* represents *promEXPA2::GUS ga1-3*; *Expa2* Col-0 is *promEXPA2::GUS* in Col-0 background. Scale bar= 25 µm

After 45-60 minutes of imbibition, GUS expression was detected only in the separated endosperms of *promDELTA-VPE::GUS* and *promEXPA2::GUS* in *ga1-3* and Col-0 background. For *promDELTA-VPE::GUS ga1-3*, GUS activity could be detected only in the micropylar endosperm, while in Col-0 background in the whole endosperm, regardless the treatment.

For *promEXPA2::GUS ga1-3*, GUS expression was present in each single cell of the endosperm with or without treatment, while in Col-0 an isolated expression in the micropylar endosperm was noticed on media without GA.

The GUS expression was seen in the whole endosperm when *promEXPA2::GUS* in Col-0 was plated on GA supplemented media. No GUS expression could be seen in the endosperms of *promSCPL51::GUS ga1-3*.

3.1.4.4 Temporal GUS expression for cluster 19 promoters

Four different time points were chosen: 6, 12, 18, 24 hours of imbibition, before the endosperms were separated from embryos and stained, for seeds containing *promDELTA-VPE::GUS*, *promSCPL51::GUS*, *promEXPA2::GUS*, in Col-0 or *ga1-3* background.

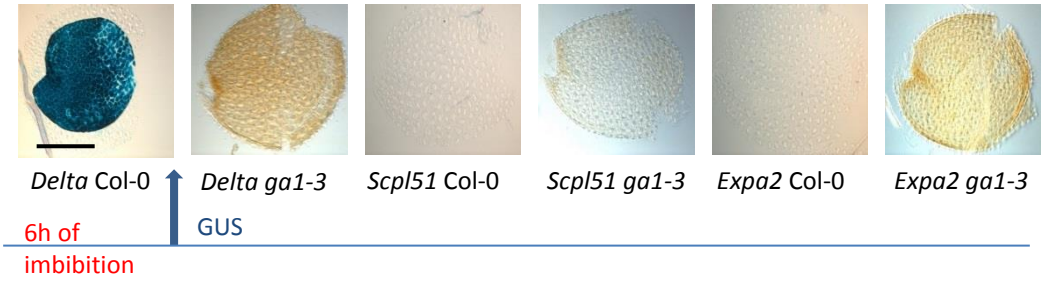

Figure 3.18 GUS expression in separated endosperms after 6 hours of imbibition on ½ MS, for Col-0 background or ½ MS + 25 µM GA, for *ga1-3* background; *promDELTA-VPE::GUS* in *ga1-3* background (*Delta ga1-3*) and Col-0 (*Delta* Col-0); *promSCPL51::GUS* in *ga1-3* background (*Scpl51 ga1-3*) and Col-0 background (*Scpl51* Col-0); *promEXPA2::GUS* in *ga1-3* background (*Expa2 ga1-3*) or Col-0 background (*Expa2* Col-0). Scale bar= 25 µm.

No GUS expression was observed in *promEXPA2::GUS* or *promSCPL51::GUS* in Col-0 or *ga1-3* background after 6 hours of imbibition on respective media. *promDELTA-VPE::GUS* could be noticed in the entire endosperm, after 6 hours of imbibition on ½ MS for Col-0 background, while no activity was observed for *ga1-3* background lines (Figure 3.18).

After 12 hours of imbibition on respective media, the endosperms were separated from the embryos and stained. The results are shown in the figure 3.19.

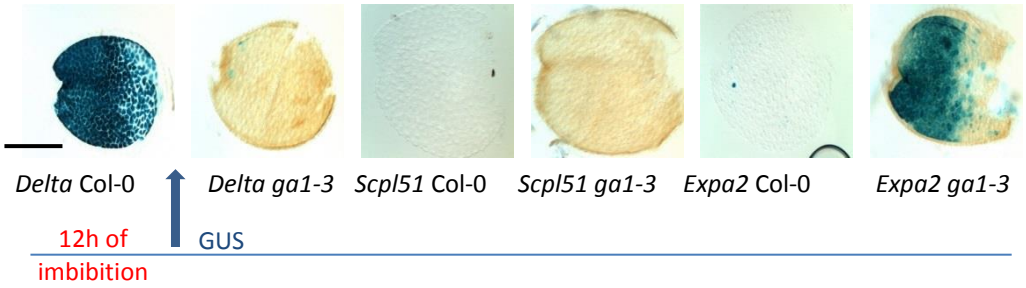

Figure 3.19 GUS expression in separated endosperms after 12 hours of imbibition on ½ MS, for Col-0 background or ½ MS + 25 µM GA, for *ga1-3* background*; promDELTA-VPE::GUS* in *ga1-3* background (*Delta ga1-3*) and Col-0 (*Delta* Col-0); *promSCPL51::GUS* in *ga1-3* background (*Scpl51 ga1-3*) and Col-0 background (*Scpl51* Col-0); *promEXPA2::GUS* in *ga1-3* background (*Expa2 ga1-3*) or Col-0 background (*Expa2* Col-0). Scale bar= 25 µm.

The GUS expression in *promDELTA-VPE::GUS*, in Col-0 background, could be noticed in all the cells of the endosperm, while in *ga1-3* background, an isolated expression could be observed in few cells of the micropylar endosperm. No GUS activity was observed for *promSCPL51::GUS*, in both backgrounds Col-0, *ga1-3*, respectively. For *promEXPA2::GUS*, only few cells of the endosperm showed GUS expression, in the Col-0 background, while for *ga1-3* background, the GUS expression was present in all the endosperm cells, except the chalazal region.

The third chosen time point to dissect the seeds separating the endosperm from embryo was at 18 hours of imbibition. The observed GUS activity is displayed in figure 3.20.

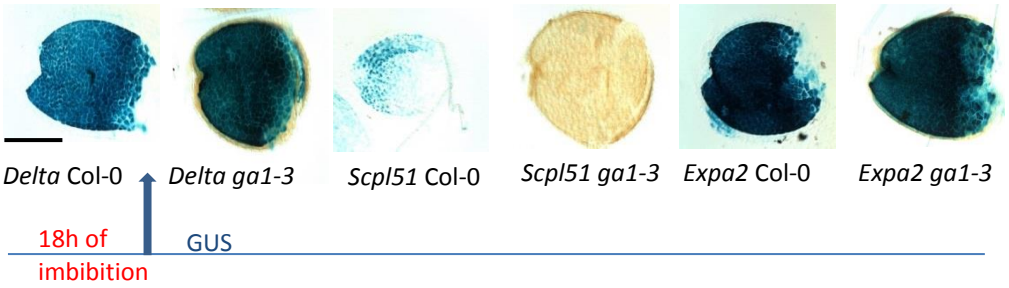

Figure 3.20 GUS expression in separated endosperms after 18 hours of imbibition on ½ MS, for Col-0 background or ½ MS + 25 µM GA, for *ga1-3* background; *promDELTA-VPE::GUS* in *ga1-3* background (*Delta ga1-3*) and Col-0 (*Delta* Col-0); *promSCPL51::GUS* in *ga1-3* background (*Scpl51 ga1-3*) and Col-0 background (*Scpl51* Col-0); *promEXPA2::GUS* in *ga1-3* background (*Expa2 ga1-3*) or Col-0 background (*Expa2* Col-0). Scale bar= 25 µm.

After 18 hours of imbibition, expression of *promDELTA-VPE::GUS* and *promEXPA2::GUS* could be observed fully expressed in both backgrounds Col-0 and *ga 1-3*, in all the endosperm cells. The *promSCPL51::GUS* expression was noticed only in the Col-0 background, in the micropylar and lateral endosperm, but no activity was detected in *ga1-3* background.

The latest time point was 24 hours of imbibition. Endosperms were separated and stained, and the results are summarized in the below images (Figure 3.21).

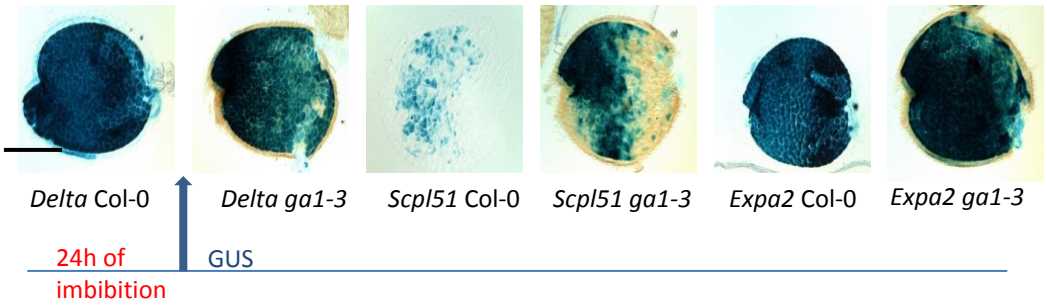

Figure 3.21 GUS expression in separated endosperms after 24 hours of imbibition on ½ MS for Col-0 background or ½ MS + 25 µM GA, for *ga1-3* background; *promDELTA-VPE::GUS* in *ga1-3* background (*Delta ga1-3*) and Col-0 (*Delta* Col-0); *promSCPL51::GUS* in *ga1-3* background (*Scpl51 ga1-3*) and Col-0 background (*Scpl51* Col-0); *promEXPA2::GUS* in *ga1-3* background (*Expa2 ga1-3*) or Col-0 background (*Expa2* Col-0). Scale bar= 25 µm.

GUS expression could be seen in the whole endosperm for *promDELTA-VPE::GUS* and *promEXPA2::GUS*, in both backgrounds, Col-0 and *ga1-3*, while for *promSCPL51::GUS*, GUS expression was concentrated in the micropylar and lateral endosperm for both backgrounds, Col-0 and *ga1-3*, respectively.

3.1.4.5 Analysis of the genetic regulation of endosperm function by cluster 19 transcription factors

In addition to defining the expression patterns of cluster 19 genes, genetic interactions were probed by analyzing the regulation of germination by transcription factors within the cluster. These include members of the bHLH, C_2C_2 and ATH families (Bassel et al., 2011).

Germination of after-ripened mutant seeds (Figure 3.22) was analyzed in the presence or absence of PAC; this approach was used to probe the relationship between transcription factors function and requirement of GA for their expression.

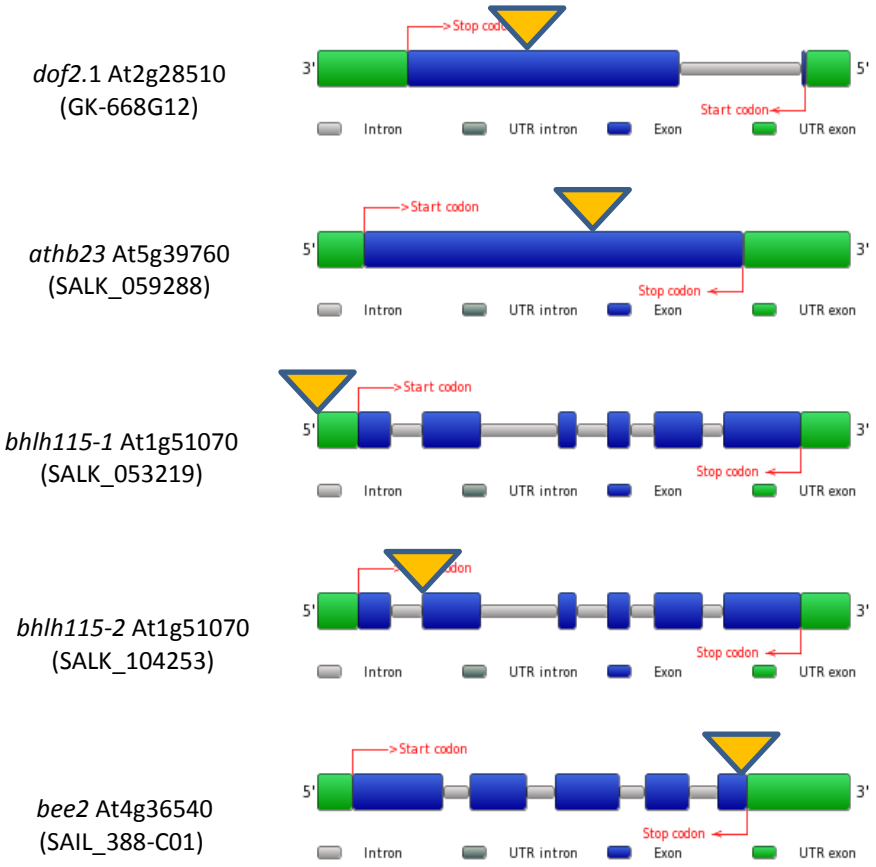

Figure 3.22 T-DNA lines used in this study with the insertion positions for cluster 19 transcription factors: *DOF2.1*, *ATHB23*, *bHLH115* and *BEE2*.

The results show that the *athb23* mutant is relatively insensitive to PAC, whilst *dof2.1*, and *athb23dof2.1* appeared more or equally sensitive than the wild type, Col-0 (Figure 3.23).

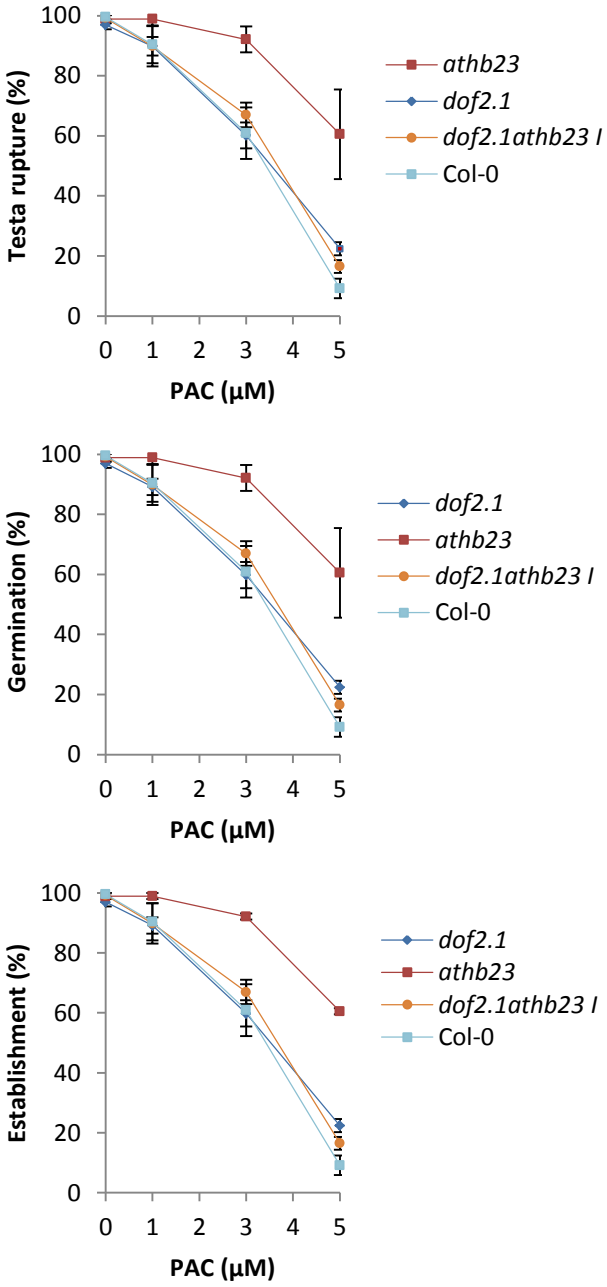

Figure 3.23 Germination assays for *athb23*, *dof2.1* and the double mutant *athb23dof2.1*. Germination was scored over 7 days, on 4 different PAC concentrations: 0, 1, 3, 5 µM. Four replicates of minimum 50 seeds for each replicate were used for each mutant. Error bars represent the standard deviation.

For *bee2*, *bhlh115-2* and the double mutant, *bee2bhlh115-2*, the same experiment was performed. *bee2* and *bee2bhlh115-2* germinated much slower

in comparison with the wild type, Col-0, while *bhlh115-2* germinated faster (Figure 3.24).

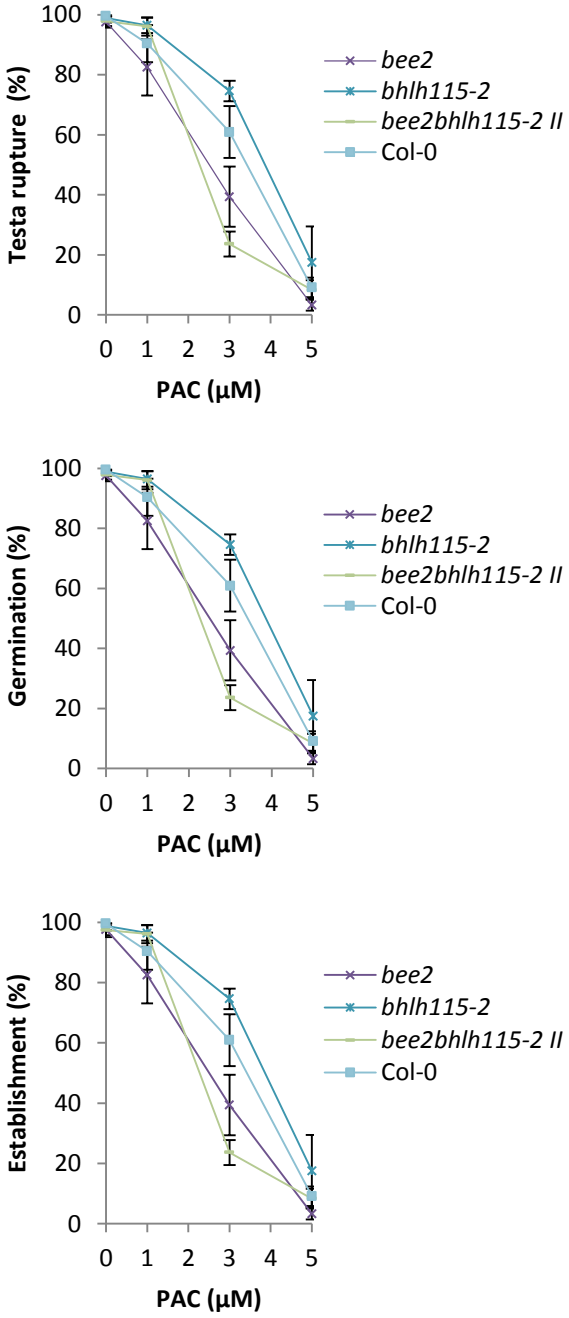

Figure 3.24 Germination assay for *bee2*, *bhlh115* and the double mutant *bee2bhlh115*. Testa rupture, germination and establishment were scored for 7 days, on 4 different PAC concentrations: 0, 1, 3, 5 µM. Four replicates of minimum 50 seeds for each replicate were used for each mutant. Error bars represent the standard deviation.

Subsequently, the response of *athb23*, *dof2.1* and the double mutant *athb23dof2.1* to stress agents including salt (NaCl) and polyethylene glycol (PEG 6000) was analysed. For this purpose, a range of concentrations were used, 0, 10, 20, 30% PEG and 0, 50, 100, 150 and 200 mM NaCl, in a germination assay of 7 days, following chilling for 48 hours at 4°C.

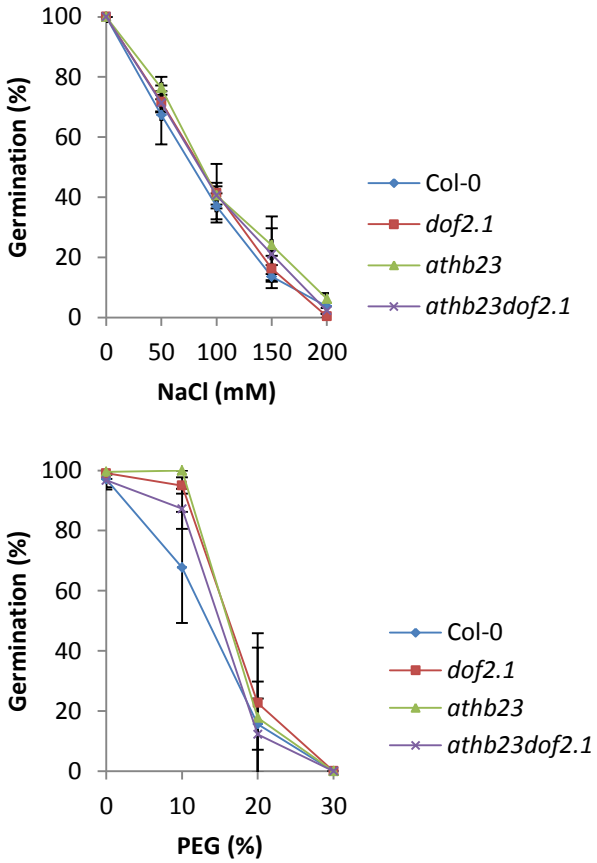

Figure 3.25 Germination scores (7th day) for *athb23*, *dof2.1* and *athb23dof2.1* on media containing stress agents: PEG (0, 10, 20, 30%) and NaCl (0, 50, 100, 150 mM). The error bars indicate standard deviation.

In figure 3.25, germination responses to different concentrations of PEG and NaCl, indicate a higher tolerance of the mutants to abiotic stresses, than the wild type Col-0. Both substances diminish water potential of cells.

To understand the relationship between transcription factors in cluster 19 and structural genes, crosses between *athb23* and *athb23dof2.1* and

promEXAP2::GUS, *promDOF2.1::DOF::GUS*, *promDELTA-VPE::GUS* and *promSCPL51::GUS*, were made.

After the seeds were genotyped and the homozygous lines selected, a germination assay on PAC was performed (Figure 3.26).

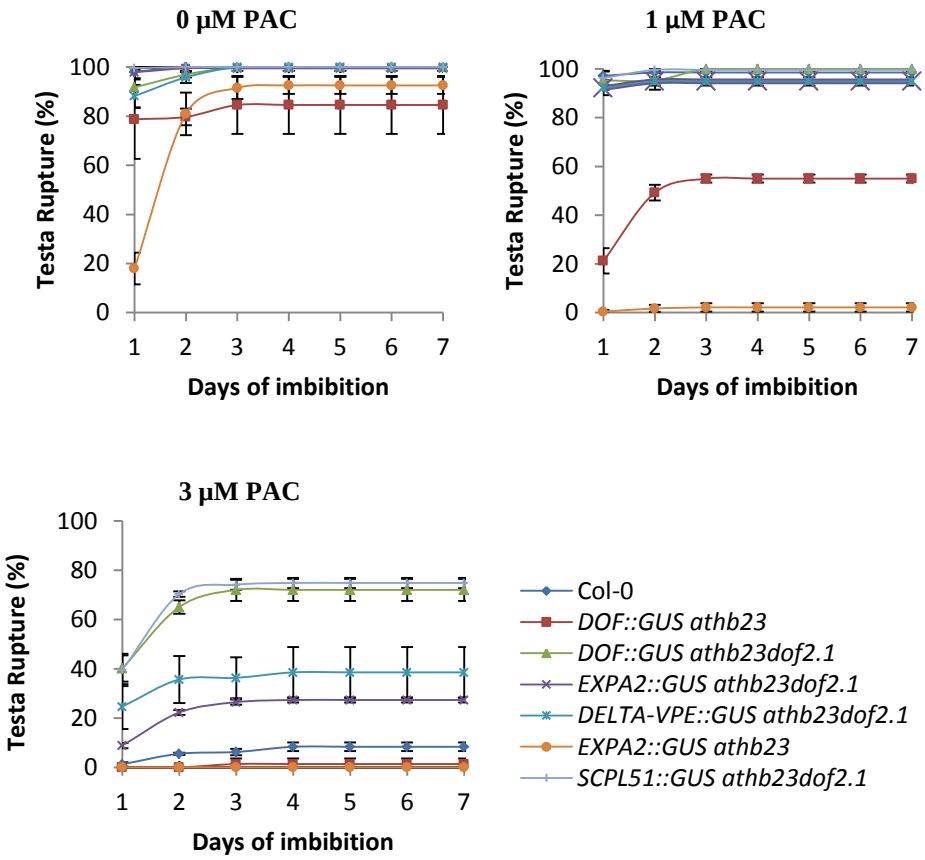

Figure 3.26 Testa rupture (%) of *athb23* and *athb23dof2.1* mutants scored for 7 days on 3 different concentrations of PAC: 0, 1 and 3 µM PAC. *promDOF2.1/EXPA2::GUS athb23* were showing testa rupture slower than the wild type, but also than the double mutants *promDOF2.1/EXPA2/DELTA-VPE/SCPL51::GUS athb23dof2.1*. Error bars indicate standard deviation.

The results show that the double mutants testa ruptured faster than the single *athb23*, on media containing a GA inhibitor agent. *promDOF2.1::DOF2.1::GUS athb23* and *promEXPA2::GUS athb23* were more sensitive to PAC than the wild type Col-0, but also than double mutants

promDOF2.1::DOF2.1::GUS athb23dof2.1 and *promEXPA2::GUS athb23dof2.1*, respectively.

The fact that *athb23* and *athb23dof2.1* mutant lines resulted from crosses with structural genes from cluster 19 were germinating differently than the *athb23* and *athb23dof2.1* lines, it might be due to the environmental conditions changes inside the growth rooms (night time temperature was changed).

Moreover, *promEXPA2::GUS* expression was monitored in the seeds resulted from crosses between the transgenic plants and a mutant of *ATHB23* (transcription factor, present in cluster 19). The analysed seeds were containing *promEXPA2::GUS* in *athb23* background, as well as in Col-0. They were imbibed in ½ MS for 6, 12, 18 and 24 hours before the endosperms were separated from embryos and stained (Figure 3.27).

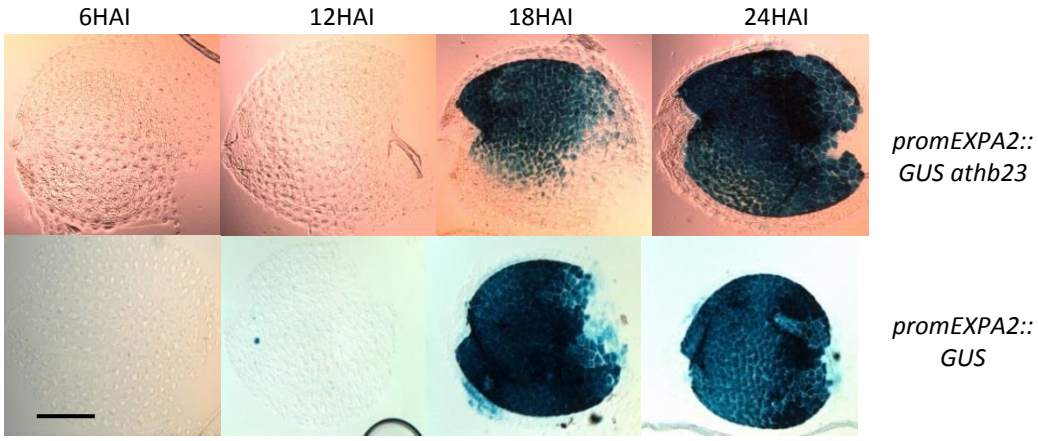

Figure 3.27 GUS expression over 24 hours of imbibition (6, 12, 18, 24 HAI= hours of imbibition) for *promEXPA2::GUS* in *athb23* background and Col-0. Scale bar= 50 μm.

The results are indicating the fact that *EXPA2* promoter expression was visible after 18 hours of imbibition, in the whole endosperm in the wild type background, while for *athb23* mutant the expression was limited to the micropylar and lateral endosperm. After 24 hours of imbibition, GUS activity for *EXPA2* promoter was similar for both backgrounds.

3.1.4.6 Testing putative interactions between EXPA2 promoter and cluster 19 transcription factors using yeast one hybrid system.

Regulation of transcription is important and underlines the gene expression pattern. This is controlled by the number, position and interactions between the *cis*-elements in gene promoters and the transcription factors. *Cis*-elements are short DNA-sequences located in the gene promoters that are bound to certain transcription factors (Castrillo et al., 2011).

To test if there are any interactions between the *EXPA2* promoter and the transcription factors from cluster 19: *ATHB23*, *BEE2*, *bHLH115* and *DOF2.1*, yeast one hybrid system was used. Possible interactions are displayed using ATHAMAP program in Figure 3.28.

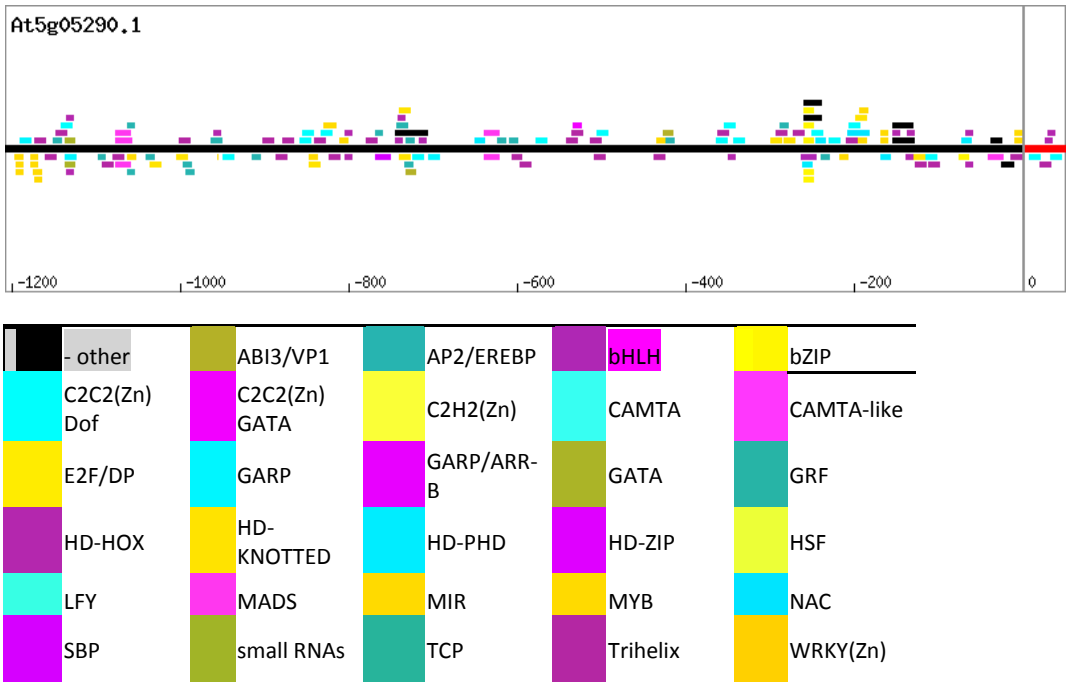

Figure 3.28 Transcription factors binding sites and small RNA target sites for *EXPA2*, 1200bp upstream ATG; displayed map using AthaMap (http://www.athamap.de).

The promoter of *EXPA2* was divided into 4 fragments: 3 fragments of 400bp and 1 fragment of 300bp (Figure 3.29). Each fragment was cloned into pHISLEU2GW vector, using Gateway cloning system (Figure 3.30).

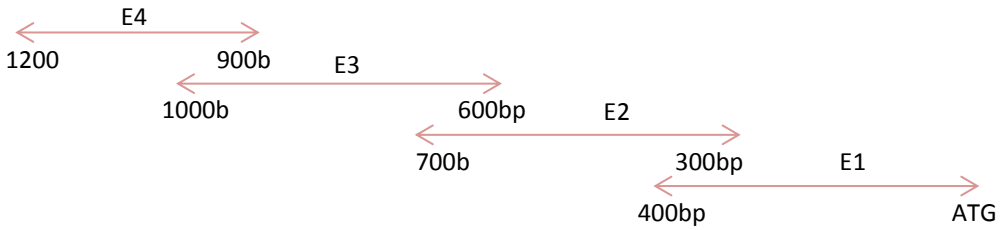

Figure 3.29 *EXPA2* promoter (1200bp upstream ATG) was split in 4 fragments of 400bp and 300bp, respectively. The last 100bp of each fragment was overlapping with the beginning of the next fragment.

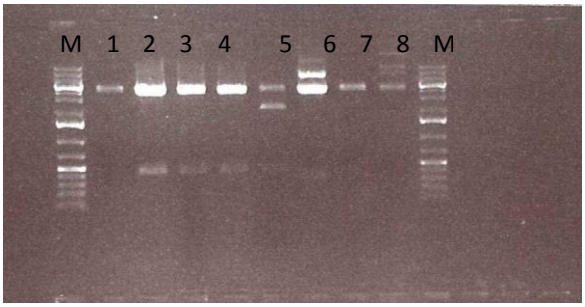

Figure 3.30 Digestion products of *EXPA2* promoter fragments cloned in pHISLEU2GW (BsrGI): *(1), (2) E1*; *(3), (4) E2*; *(5), (6) E3*; *(7), (8) E4*; M- DNA ladder 1kb+.

The transcription factors: *ATHB23* (At5g39760), *bHLH115* (At1g51070), *BEE2* (At4g36540) and *DOF2.1* (At2g28510) were amplified and cloned into pDEST22, a vector suitable for yeast transformation (Figure 3.31), using Gateway cloning system.

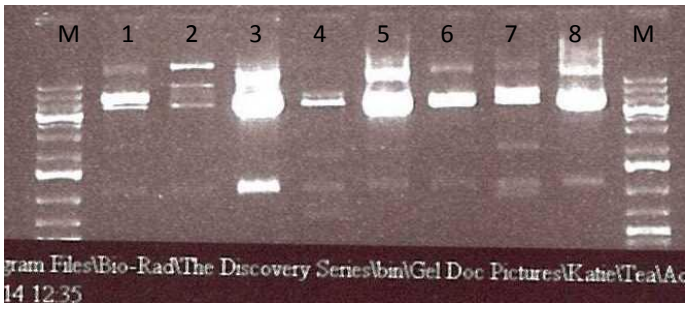

Figure 3.31 BsrGI digestion products of TFs cloned into pDEST22: *(1), (2) ATHB23*; *(3) BEE2*; *(4) bHLH*; *(5), (6) (7), (8) DOF2.1*; M- DNA ladder 1kb+.

After the DNA sequence of constructs was confirmed by Source BioScience Sequencing Labs, that the vectors are containing the correct DNA fragments, either *EXPA2* promoter fragments or the TFs, the samples were sent to Madrid, to Centre for Plant Biotechnology and Genomic, to the Laboratory of Dr. Luis Onate Sanchez.

Under his supervision, the constructs were transformed into yeast strains, the prey sequences (TFs) into *Saccharomyces cerevisiae* YM4271, together with two negative controls: Green Fluorescent Protein (GFP) and an empty plasmid. The bait sequences, the four fragments of *EXPA2* promoter, were cloned into *Saccharomyces cerevisiae* Y187 (α mating type) (Castrillo et al., under revision).

As described in Materials and Methods chapter, the plasmid used to recombine the TFs into a yeast compatible strain, was conferring auxotrophy to tryptophan, while the bait sequences were cloned into a strain with auxotrophy to leucine, enabling the selection of the transformants.

After being grown on selective media where only diploid cells could grow (- LEU, -W), the cultures containing diploid cells were mixed and plated on plates with media lacking both amino acids (DOB-LEU-W) (Figure 3.32). The diploid cells growth is an indicative for the success of mating between yeast strains containing bait and prey sequences.

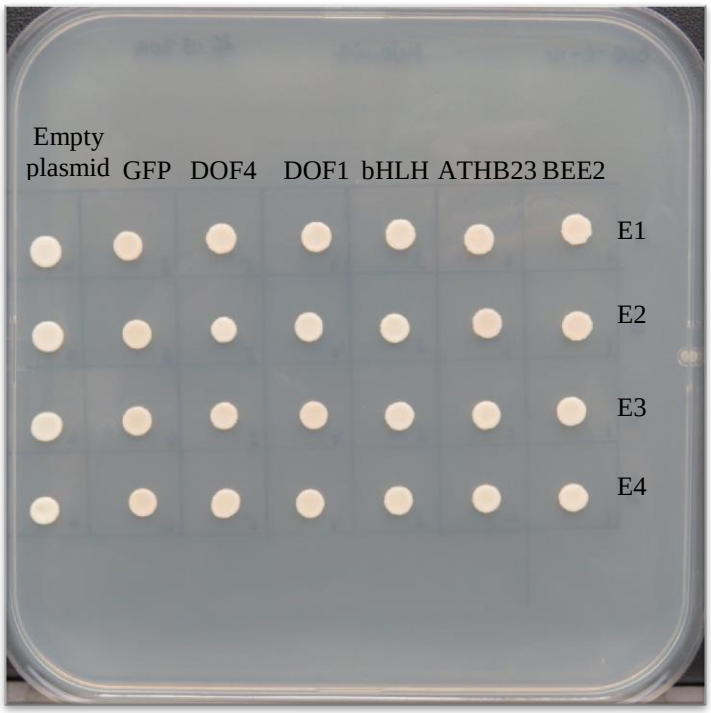

Figure 3.32 Diploids cells on selective media DOB-L-W (growing media lacking leucine and tryptophan; only diploids cells could grow). Mated cells of *EXPA2* promoter fragments (E1, E2, E3, E4) with TFs: *DOF2.1*, *bHLH115*, *ATHB23*, *BEE2* and two negative controls: GFP and an empty plasmid.

To score for diploids and positive bait-prey interactions, selective media missing histidine (Figure 3.33) and containing increasing concentrations of 3-Amino-1, 2, 4- triazole (3-AT), an inhibitor of the reporter gene *HIS3*, as described in Materials and Methods, were used (Figure 3.34).

Figure 3.33 Diploid cells grown on auxotrophic media (DOB-L-W-H). Mated cells of *EXPA2* promoter fragments (*E1*, *E2*, *E3*, *E4*) with TFs: *DOF2.1*, *bHLH115*, *ATHB23*, *BEE2* and two negative controls: GFP and an empty plasmid.

Yeast growth was reduced as soon as the histidine was removed from media. Leaky expression of *HIS3*, was titrated using different 3-AT concentrations, avoiding an increased number of false positive, but also allowing the observation of weak interactions (Figure 3.34).

The yeast growth was scored for 5 days on auxotrophic media containing different 3-AT concentrations. Yeast cells carrying the first two *EXPA2* promoter fragments (*E1* and *E2*) required 0.1 mM 3-AT to suppress the basal activity of *HIS3*, while a higher concentration was neded for *E3* and *E4* (Figure 3.34).

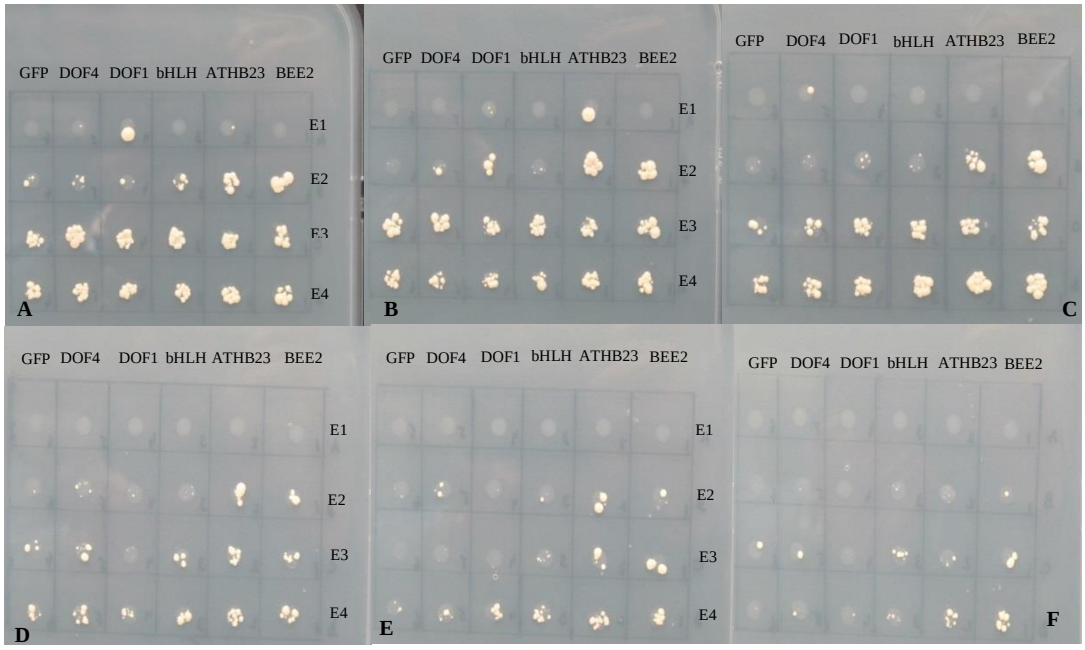

Figure 3.34 Yeast one hybrid screening of transcription factors: *DOF2.1*, *bHLH115*, *ATHB23* and *BEE2* with *EXPA2* promoter fragments: *E1*, *E2*, *E3* and *E4*, on auxotrophic media containing increasing 3-AT concentrations: *(A)*- 0.1 mM 3-AT; *(B)*- 0.3 mM 3-AT; *(C)*- 0.7 mM 3-AT; *(D)*- 1mM 3-AT; *(E)*- 2mM 3-AT; *(F)*- 3mM 3-AT.

Diploid colony size was taken into account to compare and normalize the strenghth of positive bait-prey interactions (Castrillo et al., 2011). According to this principle, the only positive interactions appeared to be between *EXPA2* third and fourth fragments, *E3* and *E4*, and *BEE2* and *ATHB23*, from the TFs.

From figure 3.34, we could see that the only matched pairs, able to grow on higher 3-AT concentrations were *E3*/*E4*- *ATHB23*/*BEE2*. The negative control stopped growing on 2 mM 3-AT.

As a preliminary result, the interacting factors appeared to be *ATHB23* and *BEE2* and the third and fourth fragments of *EXPA2* promoter (*E3* and *E4*).

3.2 Biomechanics and imaging

3.2.1. Nanoindentation of plant materials

As a preliminary study, and also to become familiar with nanoindentation, several experiments on leaves were carried out. The reason of working on leaves was because they are considered flat surfaces; flat samples reduce the noise and keep force/deflection curve shape uniform (Figure 3.35).

Four different groups of plants were tested: three mutants (arabinan deficient (*arad1*) (Harholt et al., 2006), pectin deficient (*qua2*) (Mouille et al., 2007), altered xyloglucan content (*xxt1xxt2*) (Cavalier et al., 2008) and a wild type (Col-0 for *qua2* and *xxt1xxt2*; QRT for *arad1*) as a control, to detect any changes in the cell wall stiffness.

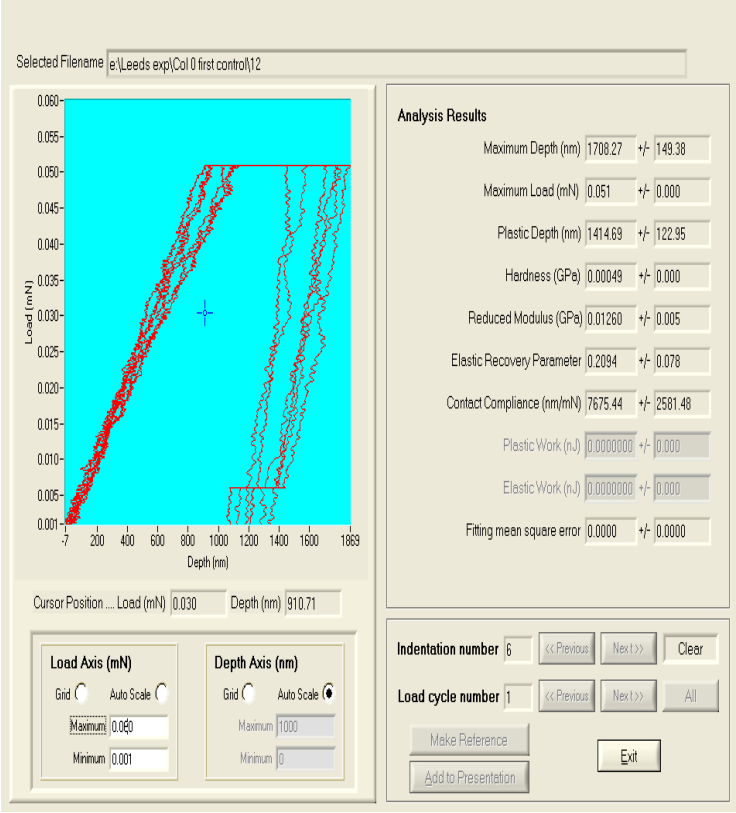

Figure 3.35 Load-displacement curves of Arabidopsis Col-0 leaves, using a spherical indenter.

The results plotted in figure 3.36, comparing the hardness and elastic modulus values of the mutants with the correspondent wild type, no significant difference could be found (two tail t-test, p>5). Using the literature results as reference, it was expected to find differences in stiffness between *qua2* and Col-0, *arad1* and QRT, the mutants having stiffer cell walls, while *xxt1xxt2* more compliant than Col-0.

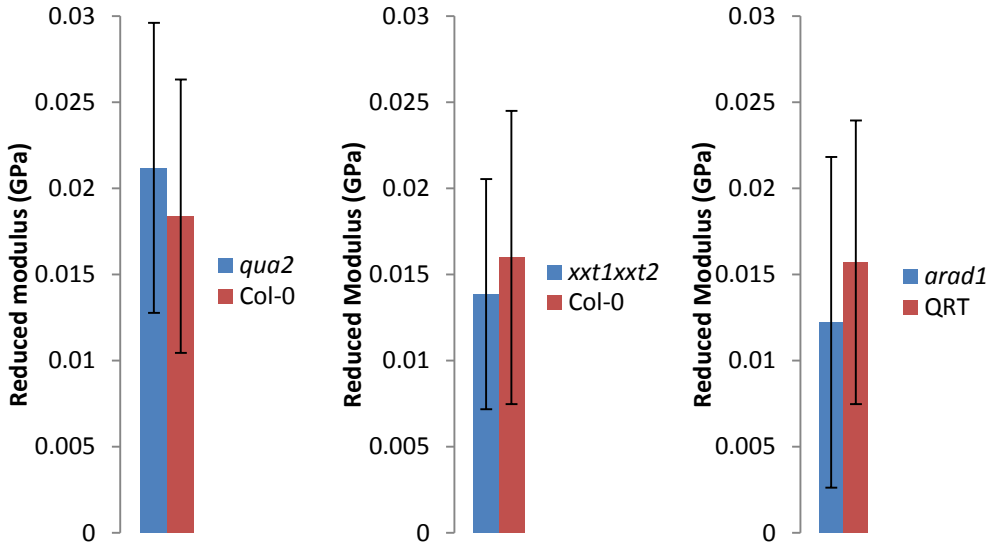

Figure 3.36 Reduced modulus (GPa) for Arabidopsis mutants *qua2*, *xxt1xxt2*, *arad1* leaves in comparison with their wild type correspondent Col-0 and QRT, respectively. Four leaves for each type were tested with 10 indentations for each, in the same area, approximatively. Error bars represent standard deviation.

Another comparison was made between the two sides of a leaf: adaxial and abaxial sides, using different loading forces. The results were plotted in figure 3.37. After running the t-test, no significant difference (p>0.5) was found between the adaxial and abaxial sides.

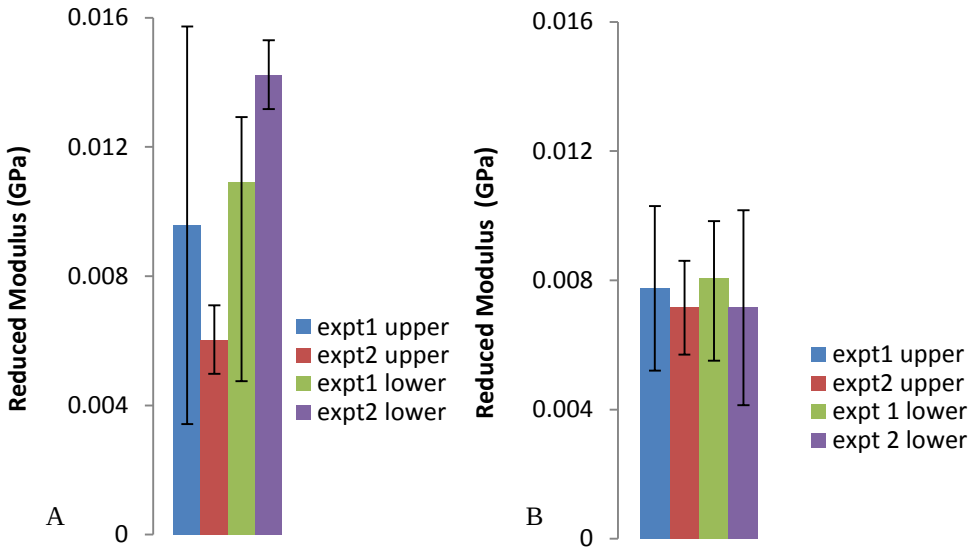

Figure 3.37 Reduced modulus (GPa) results for Arabidopsis Col-0 leaves, indented on both sides: adaxial (the upper surface of the leaf) and abaxial (the lower surface of the leaf) sides. *(A)* Maximum load was 0.2 mN; *(B)* Maximum load was 0.5 mN; expt- experiment1, 2 consisting of 10 indentations per experiment. Halves of nine leaves were used in these experiments, to be indented on both sides. Error bars represent standard deviation.

Although the results of leaves nanoindentation were not very encouraging, Lepidium dry seeds were subjected to nanoindentation tests. The nanoindentation approach was used in an attempt to generate reduced modulus values for Lepidium endosperms in different stages of germination; assuming that the changes in cell wall stiffness would be detectable.

The modulus of elasticity of a seed is a mechanical property which has been suggested as a measure of the textural attribute described as firmness (Khodabakhshian, 2012).

To test the sensitivity of the method, 10 dry cress seeds were indented, and the results appeared to be consistent (the measured mean stiffness of the seeds appeared to be constant amongst the cohort within the precision of the technique), excluding seed 7 (Fig 3.38).

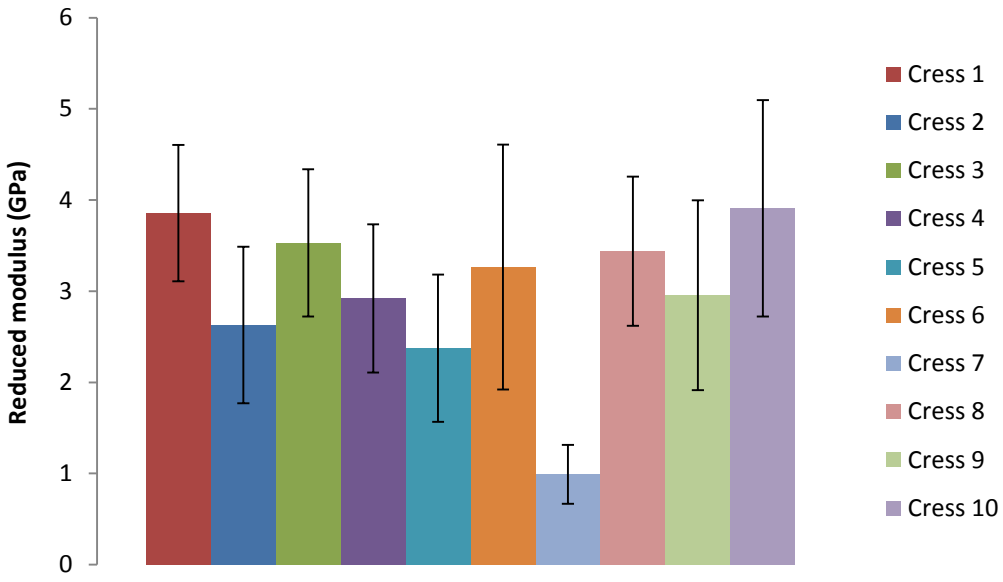

Figure 3.38 Results of nanoindentation of dry cress seeds (*Lepidium sativum*). Ten seeds were indented with 10 indentations on top of the radicle; the elastic modulus (GPa) results are displayed in columns; Error bars ± standard deviation.

Once the methodology was accepted as reliable, tests on imbibed seeds were performed. After indenting 6 Lepidium endosperms, the mean value of reduced modulus was ~100 MPa (Figure 3.39a). The cabin environment (22°C) was leading to sample dehydration, as could be visually observed (Figure 3.39b). In order to complete a set of 10 indentations, approximately 2 hours was needed. No significant difference was found between the elastic modulus for endosperms of seeds imbibed for 1 or 16 hours ($p>0.05$).

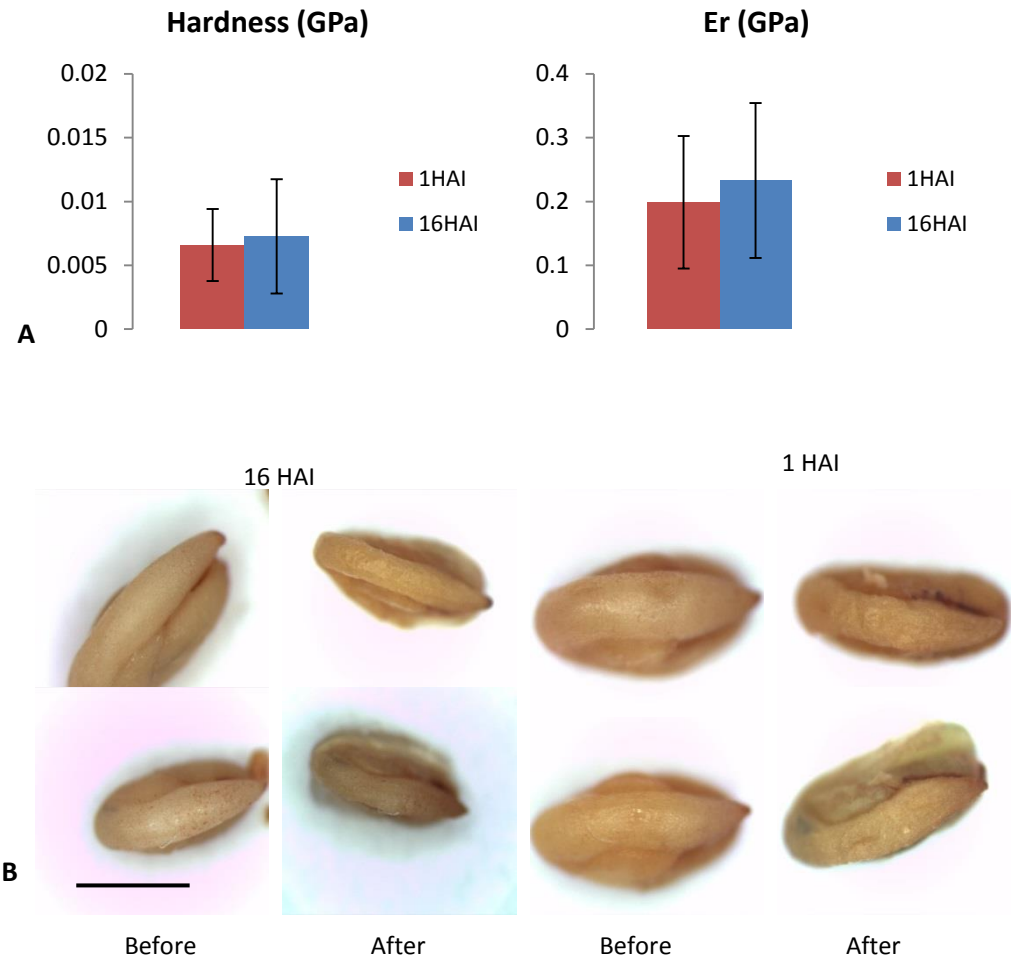

Figure 3.39 *(A)* Hardness (GPa) and reduced modulus (E_r) (GPa) for Lepidium seeds imbibed for 1 and 16 hours, respectively; *(B)* Lepidium seeds testa removed imbibed for 1, 16 hours before and after indentation (same seed). 6 seeds were indented for each time point, 10 indentations being performed on top of the radicle, aiming the same area. HAI= hours of imbibition; Error bars ± standard deviation. Scale bar= 500 µm.

3.2.2 Atomic force microscopy

Dry Arabidopsis seeds were imaged using AFM. The acquired images represent the height of the sample, a 3D reconstruction of it and also a heat map (Figure 3.40).

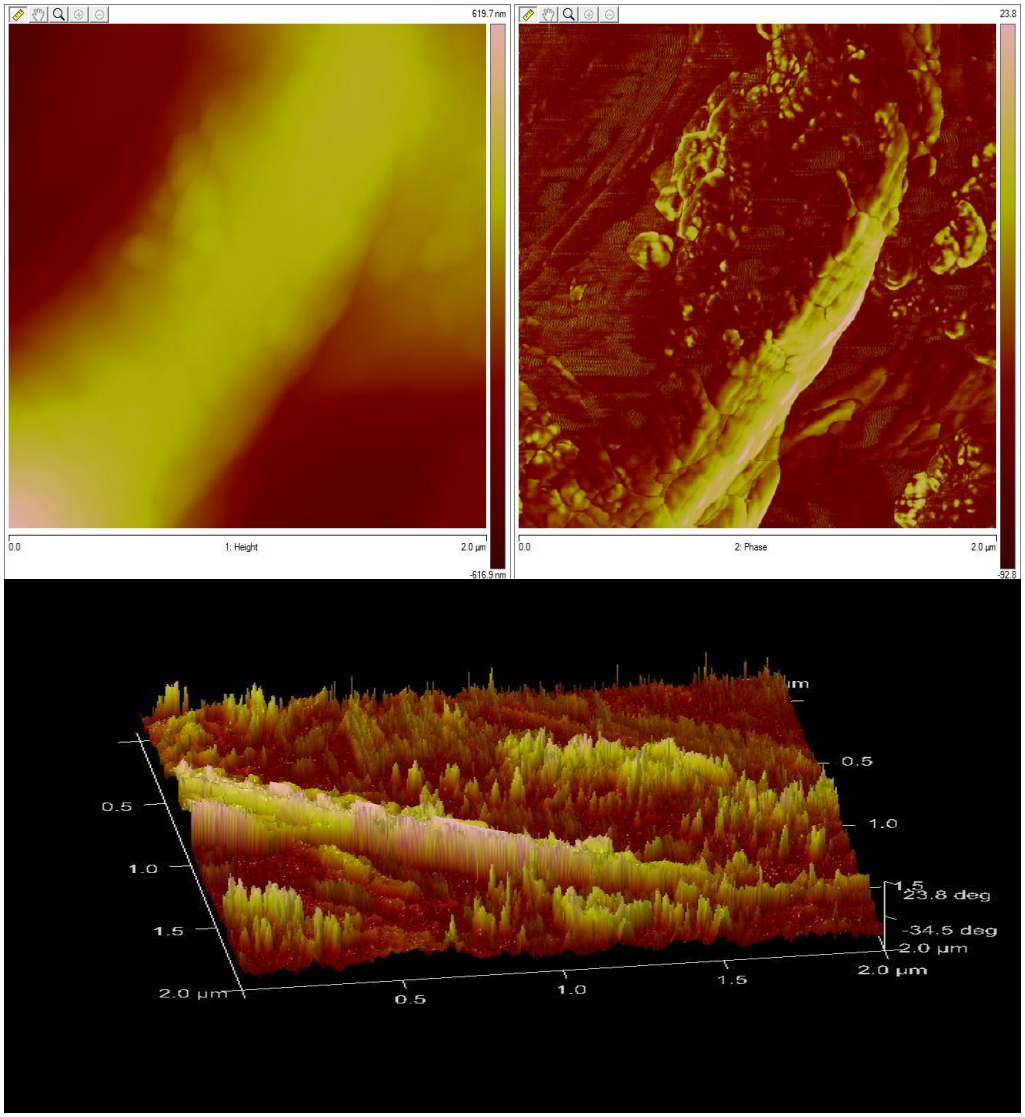

Figure 3.40 AFM images of a dry Arabidopsis seed.1: height; 2: phase (3D reconstruction); 3-3D heat map; scale bar= 2 µm.

Unfortunately no comparable data were acquired. The methodology failed completely, when imbibed Arabidopsis endosperms were imaged. The cantilever tip did not retract from the sample, impossible to generate retracting curves.

3.2.3 Imaging Lepidium seeds using micro-CT

As the various components of an organ have different x–ray attenuation coefficients, micro-computed tomography allows discrimination between liquid-filled cells and the air-filled intercellular space of the seed. Thus scans of either dry seed or imbibed seeds may be separated into those parts representing solid plant tissue and the air spaces within the tissue (Dorca-Fornell et al., 2013).

Thirty three Lepidium seeds in different stages of germination were scanned in order to visualize the changes inside the seed from a dry state to the completion of germination. In figure 3.41, seeds in different states are represented as sections of seeds. The imbibed seeds were stained with 1% IKI, while the dry seed was scanned without staining, considering that the staining solution is an aqueous solution.

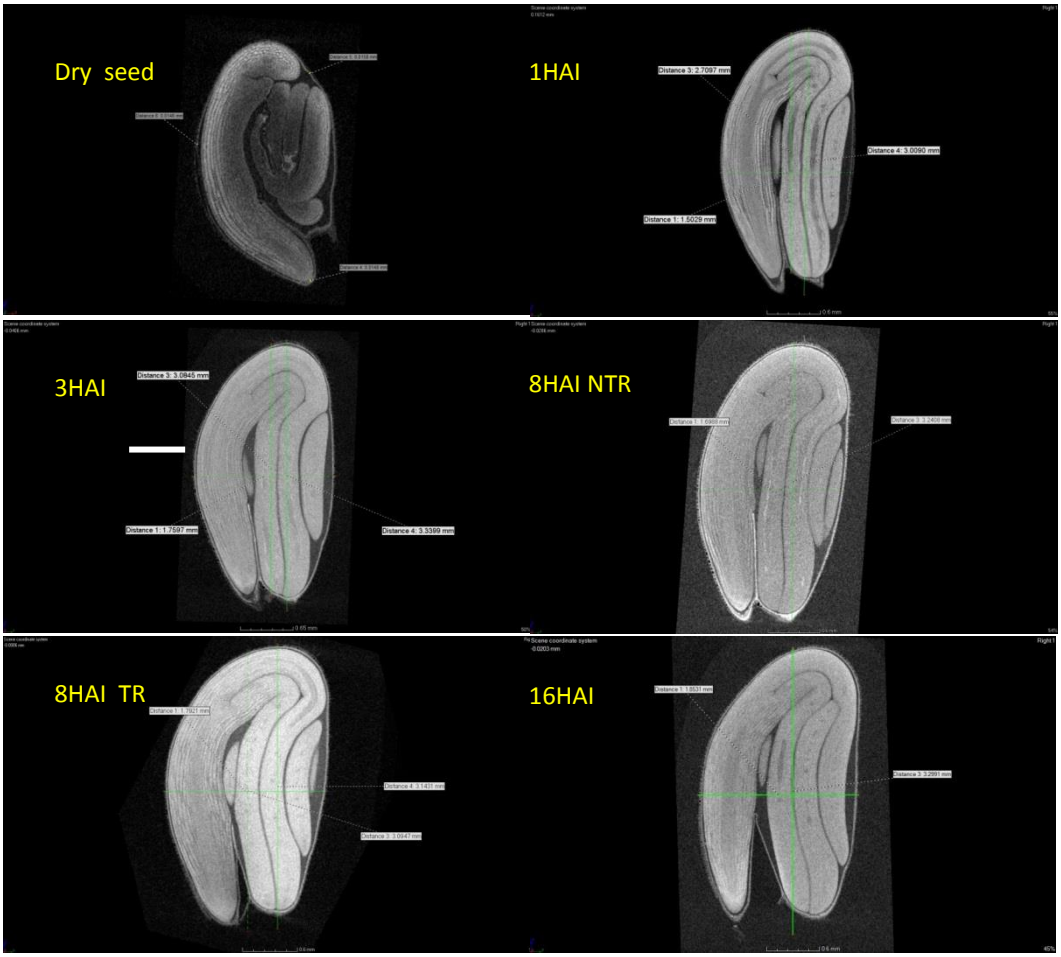

Figure 3.41 Micro-CT images of Lepidium seeds, at different imbibition time points: dry, 1hour, 3 hours, 8 hours no testa ruptured, 8 hours with testa ruptured, and 16 hours of imbibition. Scale bar= 0.06 mm. (VG Studio Max; http://www.volumegraphics.com/en/products/vgstudio-max.html)

Assuming that endosperm thickness in affected by the compression or/and stretching, using micro-CT 2D reconstructions, apparent thickness was approximated using the automatic material calibration tool within StudioMax version 2.0 (Volume Graphics, http://www.volumegraphics.com), in which the background (air) and material (testa, endosperm and embryo) are differentiated based on the grey value of individual voxels, which relates to the x–ray attenuation and hence material density of the sample.

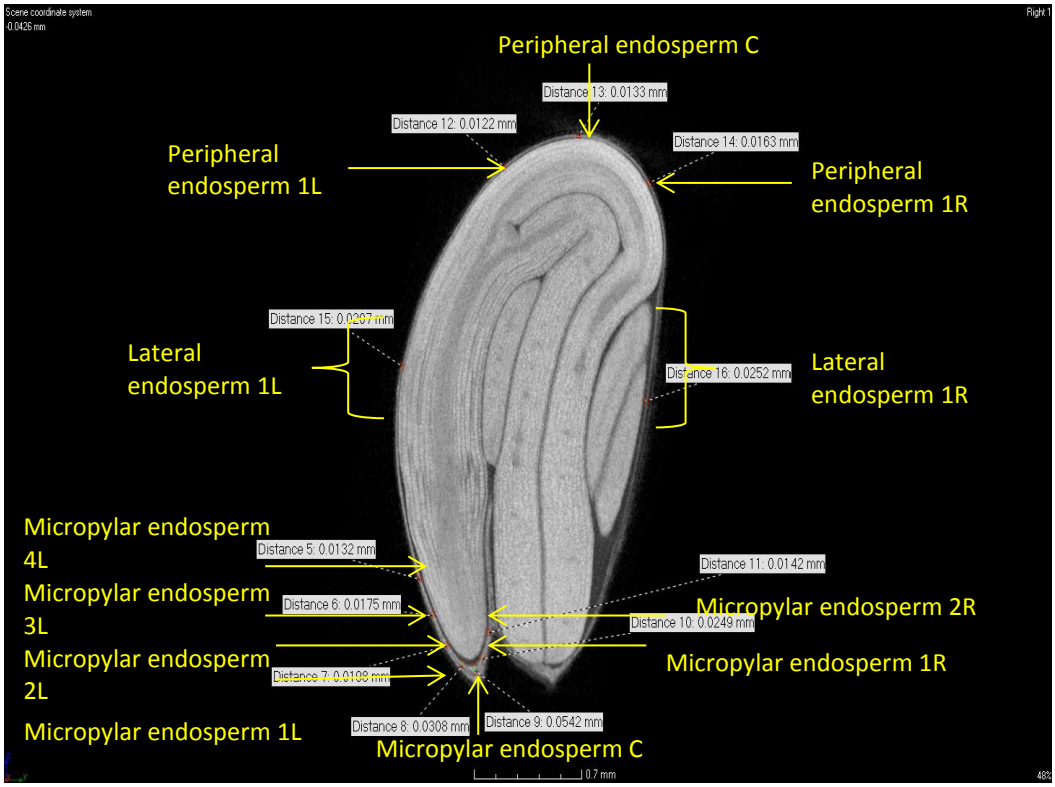

Figure 3.42 2D micro-CT of an imbibed Lepidium seed. Endosperm was divided in 3 regions: micropylar, lateral and peripheral; each region was subdivided in: central (C), lateral right (R) and left (L). Scale bar = 0.7 mm.

In dry seeds, the endosperm layer had an average thickness of ~ 15 µm in all the regions: micropylar, chalazal, and non-micropylar endosperm (Figure 3.43).

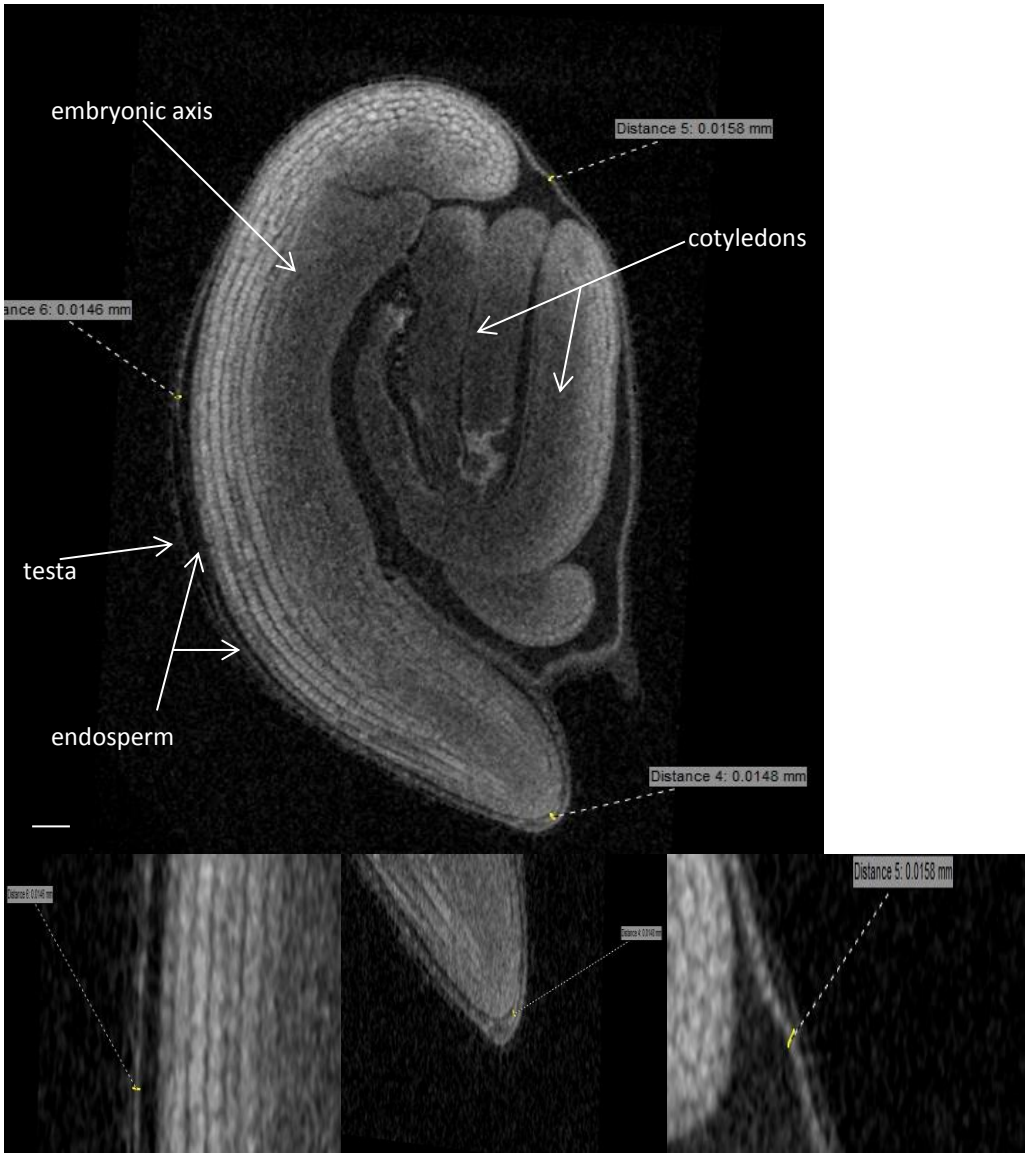

Figure 3.43 Micro-CT 2D pictures of a dry Lepidium seed. Endosperm thickness values estimated using VG Studio Max; http://www.volumegraphics.com/en/products/vgstudio-max.html. Scale bar= 0.08 mm

In an imbibed seed, before testa ruptures, the endosperm thickness increased in the micropylar region to 25 µm, while in the chalazal region remained at the same value (Figure 3.44).

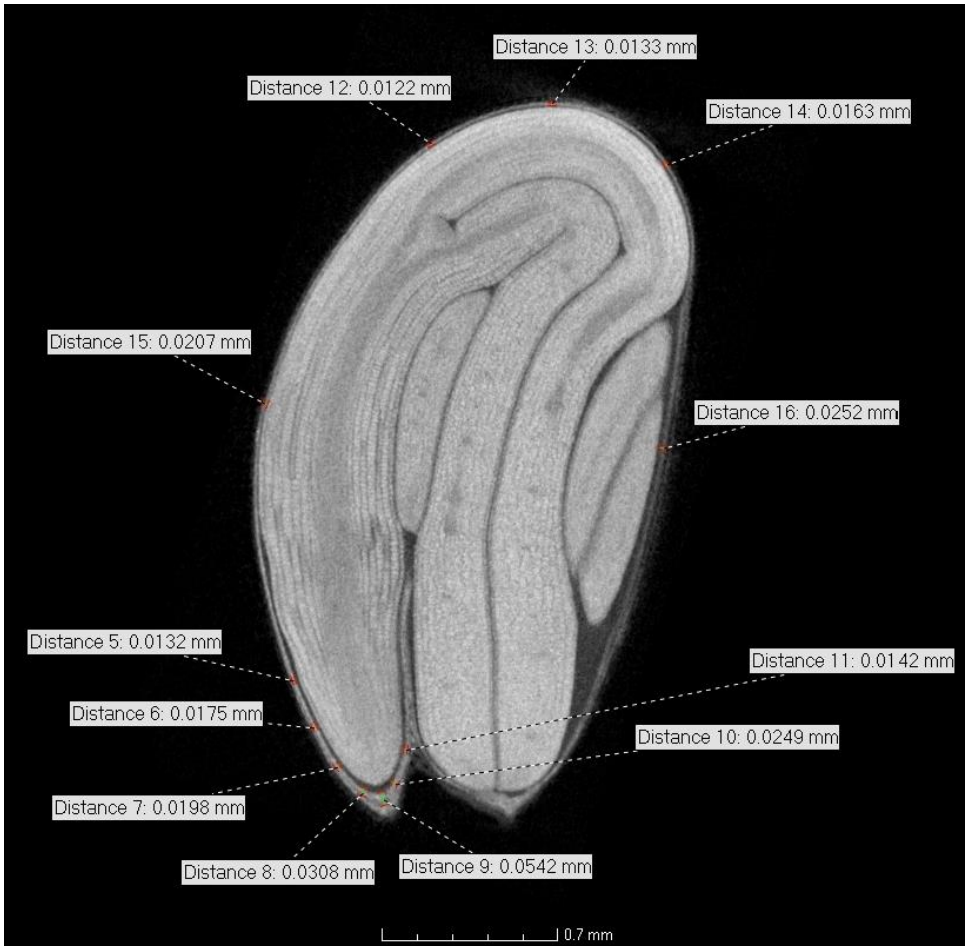

Figure 3.44 Micro-CT 2D section of a 1 hour imbibed Lepidium seed. The endosperm thickness was approximated using VG Studio Max; Scale bar= 0.7 mm. http://www.volumegraphics.com/en/products/vgstudio-max.html.

In an advanced stage of germination, after testa rupture but before endosperm rupture, the endosperm thickness had an average value in the micropylar region of 42 µm, while in the non-micropylar region only 28 µm (Figure 3.45).

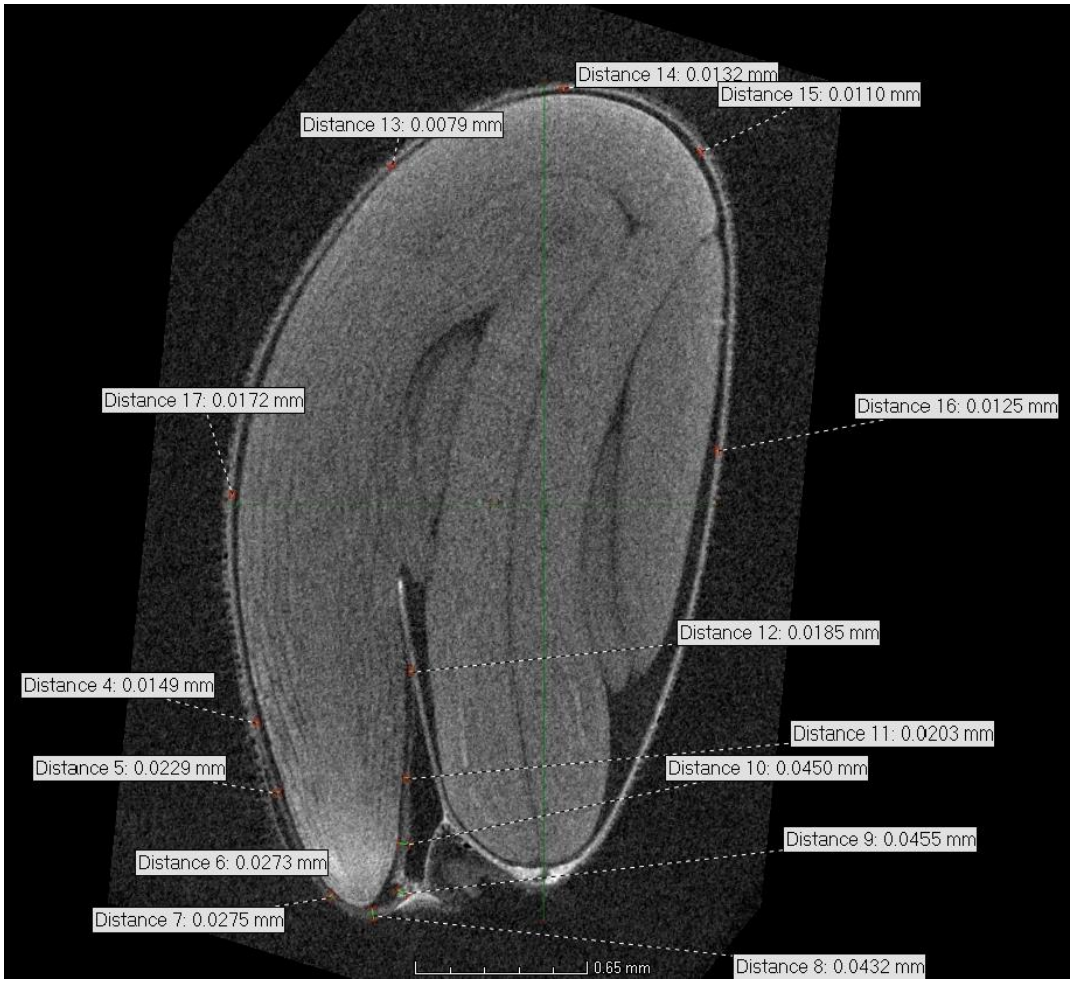

Figure 3.45 Micro-CT 2D section of an 8 hours imbibed Lepidium seed. The endosperm thickness was approximated using VG Studio Max; Scale bar= 0.65 mm. http://www.volumegraphics.com/en/products/vgstudio-max.html.

After the radicle has protruded through the endosperm, the thickness of micropylar endosperm was no longer measurable, but the values of endosperm thickness in the seed were between 16-40 µm (Figure 3.46).

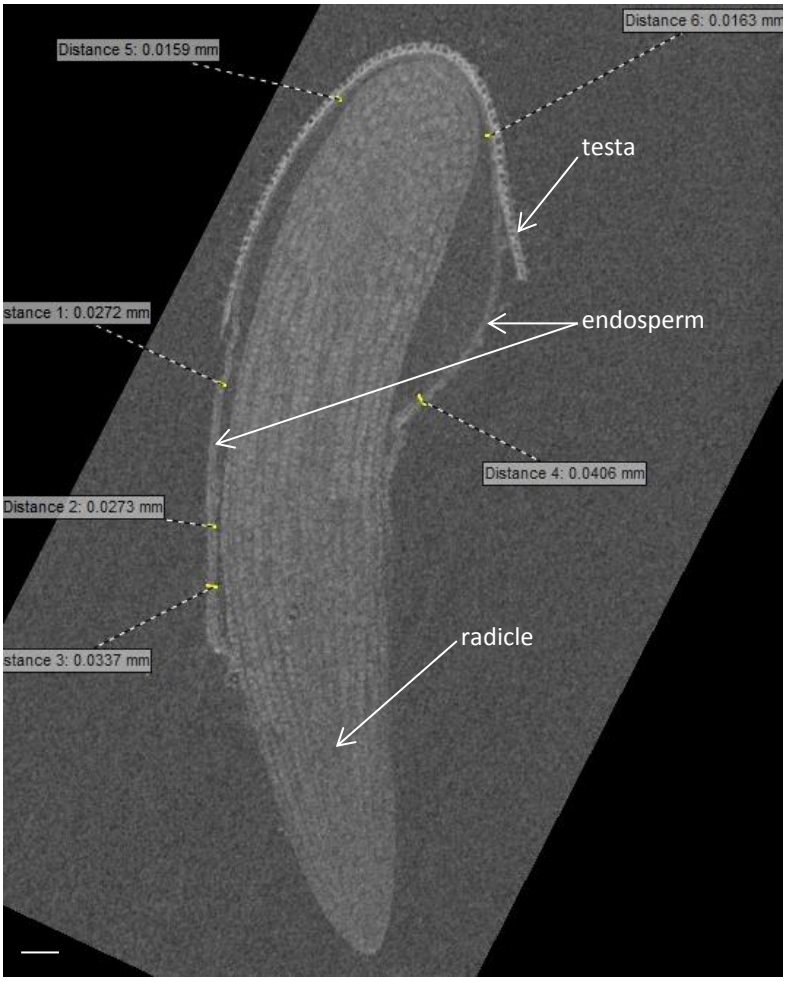

Figure 3.46 Micro-CT 2D picture of a Lepidium germinated seed using VG Studio Max; http://www.volumegraphics.com/en/products/vgstudio-max.html. The radicle protruded through the endosperm, making impossible the thickness estimation in the micropylar region. Scale bar= 0.05 mm.

After the radicle protrusion, the endosperm cells remained intact, suggesting that the rupture appears between individual cells, as was observed on eSEM scans of Arabidopsis germinating seed (Figure 3.47). It enforces the findings of Bethke et al. (2007) that the endosperm cells from radicle region exhibited vacuolation and wall weakening, enough for individual cells to be released from the layer.

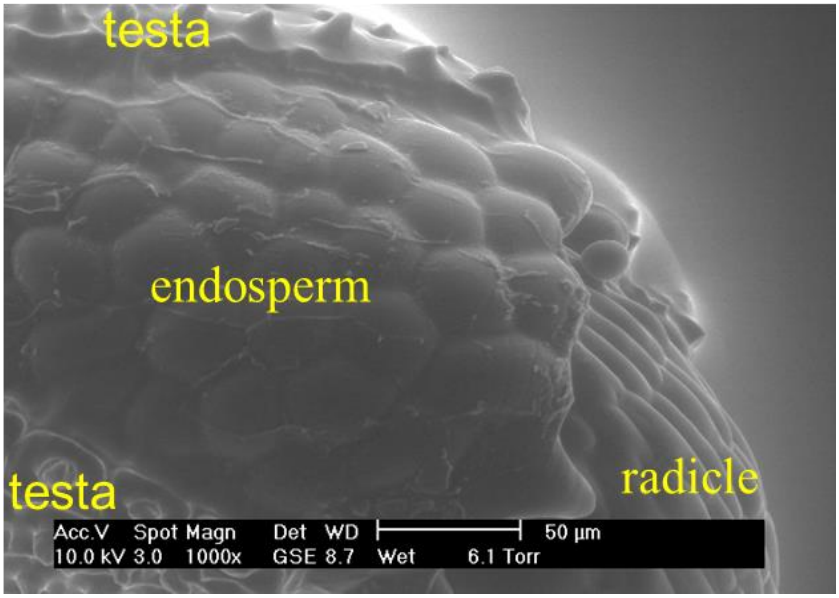

Figure 3.47 eSEM Arabidopsis germinating seed. After radicle protrusion, the endosperm cells are intact, suggesting the appearance of rupture between individual cells. Scale bar= 50 µm.

Mean values of endosperm thickness in different regions ME, LE and PE were compared as subsections, each section being divided as shown in figure 3.42, at different time points of imbibition (1, 3, 8, 16 hours) using ANOVA two ways statistical test. The results indicated a significant difference between subsections in single time points ($p<0.001$), significant difference between time points ($p<0.001$) and also a significant difference between subsections in different time points ($p<0.001$). 6 seeds for each time point were analysed. The values are displayed in figure 3.48.

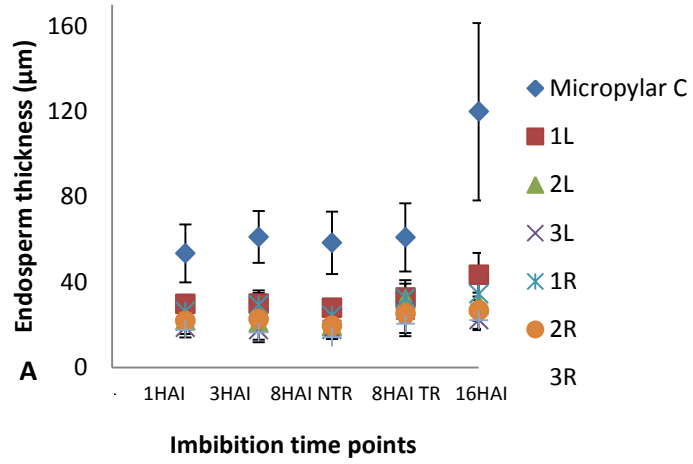

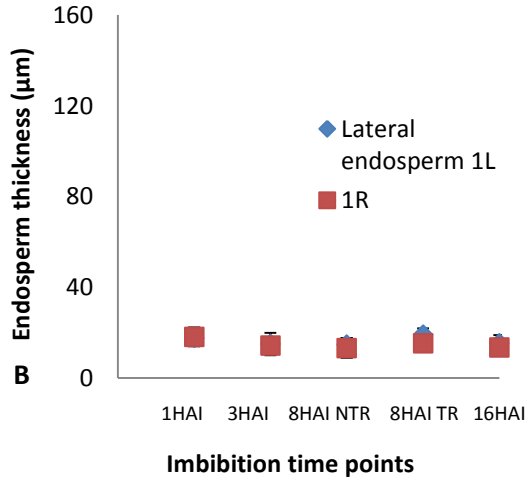

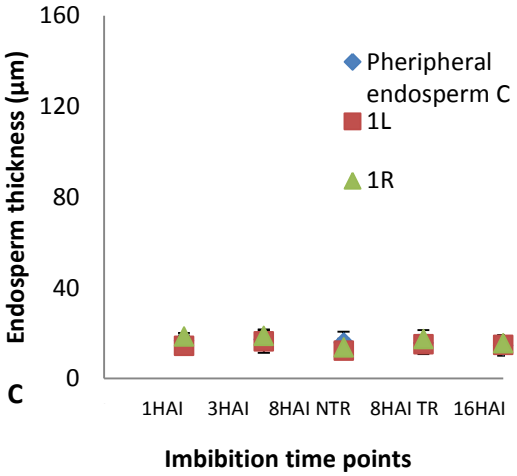

Figure 3.48 Mean values of Lepidium endosperm thickness in 3 different regions : micropylar *(A)*, lateral *(B)* , peripheral *(C)* (L= left; R= right; C= central); each region of the endosperm was divided in subregions as displayed in figure 3.42. 5 time points of imbibition (HAI= hours of imbibition): 1= 1HAI; 2= 3HAI; 3= 8HAI NTR (non testa ruptured); 4= 8HAI TR (testa ruptured); 5= 16HAI. 6 seeds were analysed for each time point. Error bars represent standard deviation.

When regions of endosperm were compared as sections, ME, LE and PE, a significant difference was found between sections in single time points ($p<0.001$), significant difference between time points as general means ($p=0.008$, $p<0.05$) but no significant difference between sections in different time points ($p=0.11$, $p>0.05$). The results are displayed in figure 3.49.

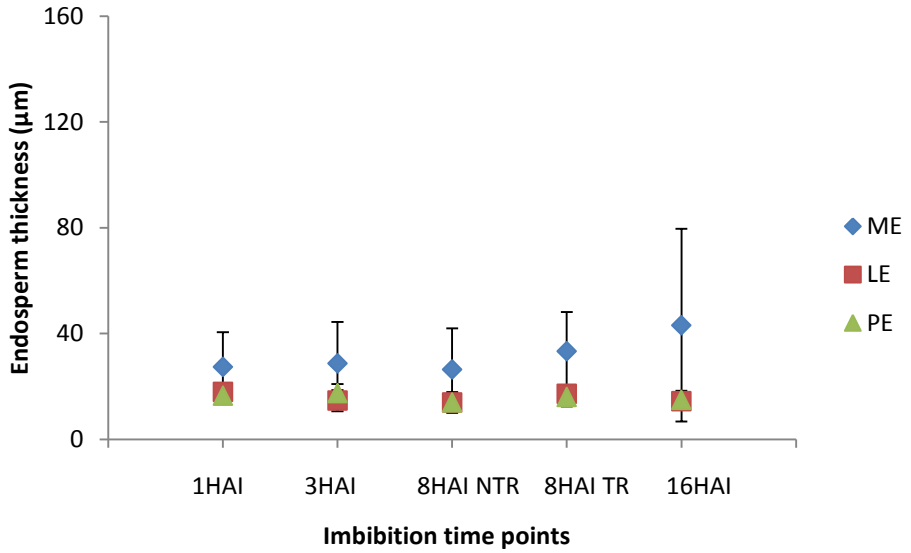

Figure 3.49 Mean values for micropylar endosperm (ME), lateral endosperm (LE) and peripheral endosperm (PE) thickness, at different moments of imbibition: 1, 3, 8 and 16 hours of imbibition (HAI); NTR= non testa ruptured; TR= testa ruptured. 6 seeds were analysed for each time point. Error bars indicate standard deviation.

3.2.4 Digital image correlation

Although no DIC work has been reported for plants, it has been successfully used to small animal tissue samples (Sutton et al., 2008). We therefore tried using it, hoping to find realistic displacement results for germinating Lepidium seeds. For this reason, imbibed seeds with testa removed, coated in Cr powder, were subjected to images acquirement for 2 hours, using an optical Leica microscope having attached a camera (Figure 3.50).

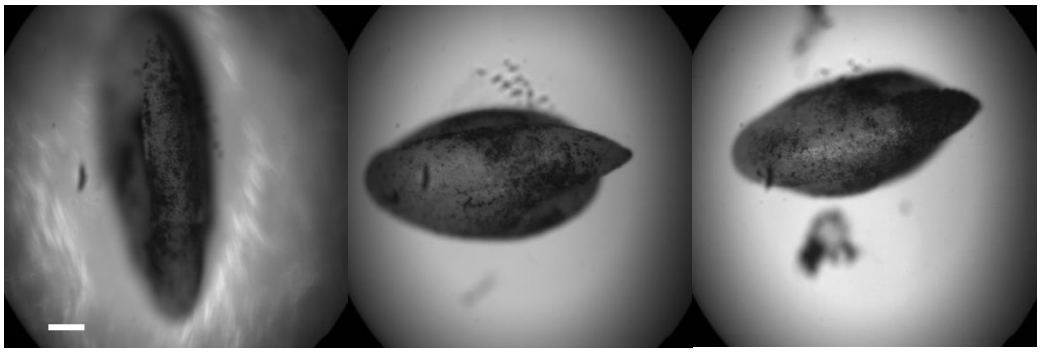

Figure 3.50 Three Lepidium seeds without testa, coated with Cr powder. Scale bar= 0.05 mm

The recorded images were analyzed using Istra 4D software, generating heat maps. After a region of interest was selected, and a reference point was chosen, the strain was represented by colours, ranging from purple to red (Figure 3.51).

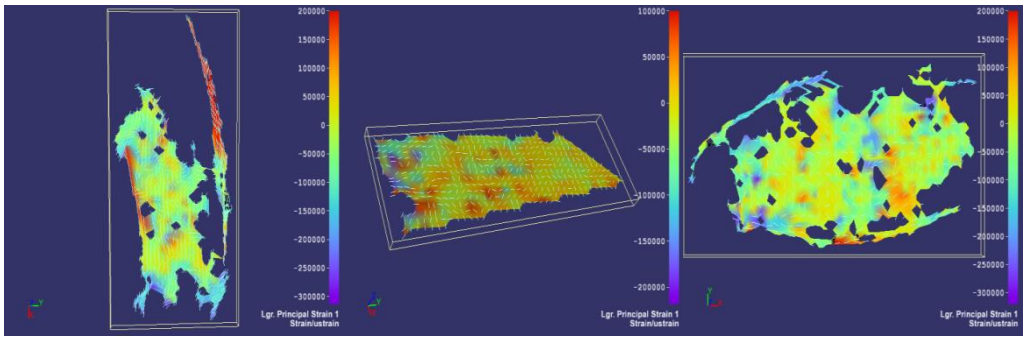

Figure 3.51 Displacement heat maps for Lepidium seeds generated using Istra 4D. The purple represents the smallest strain while at the other end the red colour, the highest (units are μstrain).

Although the generated maps were showing a certain displacement into the endosperm surface, in reality, this could not be linked to seed activity, since the endosperm was drying out because of the heat generated by the microscope lamp (Figure 3.52); the respective seed would never complete the germination, unless it was rehydrated.

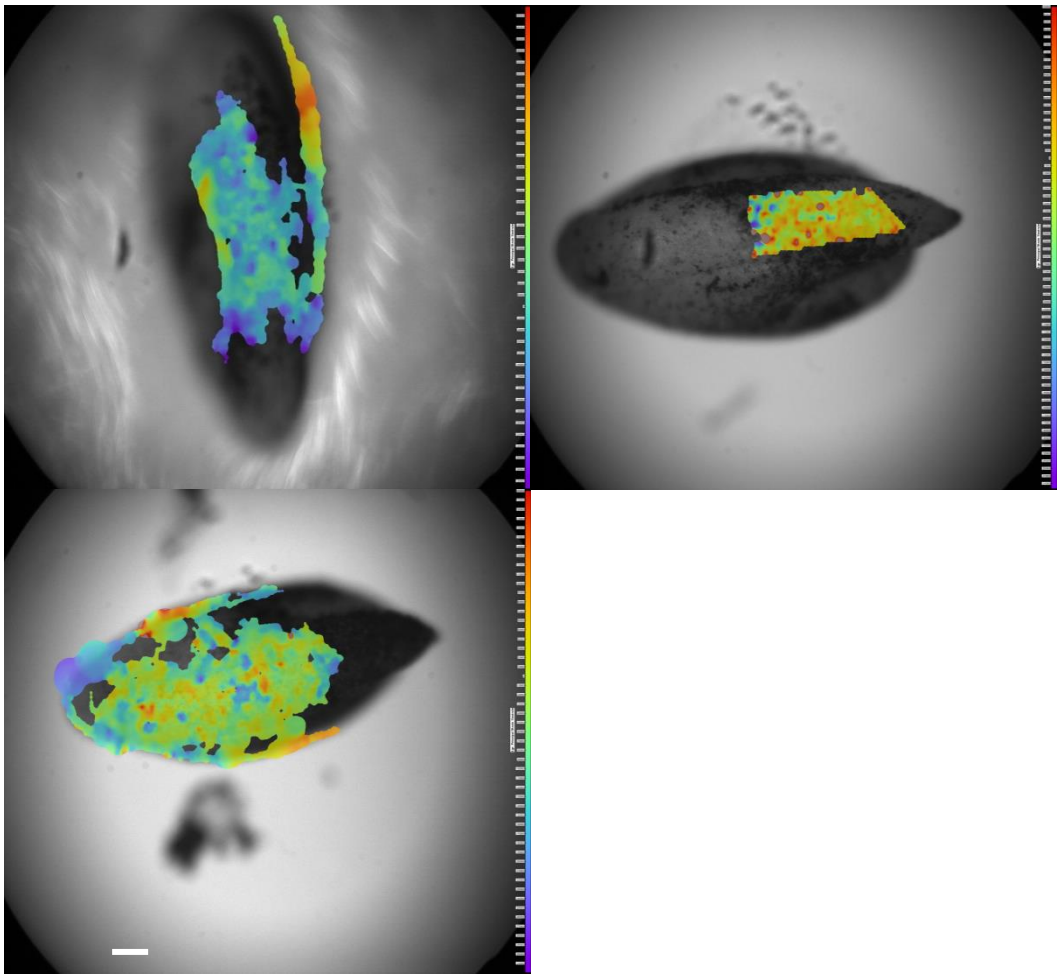

Figure 3.52 Strain heat maps for Lepidium seeds, on chosen area of interest. A uniform particle pattern was chosen, so any movement could be registered. Scale bar= 0.05 mm.

4. Discussion

4.1 Investigating molecular biomechanics

The mechanical behaviour of organisms and organs is determined by the physical properties of their components, tissues and cells. Recent biomechanics studies have started to address mechanical properties of the plant cells in living and growing tissues, at micro and nano scale, trying to elucidate growth and organ shape formation.

In this study, an attempt to detect changes in endosperm cells physical properties starting with imbibition and ending with radicle protrusion was performed. Also using imaging techniques endosperm cells through germination were visualized.

As discussed in introduction section it has been proven by various studies on different species, e.g. tomato, coffee, lettuce (Bewley, 1997; da Silva et al., 2004) and *Lepidium sativum* (Müller et al., 2006; Linkies et al., 2009) that the endosperm changes its physical properties in the micropylar region, the region covering the radicle, in order to allow the radicle to protrude.

For completing germination, not only the embryo growth is required but also the loosening of the surrounding tissues. But how does loosening happen? It is hypothesised to involve the relaxation of the cell wall tensile stress by cell wall loosing agents, a decrease in turgor pressure and enlargement, by cell wall creep (Cosgrove, 2005; Schopfer, 2006).

Marga et al., 2005, demonstrated using AFM that EXPANSIN is a loosening agent in cucumber hypocotyls, acting on the linking polymers between parallel microfibrils, rather than the whole matrix (Marga et al., 2005). There are other cell wall remodeling enzymes which are involved in endosperm loosening mainly mannanases (Nonogaki et al., 2000), glucanases (Leubner-Metzger, 2003) and endotransglycosylases (Van Sandt et al., 2007).

Not only the cell wall components and the turgor pressure are important in cell wall loosening, but also the hormones, ABA having an inhibitory effect,

delaying the endosperm rupture, while GA and ethylene are promoting the endosperm weakening (Bewley, 1997; Müller et al., 2006; Linkies et al., 2009; Finch-Savage & Leubner-Metzger, 2006).

In order to detect any changes in physical properties of the endosperm, nanoindentation and later on, AFM, were proposed as suitable methodologies. Nanoindentation was considered sensitive enough to detect differences in tissue physical properties between endosperm regions, hoping to generate results of stiffness and elasticity.

Also, imaging techniques were developed to visualize the changes happening inside the seed through germination. For this purpose, Micro-CT, eSEM and DIC were used.

4.2 Molecular dissection of endosperm specific gene expression

Understanding the role for the endosperm in germination is crucial for elucidation of the mechanisms and processes happening during this irreversible process. Several studies identified the genes expressed specifically in the endosperm during germination (Dubreucq et al., 2000; Penfield et al., 2004).

One gene *EXPANSIN A2* (*EXPA2*), has been described by Ogawa et al., 2003 (Ogawa et al., 2003) and later on used as an endosperm marker by Penfield et al., 2006 (Penfield et al., 2006). Other endosperm specific genes include proteases, transporters, and cell wall–modifying enzymes (Penfield et al., 2006).

In this study, *EXPA2* was used in the compared expression with the promoter expression of *DELTA-VPE*, *SCPL51* and *DOF 2.1*. The proposed hypothesises to be tested were concerning the *DELTA-VPE*, *DOF2.1* and *SCPL51* specificity (spatial and temporal distribution in endosperm cells during germination); to understand the effect of transcription factors from cluster 19 on germination, by observing the phenotype germination for their T-

DNA lines; and to test any putative interactions between *EXPA2* promoter and transcription factors from cluster 19.

Also, another point of interest in studying these genes was their responses to hormones, but also to establish if their expression requires an embryo signal.

4.2.1 Endosperm specific gene expression

The promoters of four genes from cluster 19, the only endosperm specific cluster, were analysed (Bassel et al., 2011). Their expression was monitored within GUS constructs. According to the results of this study, *EXPA2*, *DELTA-VPE*, *SCPL51* and *DOF2.1* were expressed only in the endosperm, but not in the embryos, suggesting an endosperm specific function for the encoded proteins.

Also, a temporal distribution was observed for *SCPL51* and *EXPA2*, which required between 12-18 hours of imbibition before expression became visible, while *DELTA-VPE* was expressed in the entire endosperm as early as 15 minutes of imbibition (the earliest time possible to separate seed tissues). DELTA-VPE was proved by Endo et al., 2012 to be an enzyme involved in cell death of testa formation, during seed development (Endo et al., 2012).

Endo et al., 2012, demonstrated that *DELTA-VPE* is endosperm specific expressed in the imbibed seeds, and that is involved in cell vacuolation. Using a mutant of this, they proved that vacuolation is a consequence of germination (Endo et al., 2012).

In order to understand if their expression was triggered by an embryonic signal, the endosperms were separated from embryos at early time imbibition points, from 15 minutes to 24 hours, and stained after being plated on ½ MS or ½ MS supplemented with GA for 24 hours.

It was found that *DELTA-VPE* does not need an embryo signal to be expressed, and also that it is GA insensitive; no difference was observed

between its expression on normal media, or media supplemented with GA. Apparently, the expression of this gene is not trigger by GA.

While *DELTA-VPE* expression was not dependent on an embryonic signal, it was not the case of *SCPL51*, which after separated from embryos and plated on normal media, no activity of the reporter gene was registered, but when external GA was added, its expression became visible by time. Therefore this shows that its expression is trigger by GA.

To assess the effect of ABA on the expression of these genes, after five days of imbibition on ½ MS with ABA, dissected endosperms were GUS stained and then imaged, revealing the fact that *EXPA2*, *DELTA-VPE* and *SCPL51* were expressed, without any inhibitory effect of ABA on their expression. This suggests that they are not involved in endosperm rupture but general endosperm function.

It was observed that *EXPA2* is expressed in the micropylar endosperm in the first hours of imbibition that its expression requires an embryonic signal and GA, and also that ABA has no effect on its expression. These results were confirmed by Yan et al., 2014, who demonstrated the key role played by *EXPA2* in germination (Yan et al., 2014).

An interesting observation was that when *promEXPA2::GUS* and *promDELTA-VPE::GUS* were transferred to a GA deficient background (*ga1-3*), their expression characteristics changed. *promDELTA-VPE::GUS* instead of showing an expression distributed in the whole endosperm, only an isolated expression in few cells of the micropylar endosperm was observed. The reduced expression of *promDELTA-VPE::GUS* in *ga1-3* background, may indicate the requirement of endogenous GA in endosperm cells before imbibition.

Also, analysing the expression of *promEXPA2::GUS* in *ga1-3* background, it revealed a temporal expression, being present in the first hours of imbibition in the micropylar endosperm, extended overtime in the whole endosperm; an enriched expression in comparison with *promEXPA2::GUS* in Col-0

background. The difference between *promEXPA2::GUS ga1-3* and *promEXPA2::GUS* was the absence of endogenous GA in *ga1-3*, and its presence in Col-0 background. Although the dissected endosperms were plated on GA supplemented media, the expression of the reporter gene was less abundant than in the *ga1-3* background.

The contradictory results of *promEXPA2::GUS* expression cannot be considered to elaborate a hypothesis, further investigations and repetition of experiments would be required in order to explain them.

Analysing the role of transcription factors from cluster 19 in germination, T-DNA lines were used in germination assays to score the germination percentage on Paclobutrazol, an inhibitor of GA biosynthesis. In the germinations assays were included double mutants, as well as the single mutants: *bee2*, *bhlh115-2, bee2bhlh115-2*, *athb23*, *dof2.1* and *athb23dof2.1*.

The results showed that *athb23* is less sensitive than Col-0 and *athb23dof2.1*, on media containing a GA inhibitor agent, germinating faster. If the GA biosynthesis was inhibited and transcription factors *ATHB23* and *DOF 2.1* were not expressed, the seeds germinated slower while if only *ATHB23* was not expressed, they germinated faster.

This fact suggests a direct effect of *DOF2.1* on *ATHB23* expression. The mutation whose phenotype is expressed is called epistatic, in this case *DOF2.1*, while the altered phenotype is called hypostatic, *ATHB23*. Epistasis is the phenomenon where the effects of one gene are modified by one or several other genes (Rasmusson & Phillips, 1997).

When *bee2*, *bhlh115-2*, *bee2bhlh115-2* were subjected to the same treatment, *bee2* and *bee2bhlh115-2* germinated much slower in comparison with the wild type, Col-0, while *bhlh115-2* germinated faster.

Because only *athb23* and *athb23dof2.1* showed a germination phenotype, they were selected to be used in crosses with *promEXAP2::GUS*, *promDOF2.1::DOF2.1::GUS*, *promDELTA-VPE::GUS* and *promSCPL51::GUS*. The homozygous seeds were plated on PAC, but for

athb23 mutant lines, a reduced germination could be observed, in opposition with previous results. Due to the changes of the environmental conditions into the growth rooms (night time temperature changed, Mike Holdsworth personal communication) the germination phenotype could not be reproduced.

It is known that transcription factors are involved in stress responses (Nakashima et al., 2012) by overexpression they provide high tolerance to drought and salt. When *athb23*, *dof2.1* and *athb23dof2.1* were plated on different concentration of PEG and NaCl, the germination scores were higher than for the wild type, Col-0, suggesting that not only overexpression but also knockout of transcription factors can affect germination by maintaining a higher water potential of cells, emphasizing the role of endosperm in stress tolerance.

4.2.2 Control of seed germination by *EXPA2*

The Arabidopsis *EXPA2* was found to be expressed highly in endosperm and described as an early GA-induced transcript during seed germination (Ogawa et al., 2003).

Using an *EXPA2* mutant (Salk_117075, T-DNA insertion in the promoter region), *exp2-1*, Yan and al., 2014, demonstrated that mutant seeds, in which the expression of *EXPA2* was almost completely supressed, germinated significantly slower than the wild type, confirming its importance for seed germination (Yan et al., 2014).

Also, when plated on media containing osmotic stress factors such as NaCl and PEG, *expa2-1* seeds were showing a higher sensitivity than the wild type Col-0, while the overexpression mutant seeds showed an improved tolerance to stress factors than the wild type, Col-0.

In this study it was used a different T-DNA line (SALK_137972C, T-DNA insertion in the coding region), *expa2-2*, observing that mutant seeds had a

reduced germination in comparison with the wild type Col-0, on media containing an inhibitor of GA biosynthesis.

It is known that GA promotes germination (Groot & Karssen, 1987) and also Yan et al., 2014, showed that *EXPA2* is involved in the GA-mediated seed germination, enforcing the results from *expa2-2* germination scores on media containing an inhibitor of GA biosynthesis.

It was observed a reduce germination for *expa2-2*, when the endogenous GA was blocked by PAC, in comparison with the wild type, Col-0. This fact supports the idea of which between *EXPA2*, GA and seed germination is a direct interdependency. Also, it suggests the role of *EXPA2* on endosperm loosening, the mutant seeds lacking its expression showed a reduced germination in comparison with the wild type.

4.2.3 Putative interaction between *EXPA2* promoter fragments and transcription factors from cluster 19

In the last years, yeast one hybrid system was frequently used to reveal the control of transcription in plants, allowing in very short time identification of *cis*-elements of a promoter and the transcription factors which they interact with (Castrillo et al., 2011).

To test if there was any interaction between the *EXPA2* promoter and transcription factors from cluster 19, yeast one hybrid system was used. After the constructs were grown in the yeast strain as baits, preys, respectively, the yeast growth was scored after five days on selective media, containing an inhibitor of the reporter gene used.

In this study the bait sequences represented by *EXPA2* fragments, four fragments of 400bp each, were mated with the prey sequences *BEE2*, *ATHB23*, *DOF2.1* and *bHLH115*, and grown on selective media, allowing the growth and development only of the diploid cells.

Comparing the colony size, as a principle of interaction (Castrillo et al., 2011), the results indicated a possible interaction between the third and fourth fragment of *EXPA2* (*E3*, *E4*) promoter and *ATHB23* and between the fourth fragment of *EXPA2* promoter (*E4*) with *BEE2*, but further experiments are required to confirm the result, as positive interactions.

Although the *cis*-elements in the *EXPA2* promoter fragments 3 (*E3*) and 4 (*E4*) indicated specific bindings with *DOF2.1*, and fragments 1 (*E1*) with *bHLH115* or *BEE2*, apparently, fragments 3 and 4 (*E3*, *E4*) interact with *ATHB23* and *BEE2*, according to yeast one hybrid system preliminary results.

4.3 Biomechanical dissection of endosperm function

Lee et al., 2013, suggested that Arabidopsis and Lepidium endosperm cell walls contain cellulose, homogalacturonan, arabinan, and xyloglucan, with the difference that Lepidium endosperm cell walls contain extensin (Lee et al., 2013). Also, the micropylar endosperm of Lepidium consists of one, two cell layers, not a monolayer as in Arabidopsis.

Discussing the physical properties of cell wall components, it gives an idea of physical properties of the cell wall. Cellulose microfibrils being inelastic and having a high tensile strength, were proposed to control the organ shape (Baskin, 2005). Also, they increase the wall strength by cross-linking with xyloglucans (Wolf et al., 2012), through hydrogen bonds disrupted by expansins (Cosgrove, 2001).

A series of glycosidases were reported to alter the structure of xyloglucans and the interactions with cellulose (Park & Cosgrove, 2012), but it was not enough to produce polymer creep which allows cell extension. Dick-Perez et al., 2011, suggested that pectin plays an important role in cell wall extensibility (Dick-Pérez et al., 2011).

There is direct connection between the pH and growth, Rayle in 1973, developed a theory according which the influx of hydrogen ions causes loosening of cell wall, allowing cell expansion through polymer creep (Rayle,

1973). This acid growth theory, sustain the activity of expansins in cell wall expansion (Cho & Cosgrove, 2000).

Although many studies were investigating the cell wall growth, very little is known about endosperm cell wall in germinating seeds. Most of the studies cover the biochemical aspect, while for mechanical tests only seeds with a certain size were analysed. For Arabidopsis, despite the fact that its genome was decoded, it is still unclear how plants cells are growing.

According to Muller et al., a force of 37.8 ± 2.5 mN was necessary to puncture the Lepidium endosperm at 8 hours of imbibition, just after testa rupture, and only 19.5 ± 1.7 mN was necessary at 18 hours of imbibition, when the endosperm ruptured. So, according to literature references, there are differences in endosperm strength and fracture toughness during germination and between its regions (Müller et al., 2006; Linkies et al., 2009).

When nanoindentation was suggested to be a suitable approach to detect the difference in stiffness of endosperm in different regions, it was already known that endosperm is weakening in the micropylar region prior radicle protrusion in *Lepidium sativum* seeds from puncture force experiments (Müller et al., 2006).

Indenting Lepidium seeds in a dry state, having the entire testa on, basically the testa was the indented tissue, consistent results for stiffness and hardness were found. It was not the same with testa removed imbibed seeds for 1 hour or 16 hours, where no significant difference in stiffness could be detected between the respective time points. It is known that larger sample size lead to increased precision of the results.

After nanoindentation could not detect the expected differences, AFM seemed to be a better option. Using a first generation machine, it was impossible to scan imbibed Arabidopsis seed; the cantilever tip remained attached to the sample, so no retraction curves were generated. Thus, no values could be generated for adhesion, hardness or elastic modulus.

The first attempt using nanoindentation to detect the differences in cell wall stiffness was performed on leaves of different Arabidopsis mutants, which were lacking one of the cell wall components: arabinan deficient (*arad1*), pectin deficient (*qua2)*, xyloglucan deficient (*xxt1xxt2*) and the wild types (Col 0 for *qua2* and *xxt1xx2*; QRT for *arad1*) as a control.

The statistical analysis of the preliminary results showed no significant differences concerning the stiffness of the leaves, although it might be expected that *qua2* (Mouille et al., 2007) and *arad1* (Harholt et al., 2006) would have stiffer walls, while *xxt1xxt2* (Cavalier et al., 2008) more compliant.

Also, when compare the sides of the leaf, the abaxial and adaxial, no significant difference was found, although the adaxial was expected to be stiffer (Braybrook & Kuhlemeier, 2010). However, the scatter results, reflected by high standard deviation values, can be explained by the irregular surface, due to the presence of hairs and stomatal apertures.

4.3.1 Imaging Lepidium seeds using micro-CT

Assuming that the seed structure is changing through germination, Lepidium seeds in different state of imbibition were scanned using micro-CT. Also, using StudioMax version 2.0 (Volume Graphics, http://www.volumegraphics.com), the endosperm thickness was approximated and compared for 32 seeds for four different time points of imbibition: 1, 3, 8 and 16 hours of imbibition. These estimations, when being compared using ANOVA multiple variance statistical test, showed no significant difference in thickness by time between regions of the endosperm but significant difference between subregions as shown in Results section.

Although the samples were not embedded in resin the IKI staining could generate an average of volume shrinkage of 40% in soft tissues (Buytaert et al., 2014) also the ethanol dehydration could have similar effects on seeds. The effect can be measured by comparing the volume of the unstained sample with a stained one, considering the volume reduction when analysing the results.

In this study there was not a direct comparison between an unstained hydrated seed and IKI stained ethanol dehydrated samples, the shrinkage being assumed to be produced uniform in all the cells, regardless their anisotropy, thus the results being directly comparable.

How the fact that the endosperm is not changing in thickness, can be explained? It is known that the turgor pressure is keeping the cell wall in tension, and that at a certain value it triggers the extension of the cell wall (Boyer, 2009). In order to hold this pressure, the cell wall is reinforced by new biosynthesized material, so the enlargement is taking place simultaneously with cell wall biosynthesis (Kutschera, 1990).

From micro-CT images, it could be concluded that the endosperm thickness remained constant for Lepidium seeds; also using eSEM to image the endosperm structure in Arabidopsis seeds, it could be noticed that the endosperm rupture occurs between individual cells, its structure remaining intact after radicle protrusion.

Another important issue would be the extension direction of the endosperm cells, from eSEM scans, being visible a width enlargement in the first hours of imbibition and ending-up with a lengthwise enlargement. So, whatever is happening in the cell wall, in terms of remodeling and restructuring, it influences the growth directions. It will be very interesting if a model of embryo growth will become available, so the endosperm expansion will be fully understood.

4.3.2 Correlating gene activity with endosperm rupture in seed germination

This study confirmed the spatial and temporal distribution of endosperm specific genes during germination; it identified new interactions between transcription factors *ATHB23* and *BEE2* and the promoter of *EXPA2*, genes belonging to the same cluster, endosperm specific, according to SeedNet

(Bassel et al., 2011). It also, revealed an epistatic relationship between two transcription factors of cluster 19, *ATHB23* and *DOF2.1*.

Using eSEM it was suggested that Arabidopsis endosperm rupture occurs between individual cells, highlighting the fact that endosperm cells in the radicle region, vacuolated and weakened enough for individual cells to be released (Bethke et al., 2007). Bethke et al. proven that there is a direct interdependency between number and size of vacuoles in Arabidopsis endosperm cells and cell wall thickness. If at the beginning of the germination, a nondormant seed has a various numbers of small vacuoles in endosperm cells, at the end of it one single big vacuole was noticed. Also, endosperm cells are synthesising enzymes that are degrading the cell wall to a thin band (Bethke et al., 2007).

Based on Bethke et al. observations on endosperm cell-wall thickness (Bethke et al., 2007) seeds of *Lepidium sativum* were scanned using micro-CT. The micro-CT images of Lepidium seeds were used to approximate the apparent thickness of the endosperm cell layer at different time points of imbibition. The results showed statistically significant differences in thickness between different regions of endosperm, ME, LE and PE, as well as between their subregions. Although there was a significant difference between subregions by time, no correlation was found between regions and time.

4.3.3 Conclusion

Studying genes that are endosperm specific, it was attempted to correlate gene expression with changes in endosperm physical properties during germination.

In this study, a link between gene expression and changes in physical properties of the endosperm was probed. Also, visualization of changes inside the seed through germination was accomplished by micro-CT imaging, while eSEM revealed a rupture between individual cells before radicle protrusion.

Knowing that the Arabidopsis endosperm cells near radicle tip are becoming less angular compared with the rest of the endosperm cells during germination, suggesting that the cell walls are thinning and weakening, estimated values for Lepidium endosperm thickness were compared for different imbibition time points, in different regions. Thus, a significant difference was found between the ME, LE and PE suggesting that endosperm cells are expanding differently, the fastest being the region around the radicle tip.

Also, this study confirmed the prediction of the SeedNet concerning tissue specificity of cluster 19 genes *EXPA2*, *DELTA-VPE*, *SCPL51* and *DOF2.1*, as being endosperm specific, their promoters' expression being observed only in the endosperm but not in the embryo.

Along with the specificity of expression, it was revealed a temporal and spatial distribution of these genes expression, 12-18 hours being necessary for the expression of *SCPL51* and *EXPA2* to become visible first in the micropylar endosperm expanding by time, while *DELTA-VPE* was expressed in the entire endosperm cells after 15 minutes of imbibition.

Another interesting observation was the signal required for their expression: *DELTA-VPE* appeared to be independent of an embryonic signal being insensitive to GA and ABA; *EXPA2* required an embryonic signal and GA to be expressed, being insensitive to ABA, while *SCPL51* needed an embryonic signal and GA for its expression, ABA having no effect on it.

Analysing the role of transcription factors from cluster 19 in germination, T-DNA lines were assessed by germination assays, revealed the epistatic relationship between *DOF2.1* and *ATHB23*.

Knowing the role of transcription factors in stress responses, cluster 19 transcription factors knockouts were observed in germination assays (*athb23*, *dof 2.1*, *athb23dof2.1*, *bee2*, *bhlh115-2* and *bee2bhlh115-2*). The germination scores suggested that not only overexpression but also knockout of transcription factors can affect germination by maintaining a higher water potential of cells, emphasizing the role of the endosperm in stress tolerance.

Putative interactions between *EXPA2* promoter fragments and transcription factors from cluster 19 were tested using yeast one hybrid system. Apparently, fragments 3 and 4 of *EXPA2* promoter interacted with *ATHB23* and *BEE2*, but further confirmations are required.

4.4 Future work

4.4.1. Confirming the role of *EXPA2* in endosperm function

Further investigations will be necessary to validate the preliminary results obtained in this thesis, showing an interaction between *EXPA2* promoter fragments and *ATHB23* and *BEE2*, and also to confirm that it is not a false positive.

Another interesting approach would be the comparison of the two *EXPA2* T-DNA lines, *expa2-1* and *expa2-2*, to reveal the effect of the insertion position on seed capacity to germinate, but also to observe the behaviour of *expa2-2* on media containing salt and osmotic stress factors.

4.4.2 Adjustments of biomechanics and imaging approaches

In terms of biomechanics, AFM remains the only sensitive methodology to sense the differences between endosperm cell walls physical properties, but with condition of using the latest generation machines.

Also, nanoindentation cannot be excluded from the methodologies to test seed tissues, but it requires an improvement of the conditions of indentation, such as: proper visualization of the indenting points and also the turgidity of the samples, maybe the use of an aquatic cell. All of these will allow the selection of interested region, but also will minimise the scatter of results, by maintain the same turgor pressure in the indented cells.

For imaging, micro-CT is a technique which will evolve fast enough so the Arabidopsis seeds could be imaged and tissue dimensions inside the seed could be estimated, with minimum errors.

DIC although is novel in plant biomechanics, it is promising, and an adjustment of the recording conditions (keeping the endosperm hydrated all along the process) and also of the particle pattern, could bring the expected results.

4.4.3 New techniques to be used in endosperm physical properties assessment

Other experimental approaches used to quantify physical parameters at cellular and subcellular levels include: micropipette aspiration (measures the suction pressure necessary to suck a single cell into a micropipette) (Hochmuth, 2000) to measure the endosperm elasticity; use of microneedles (Dennerll et al., 1989) or optical tweezers (Hénon et al., 1999) to measure the forces needed to deform cells shape (micropylar endosperm cells prior radicle protrusion).

Although it was applied only on animal cells, the magnetic rotational microrheology (Wilhelm et al., 2003) could be successfully used for plant cells,

providing information on viscoelastic shear moduli of the cytoplasm (how vacuolation changes the viscosity of endosperm cells, upon imbibition) avoiding the interference with the cell wall.

Another approach used successfully to assess plant cell turgidity was the pressure probe, which cannot be used for seeds do to the higher content of lipids and the lack of vacuolation in dry seeds, but promising remains the tonometer approach for imbibed endosperms. The tonometer approach can measure the turgor pressure of cells, by applying a spherical glass probe onto the cell surface with a known force (Lintilhac et al., 2000; Wei, 2001).

Small deformation oscillatory rheology is a technique that measures the viscosity of a material after being subjected to an oscillating shear stress, approach being part of the tensile and compression tests, used to assess components of the cell wall, individually. These methodologies are generating shear modulus and dynamic viscosity values (Schopfer, 2006; Kutschera, 1996; Wang et al., 2004). This new method has been used to show that Young's modulus of cultured tomato cell walls is at its lowest at pH 4.5, the pH optimum for expansin activity (Wang et al., 2004).

5. Bibliography

Arteca, Richard N, and Jeannette M Arteca. 2008. "Effects of brassinosteroid, auxin, and cytokinin on ethylene production in *Arabidopsis thaliana* Plants." *Journal of Experimental Botany* 59 (11): 3019–26.

Bader, Gary, and Christopher Hogue. 2003. "An automated method for finding molecular complexes in large protein interaction networks." *BMC Bioinformatics* 4 (1): 2.

Baskin, Carol C. 2003. "Breaking physical dormancy in seeds - focussing on the lens." *New Phytologist* 158 (2): 229–32.

Baskin, Jerry M., and Carol C. Baskin. 2004. "A classification system for seed dormancy." *Seed Science Research* 14: 1–16.

Baskin, Tobias I. 2005. "Anisotropic expansion of the plant cell wall." *Annual Review of Cell and Developmental Biology* 21 (January). Annual Reviews, 4139 El Camino Way, PO BOX 10139, Palo Alto, CA 94303-0139 USA: 203–22.

Bassel, George W, Hui Lan, Enrico Glaab, Daniel J Gibbs, Tanja Gerjets, Natalio Krasnogor, Anthony J Bonner, Michael J Holdsworth, and Nicholas J Provart. 2011. "Genome-wide network model capturing seed germination reveals coordinated regulation of plant cellular phase transitions." *Proceedings of the National Academy of Sciences of the United States of America* 108 (23): 9709–14.

Bassel, George W, Petra Stamm, Gabriella Mosca, Pierre Barbier de Reuille, Daniel J Gibbs, Robin Winter, Ales Janka, Michael J Holdsworth, and Richard S Smith. 2014. "Mechanical constraints imposed by 3D cellular geometry and arrangement modulate growth patterns in the Arabidopsis embryo." *Proceedings of the National Academy of Sciences of the United States of America* 111 (23): 8685–90.

Beaudoin, N, C Serizet, F Gosti, and J Giraudat. 2000. "Interactions between abscisic acid and ethylene signaling cascades." *The Plant Cell* 12 (7): 1103–15.

Berger, Frédéric, Paul E Grini, and Arp Schnittger. 2006. "Endosperm: an integrator of seed growth and development." *Current Opinion in Plant Biology* 9 (6): 664–70.

Bethke, Paul C, Igor G L Libourel, Natsuyo Aoyama, Yong-Yoon Chung, David W Still, and Russell L Jones. 2007. "The Arabidopsis aleurone layer responds to nitric oxide, gibberellin, and abscisic acid and is sufficient and necessary for seed dormancy." *Plant Physiology* 143 (3): 1173–88.

Bewley, J. D. 1997. “Seed germination and dormancy.” *The Plant Cell* 9 (7): 1055–66.

Bewley, J. Derek. 1997. “Breaking down the walls — a role for endo-β-mannanase in release from seed dormancy?” *Trends in Plant Science* 2 (12): 464–69.

Bewley, J. Derek, and Michael Black. 1994. *Seeds*. Springer.

Bewley, J. Derek, Kent Bradford, Henk Hilhorst, and Hiroyuki Nonogaki. 2013. *Seeds: Physiology of Development, Germination and Dormancy*. Springer Science & Business Media.

Bialek, K, and J D Cohen. 1989. “Free and conjugated indole-3-acetic acid in developing bean seeds.” *Plant Physiology* 91 (2): 775–79.

Boisnard-Lorig, C. 2001. “Dynamic Analyses of the expression of the HISTONE::YFP fusion protein in Arabidopsis show that syncytial endosperm is divided in mitotic domains.” *The Plant Cell Online* 13 (3): 495–509.

Bolduc, J-E, L J Lewis, C-E Aubin, and A Geitmann. 2006. “Finite-element analysis of geometrical factors in micro-indentation of pollen tubes.” *Biomechanics and Modeling in Mechanobiology* 5 (4): 227–36.

Bornert, M., F. Brémand, P. Doumalin, J.-C. Dupré, M. Fazzini, M. Grédiac, F. Hild, et al. 2008. “Assessment of digital image correlation measurement errors: methodology and results.” *Experimental Mechanics* 49 (3): 353–70.

Boyer, John S. 2009. “Evans Review : Cell wall biosynthesis and the molecular mechanism of plant enlargement.” *Functional Plant Biology* 36 (5). CSIRO Publishing: 383.

Braam, Janet. 2005. “In touch: plant responses to mechanical stimuli.” *The New Phytologist* 165 (2): 373–89.

Braidwood, Luke, Christian Breuer, and Keiko Sugimoto. 2013. “My body is a cage: mechanisms and modulation of plant cell growth.” *The New Phytologist*, August.

Braybrook, Siobhan A, and Cris Kuhlemeier. 2010. “How a plant builds leaves.” *The Plant Cell* 22 (4): 1006–18.

Braybrook, Siobhan A, and Alexis Peaucelle. 2013. “Mechano-chemical aspects of organ formation in *Arabidopsis thaliana*: the relationship between auxin and pectin.” *PloS One* 8 (3): e57813.

Briscoe, B.J., K.K. Liu, and D.R. Williams. 1998. “Adhesive contact deformation of a single microelastomeric sphere.” *Journal of Colloid and Interface Science* 200 (2): 256–64.

Brown, R. C., Betty E. Lemmon, Hong Nguyen, and Odd-Arne Olsen. 1999. “Development of endosperm in *Arabidopsis thaliana*.” *Sexual Plant Reproduction* 12 (1): 32–42.

Burgert, Ingo. 2006. “Exploring the micromechanical design of plant cell walls.” *American Journal of Botany* 93 (10): 1391–1401.

Burton, Rachel A, Michael J Gidley, and Geoffrey B Fincher. 2010. “Heterogeneity in the chemistry, structure and function of plant cell walls.” *Nature Chemical Biology* 6 (10). Nature Publishing Group, a division of Macmillan Publishers Limited. All Rights Reserved. 724–32.

Buytaert, Jan, Jana Goyens, Daniel De Greef, Peter Aerts, and Joris Dirckx. 2014. “Volume shrinkage of bone, brain and muscle tissue in sample preparation for micro-CT and light sheet fluorescence microscopy (LSFM).” *Microscopy and Microanalysis : The Official Journal of Microscopy Society of America, Microbeam Analysis Society, Microscopical Society of Canada*, June, 1–10.

Caffall, Kerry Hosmer, and Debra Mohnen. 2009. “The structure, function, and biosynthesis of plant cell wall pectic polysaccharides.” *Carbohydrate Research* 344 (14): 1879–1900.

Carrillo, Fernando, Shikha Gupta, Mehdi Balooch, Sally J. Marshall, Grayson W. Marshall, Lisa Pruitt, and Christian M. Puttlitz. 2011. “Nanoindentation of polydimethylsiloxane elastomers: effect of crosslinking, work of adhesion,and fluid environment on elastic modulus’ [J. Mater.Res. 20, 2820 (2005)].” *Journal of Materials Research* 21 (02). Cambridge University Press: 535–37.

Castrillo, Gabriel, Franziska Turck, Magalie Leveugle, Alain Lecharny, Pilar Carbonero, George Coupland, Javier Paz-Ares, and Luis Oñate-Sánchez. 2011. “Speeding cis-trans regulation discovery by phylogenomic analyses coupled with screenings of an arrayed library of Arabidopsis transcription factors.” Edited by Miguel A. Blazquez. *PloS One* 6 (6). Public Library of Science: e21524.

Cavalier, David M, Olivier Lerouxel, Lutz Neumetzler, Kazuchika Yamauchi, Antje Reinecke, Glenn Freshour, Olga A Zabotina, et al. 2008. “Disrupting two *Arabidopsis thaliana* xylosyltransferase genes results in plants deficient in xyloglucan, a major primary cell wall component.” *The Plant Cell* 20 (6): 1519–37.

Chapman, Elisabeth J, and Mark Estelle. 2009. “Mechanism of auxin-regulated gene expression in plants.” *Annual Review of Genetics* 43 (January): 265–85.

Chehab, E Wassim, Chen Yao, Zachary Henderson, Se Kim, and Janet Braam. 2012. “Arabidopsis touch-induced morphogenesis is jasmonate mediated and protects against pests.” *Current Biology : CB* 22 (8): 701–6.

Chen, F, P Dahal, and K J Bradford. 2001. “Two Tomato expansin genes show divergent expression and localization in embryos during seed development and germination.” *Plant Physiology* 127 (3): 928–36.

Cho, H T, and D J Cosgrove. 2000. “altered expression of expansin modulates leaf growth and pedicel abscission in *Arabidopsis thaliana*.” *Proceedings of the National Academy of Sciences of the United States of America* 97 (17): 9783–88.

Clair, Bruno, Richard Arinero, Gérard Lévèque, Michel Ramonda, and Bernard Thibaut. 2003. “Imaging the mechanical properties of wood cell layers by atomic force modulation microscopy.” *IAWA Journal* 24.

Clerkx, Emile J M, Hetty Blankestijn-De Vries, Gerda J Ruys, Steven P C Groot, and Maarten Koornneef. 2003. “Characterization of green seed, an enhancer of abi3-1 in Arabidopsis that affects seed longevity.” *Plant Physiology* 132 (2): 1077–84.

Cloetens, Peter, Régis Mache, Michel Schlenker, and Silva Lerbs-Mache. 2006. “Quantitative phase tomography of Arabidopsis seeds reveals intercellular void network.” *Proceedings of the National Academy of Sciences of the United States of America* 103 (39): 14626–30.

Coen, Enrico, Anne-Gaëlle Rolland-Lagan, Mark Matthews, J Andrew Bangham, and Przemyslaw Prusinkiewicz. 2004. “The genetics of geometry.” *Proceedings of the National Academy of Sciences of the United States of America* 101 (14): 4728–35.

Cosgrove, D. J. 2001. “Wall structure and wall loosening. a look backwards and forwards.” *Plant Physiology* 125 (1): 131–34.

Cosgrove, Daniel J. 2005. “Growth of the plant cell wall.” *Nature Reviews. Molecular Cell Biology* 6 (11): 850–61.

Da Silva, E A Amaral, Peter E Toorop, Adriaan C van Aelst, and Henk W M Hilhorst. 2004. “Abscisic acid controls embryo growth potential and endosperm cap weakening during coffee (*Coffea arabica* cv. *rubi*) seed germination.” *Planta* 220 (2): 251–61.

Damude, Howard G, and Anthony J Kinney. 2007. “Engineering Oilseed plants for a sustainable, land-based source of long chain polyunsaturated fatty acids.” *Lipids* 42 (3): 179–85.

Davies, Lynette M, and Philip J Harris. 2003. “Atomic force microscopy of microfibrils in primary cell walls.” *Planta* 217 (2): 283–89.

Davies, P.J. 1995. “Plant hormones.” *Kluwer Academic Publishers*.

Debeaujon, I, and M Koornneef. 2000. “Gibberellin requirement for Arabidopsis seed germination is determined both by testa characteristics and embryonic abscisic acid.” *Plant Physiology* 122 (2): 415–24.

DellaPenna, Dean. 2005. “Progress in the dissection and manipulation of vitamin E synthesis.” *Trends in Plant Science* 10 (12): 574–79.

Dekkers, Bas J W, Simon Pearce, R P van Bolderen-Veldkamp, Alex Marshall, Pawel Widera, James Gilbert, Hajk-Georg Drost, et al. 2013. “Transcriptional dynamics of two seed compartments with opposing roles in Arabidopsis seed germination.” *Plant Physiology* 163 (1). American Society of Plant Biologists: 205–15.

Dennerll, T J, P Lamoureux, R E Buxbaum, and S R Heidemann. 1989. “The cytomechanics of axonal elongation and retraction.” *The Journal of Cell Biology* 109 (6 Pt 1): 3073–83.

Dick-Pérez, Marilú, Yuan Zhang, Jennifer Hayes, Andre Salazar, Olga A Zabotina, and Mei Hong. 2011. “Structure and interactions of plant cell-wall polysaccharides by two- and three-dimensional magic-angle-spinning solid-state NMR.” *Biochemistry* 50 (6): 989–1000.

Doerner, M.F., and W.D. Nix. 2011. “A method for interpreting the data from depth-sensing indentation instruments.” *Journal of Materials Research* 1 (04). Cambridge University Press: 601–9.

Dorca-Fornell, Carmen, Radoslaw Pajor, Christoph Lehmeier, Marísa Pérez-Bueno, Marion Bauch, Jen Sloan, Colin Osborne, et al. 2013. “Increased leaf mesophyll porosity following transient retinoblastoma-related protein silencing is revealed by microcomputed tomography imaging and leads to a system-level physiological response to the altered cell division pattern.” *The Plant Journal : For Cell and Molecular Biology* 76 (6): 914–29.

Dubreucq, Bertrand, Nathalie Berger, Emmanuel Vincent, Murielle Boisson, Georges Pelletier, Michel Caboche, and Loic Lepiniec. 2000. “The Arabidopsis AtEPR1 extensin-like gene is specifically expressed in endosperm during seed germination.” *The Plant Journal* 23 (5): 643–52.

Ebenstein, Donna M., and Lisa A. Pruitt. 2006. “Nanoindentation of biological materials.” *Nano Today* 1 (3): 26–33.

Endo, Akira, Kiyoshi Tatematsu, Kousuke Hanada, Lisza Duermeyer, Masanori Okamoto, Keiko Yonekura-Sakakibara, Kazuki Saito, et al. 2012. "Tissue-specific transcriptome analysis reveals cell wall metabolism, flavonol biosynthesis and defense responses are activated in the endosperm of germinating *Arabidopsis thaliana* seeds." *Plant & Cell Physiology* 53 (1): 16–27.

Feng, Suhua, Cristina Martinez, Giuliana Gusmaroli, Yu Wang, Junli Zhou, Feng Wang, Liying Chen, et al. 2008. "Coordinated regulation of *Arabidopsis thaliana* development by light and gibberellins." *Nature* 451 (7177). Nature Publishing Group: 475–79.

Fenner, Michael, and Ken Thompson. 2005. *The ecology of seeds*. Cambridge University Press.

Fernandes, Anwesha N, Xinyong Chen, Colin A Scotchford, James Walker, Darren M Wells, Clive J Roberts, and Nicola M Everitt. 2012. "Mechanical properties of epidermal cells of whole living roots of *Arabidopsis thaliana*: an atomic force microscopy study." *Physical Review. E, Statistical, Nonlinear, and Soft Matter Physics* 85 (2 Pt 1): 021916.

Finch-Savage, William E, and Gerhard Leubner-Metzger. 2006. "Seed dormancy and the control of germination." *The New Phytologist* 171 (3): 501–23.

Finkelstein, R R, and T J Lynch. 2000. "The Arabidopsis abscisic acid response gene abi5 encodes a basic leucine zipper transcription factor." *The Plant Cell* 12 (4): 599–609.

Fischer-Cripps, A.C. 2006. "Critical review of analysis and interpretation of nanoindentation test data." *Surface and Coatings Technology* 200 (14-15): 4153–65.

Fu, Xiangdong, and Nicholas P Harberd. 2003. "Auxin promotes Arabidopsis root growth by modulating gibberellin response." *Nature* 421 (6924): 740–43.

Fung, Y. C. 1993. *Biomechanics: mechanical properties of living tissues*. Springer.

Geitmann, Anja. 2006. "Experimental approaches used to quantify physical parameters at cellular and subcellular levels." *American Journal of Botany* 93 (10): 1380–90.

Geitmann, Anja, and Joseph K E Ortega. 2009. "Mechanics and modeling of plant cell growth." *Trends in Plant Science* 14 (9): 467–78.

Ghassemian, M, E Nambara, S Cutler, H Kawaide, Y Kamiya, and P McCourt. 2000. “Regulation of abscisic acid signaling by the ethylene response pathway in Arabidopsis.” *The Plant Cell* 12 (7): 1117–26.

Goldsbury, Claire, and Simon Scheuring. 2002. “Introduction to atomic force microscopy (AFM) in biology.” *Current Protocols in Protein Science / Editorial Board, John E. Coligan ... [et Al.]* Chapter 17 (November): Unit 17.7.

Graeber, Kai, Ada Linkies, Kerstin Müller, Andrea Wunchova, Anita Rott, and Gerhard Leubner-Metzger. 2010. “Cross-species approaches to seed dormancy and germination: conservation and biodiversity of ABA-regulated mechanisms and the Brassicaceae DOG1 genes.” *Plant Molecular Biology* 73 (1-2): 67–87.

Griffiths, Jayne, Kohji Murase, Ivo Rieu, Rodolfo Zentella, Zhong-Lin Zhang, Stephen J Powers, Fan Gong, et al. 2006. “Genetic characterization and functional analysis of the GID1 gibberellin receptors in Arabidopsis.” *The Plant Cell* 18 (12): 3399–3414.

Groot, S P, and C M Karssen. 1987. “Gibberellins regulate seed germination in tomato by endosperm weakening: a study with gibberellin-deficient mutants.” *Planta* 171 (4): 525–31.

Hahm, Tae-Shik, Sung-Jin Park, and Y Martin Lo. 2009. “Effects of germination on chemical composition and functional properties of sesame (*Sesamum indicum* L.) seeds.” *Bioresource Technology* 100 (4): 1643–47.

Harholt, Jesper, Jacob Krüger Jensen, Susanne Oxenbøll Sørensen, Caroline Orfila, Markus Pauly, and Henrik Vibe Scheller. 2006. “ARABINAN DEFICIENT 1 is a putative arabinosyltransferase involved in biosynthesis of pectic arabinan in Arabidopsis.” *Plant Physiology* 140 (1): 49–58.

He, Jun-Xian, Joshua M Gendron, Yu Sun, Srinivas S L Gampala, Nathan Gendron, Catherine Qing Sun, and Zhi-Yong Wang. 2005. “BZR1 is a transcriptional repressor with dual roles in brassinosteroid homeostasis and growth responses.” *Science (New York, N.Y.)* 307 (5715): 1634–38.

Hénon, S, G Lenormand, A Richert, and F Gallet. 1999. “A new determination of the shear modulus of the human erythrocyte membrane using optical tweezers.” *Biophysical Journal* 76 (2): 1145–51.

Hentrich, Mathias, Christine Böttcher, Petra Düchting, Youfa Cheng, Yunde Zhao, Oliver Berkowitz, Josette Masle, Joaquín Medina, and Stephan Pollmann. 2013. “The Jasmonic acid signaling pathway is linked to auxin homeostasis through the modulation of YUCCA8 and YUCCA9 gene expression.” *The Plant Journal : For Cell and Molecular Biology* 74 (4): 626–37.

Heyl, Alexander, Michael Riefler, Georgy A Romanov, and Thomas Schmülling. 2012. “Properties, functions and evolution of cytokinin receptors.” *European Journal of Cell Biology* 91 (4): 246–56.

Hochmuth, R M. 2000. “Micropipette aspiration of living cells.” *Journal of Biomechanics* 33 (1): 15–22.

Holdsworth, Michael J, Leónie Bentsink, and Wim J J Soppe. 2008. “Molecular networks regulating Arabidopsis seed maturation, after-ripening, dormancy and germination.” *The New Phytologist* 179 (1): 33–54.

Hooley, R. 1994. “Gibberellins: perception, transduction and responses.” *Plant Molecular Biology* 26 (5): 1529–55.

Jacobsen, J V, and E Pressman. 1979. “A structural study of germination in celery (*Apium graveolens* L.) seed with emphasis on endosperm breakdown.” *Planta* 144 (3): 241–48.

Jiménez, Víctor M. 2005. “Involvement of plant hormones and plant growth regulators on in vitro somatic embryogenesis.” *Plant Growth Regulation* 47 (2-3): 91–110.

Kaminuma, Eli, Takeshi Yoshizumi, Takuji Wada, Minami Matsui, and Tetsuro Toyoda. 2008. “Quantitative analysis of heterogeneous spatial distribution of Arabidopsis leaf trichomes using micro x-ray computed tomography.” *The Plant Journal : For Cell and Molecular Biology* 56 (3): 470–82.

Kendrick, Mandy D, and Caren Chang. 2008. “Ethylene signaling: new levels of complexity and regulation.” *Current Opinion in Plant Biology* 11 (5): 479–85.

Khodabakhshian, R. 2012. “Elastic behavior of sunflower seed and its kernel.” *Commission of Agricultural and Biosystems Engineering (CIGR).*

Köhler, Lothar, and Hanns-Christof Spatz. 2002. “Micromechanics of plant tissues beyond the linear-elastic range.” *Planta* 215 (1): 33–40.

Koornneef, M, M L Jorna, D L Brinkhorst-van der Swan, and C M Karssen. 1982. “The isolation of abscisic acid (*aba*) deficient mutants by selection of induced revertants in non-germinating gibberellin sensitive lines of *Arabidopsis thaliana* (L.) heynh.” *TAG. Theoretical and Applied Genetics. Theoretische Und Angewandte Genetik* 61 (4): 385–93.

Koornneef, M, and J H van der Veen. 1980. “Induction and analysis of gibberellin sensitive mutants in *Arabidopsis thaliana* (L.) heynh.” *TAG. Theoretical and Applied Genetics. Theoretische Und Angewandte Genetik* 58 (6): 257–63.

Koornneef M., Karssen C. M. 1994. *Arabidopsis*. Edited by Somerville C. R. Meyerowitz E. M. Cold Spring Harbor Laboratory Press.

Koornneef, Maarten, Leónie Bentsink, and Henk Hilhorst. 2002. "Seed dormancy and germination." *Current Opinion in Plant Biology* 5 (1): 33–36.

Kucera, Birgit, Marc Alan Cohn, and Gerhard Leubner-Metzger. 2005. "Plant hormone interactions during seed dormancy release and germination." *Seed Science Research* 15 (4). Cambridge University Press: 281–307.

Kutschera, U. 1990. "Cell-wall synthesis and elongation growth in hypocotyls of *Helianthus annuus* L." *Planta* 181 (3): 316–23.

Kutschera, U. 1996. "Cessation of cell elongation in rye coleoptiles is accompanied by a loss of cell-wall plasticity." *Journal of Experimental Botany* 47 (9): 1387–94.

L.M. Vleeshouwers, H.J. Bouwmeester. 1995. "Redefining seed dormancy: an attempt to integrate physiology and ecology." *J. Ecology 83 (1995) 1031-1037.*

Lee, Keun Pyo, Urszula Piskurewicz, Veronika Turecková, Miroslav Strnad, and Luis Lopez-Molina. 2010. "A seed coat bedding assay shows that rgl2-dependent release of abscisic acid by the endosperm controls embryo growth in Arabidopsis dormant seeds." *Proceedings of the National Academy of Sciences of the United States of America* 107 (44): 19108–13.

Lee, Kieran J D, Valérie Cornuault, Iain W Manfield, Marie-Christine Ralet, and J Paul Knox. 2013. "Multi-scale spatial heterogeneity of pectic rhamnogalacturonan i (rg-i) structural features in tobacco seed endosperm cell walls." *The Plant Journal : For Cell and Molecular Biology* 75 (6): 1018–27.

Lee, KJD, and BJW Dekkers. 2012. "Distinct cell wall architectures in seed endosperms in representatives of the Brassicaceae and Solanaceae." *Plant Journal* 160 (3): 1551–66.

Lee, Sorcheng, Hui Cheng, Kathryn E King, Weefuen Wang, Yawen He, Alamgir Hussain, Jane Lo, Nicholas P Harberd, and Jinrong Peng. 2002. "Gibberellin regulates Arabidopsis seed germination via RGL2, a GAI/RGA-like gene whose expression is up-regulated following imbibition." *Genes & Development* 16 (5): 646–58.

Leubner-Metzger, G, L Petruzzelli, R Waldvogel, R Vögeli-Lange, and F Meins. 1998. "Ethylene-responsive element binding protein (EREBP) expression and the transcriptional regulation of class I beta-1,3-glucanase during tobacco seed germination." *Plant Molecular Biology* 38 (5): 785–95.

Leubner-Metzger, G. 2003. “Functions and regulation of β-1,3-glucanases during seed germination, dormancy release and after-ripening.” *Seed Science Research* 13 (1). Cambridge University Press: 17–34.

Leung, J, S Merlot, and J Giraudat. 1997. “The Arabidopsis ABSCISIC ACID-INSENSITIVE2 (ABI2) and ABI1 genes encode homologous protein phosphatases 2C involved in abscisic acid signal transduction.” *The Plant Cell* 9 (5): 759–71.

Li, J, and J Chory. 1997. “A putative leucine-rich repeat receptor kinase involved in brassinosteroid signal transduction.” *Cell* 90 (5): 929–38.

Liljegren, S J, G S Ditta, Y Eshed, B Savidge, J L Bowman, and M F Yanofsky. 2000. “SHATTERPROOF MADS-box genes control seed dispersal in Arabidopsis.” *Nature* 404 (6779): 766–70.

Linkies, Ada, and Gerhard Leubner-Metzger. 2012. “Beyond gibberellins and abscisic acid: how ethylene and jasmonates control seed germination.” *Plant Cell Reports* 31 (2): 253–70.

Linkies, Ada, Kerstin Müller, Karl Morris, Veronika Turecková, Meike Wenk, Cassandra S C Cadman, Françoise Corbineau, et al. 2009a. “Ethylene Interacts with abscisic acid to regulate endosperm rupture during germination: a comparative approach using *Lepidium sativum* and *Arabidopsis thaliana*.” *The Plant Cell* 21 (12): 3803–22.

Lintilhac, P M, C Wei, J J Tanguay, and J O Outwater. 2000. “Ball tonometry: a rapid, nondestructive method for measuring cell turgor pressure in thin-walled plant cells.” *Journal of Plant Growth Regulation* 19 (1): 90–97.

Liu, Po-Pu, Nobuya Koizuka, Tanja M Homrichhausen, Jessica R Hewitt, Ruth C Martin, and Hiroyuki Nonogaki. 2005. “Large-scale screening of Arabidopsis enhancer-trap lines for seed germination-associated genes.” *The Plant Journal : For Cell and Molecular Biology* 41 (6): 936–44.

Liu, Po-Pu, Taiowa A Montgomery, Noah Fahlgren, Kristin D Kasschau, Hiroyuki Nonogaki, and James C Carrington. 2007. “Repression of AUXIN RESPONSE FACTOR10 by microRNA160 is critical for seed germination and post-germination stages.” *The Plant Journal : For Cell and Molecular Biology* 52 (1): 133–46.

Liu, Xiaodong, Hong Zhang, Yang Zhao, Zhengyan Feng, Qun Li, Hong-Quan Yang, Sheng Luan, Jianming Li, and Zu-Hua He. 2013. “Auxin controls seed dormancy through stimulation of abscisic acid signaling by inducing ARF-mediated ABI3 activation in Arabidopsis.” *Proceedings of the National Academy of Sciences of the United States of America* 110 (38): 15485–90.

Lockhart, James A. 1965. “An analysis of irreversible plant cell elongation.” *Journal of Theoretical Biology* 8 (2): 264–75.

Lopez-Molina, Luis, Sébastien Mongrand, Derek T McLachlin, Brian T Chait, and Nam-Hai Chua. 2002. “ABI5 acts downstream of ABI3 to execute an ABA-dependent growth arrest during germination.” *The Plant Journal : For Cell and Molecular Biology* 32 (3): 317–28.

Ma, Yue, Izabela Szostkiewicz, Arthur Korte, Danièle Moes, Yi Yang, Alexander Christmann, and Erwin Grill. 2009. “Regulators of PP2C phosphatase activity function as abscisic acid sensors.” *Science (New York, N.Y.)* 324 (5930): 1064–68.

Manz, Bertram, Kerstin Müller, Birgit Kucera, Frank Volke, and Gerhard Leubner-Metzger. 2005. “Water uptake and distribution in germinating tobacco seeds investigated in vivo by nuclear magnetic resonance imaging.” *Plant Physiology* 138 (3): 1538–51.

Marga, Francoise, Michel Grandbois, Daniel J Cosgrove, and Tobias I Baskin. 2005. “Cell wall extension results in the coordinate separation of parallel microfibrils: evidence from scanning electron microscopy and atomic force microscopy.” *The Plant Journal : For Cell and Molecular Biology* 43 (2): 181–90.

Martínez-Andújar, Cristina, Wioletta E Pluskota, George W Bassel, Masashi Asahina, Piotr Pupel, Theresa T Nguyen, Noriko Takeda-Kamiya, et al. 2012. “Mechanisms of hormonal regulation of endosperm cap-specific gene expression in tomato seeds.” *The Plant Journal : For Cell and Molecular Biology* 71 (4): 575–86.

Matilla, A.J., and M.A. Matilla-Vázquez. 2008. “Involvement of ethylene in seed physiology.” *Plant Science* 175 (1-2). Elsevier: 87–97.

Matilla, Angel J. 2007. “Ethylene in seed formation and germination.” *Seed Science Research* 10 (02). Cambridge University Press: 111–26.

McGinnis, K. M. 2003. “The Arabidopsis SLEEPY1 gene encodes a putative F-box subunit of an SCF E3 ubiquitin ligase.” *The Plant Cell Online* 15 (5): 1120–30.

Metscher, Brian D. 2009. “MicroCT for comparative morphology: simple staining methods allow high-contrast 3D imaging of diverse non-mineralized animal tissues.” *BMC Physiology* 9 (1): 11.

Meyer, K, M P Leube, and E Grill. 1994. “A protein phosphatase 2C involved in ABA signal transduction in *Arabidopsis thaliana*.” *Science (New York, N.Y.)* 264 (5164): 1452–55.

Milani, Pascale, Siobhan A Braybrook, and Arezki Boudaoud. 2013. "Shrinking the hammer: micromechanical approaches to morphogenesis." *Journal of Experimental Botany* 64 (15): 4651–62.

Milani, Pascale, Maryam Gholamirad, Jan Traas, Alain Arnéodo, Arezki Boudaoud, Françoise Argoul, and Olivier Hamant. 2011. "*In vivo* analysis of local wall stiffness at the shoot apical meristem in arabidopsis using atomic force microscopy." *The Plant Journal : For Cell and Molecular Biology* 67 (6): 1116–23.

Miller CO, F Skoog, MH Von Saltza and FM Strong. 1955. "Kinetin, a cell division faction from deoxyribonucleic acid." *J Am Chem Soc* Miller CO, (77): 1392–93.

Mirabet, Vincent, Pradeep Das, Arezki Boudaoud, and Olivier Hamant. 2011. "The role of mechanical forces in plant morphogenesis." *Annual Review of Plant Biology* 62 (January): 365–85.

Mockaitis, Keithanne, and Mark Estelle. 2008. "Auxin receptors and plant development: a new signaling paradigm." *Annual Review of Cell and Developmental Biology* 24 (January): 55–80.

Mok, David WS, and Machteld C Mok. 2001. "Cytokinin metabolism and action." *Annual Review of Plant Physiology and Plant Molecular Biology* 52 (June): 89–118.

Mooney, S.J. 2006. "Three-dimensional visualization and quantification of soil macroporosity and water flow patterns using computed tomography." *Soil Use and Management* 18 (2): 142–51.

Morris, Karl, Ada Linkies, Kerstin Müller, Krystyna Oracz, Xiaofeng Wang, James R Lynn, Gerhard Leubner-Metzger, and William E Finch-Savage. 2011. "Regulation of seed germination in the close Arabidopsis relative *Lepidium sativum*: a global tissue-specific transcript analysis." *Plant Physiology* 155 (4): 1851–70.

Mouille, Grégory, Marie-Christine Ralet, Céline Cavelier, Cathlene Eland, Delphine Effroy, Kian Hématy, Lesley McCartney, et al. 2007. "Homogalacturonan synthesis in *Arabidopsis thaliana* requires a Golgi-localized protein with a putative methyltransferase domain." *The Plant Journal : For Cell and Molecular Biology* 50 (4): 605–14.

Moulia, Bruno. 2013. "Plant biomechanics and mechanobiology are convergent paths to flourishing interdisciplinary research." *Journal of Experimental Botany* 64 (15): 4617–33.

Müller, Kerstin, Stefanie Tintelnot, and Gerhard Leubner-Metzger. 2006a. "Endosperm-limited Brassicaceae seed germination: abscisic acid inhibits embryo-induced endosperm weakening of *Lepidium Sativum* (cress) and

endosperm rupture of cress and *Arabidopsis thaliana*." *Plant & Cell Physiology* 47 (7): 864–77.

Nakashima, Kazuo, Yasunari Fujita, Norihito Kanamori, Takeshi Katagiri, Taishi Umezawa, Satoshi Kidokoro, Kyonoshin Maruyama, et al. 2009. "Three Arabidopsis SnRK2 Protein Kinases, SRK2D/SnRK2.2, SRK2E/SnRK2.6/OST1 and SRK2I/SnRK2.3, involved in ABA signaling are essential for the control of seed development and dormancy." *Plant & Cell Physiology* 50 (7): 1345–63.

Nakashima, Kazuo, Hironori Takasaki, Junya Mizoi, Kazuo Shinozaki, and Kazuko Yamaguchi-Shinozaki. 2012. "NAC Transcription factors in plant abiotic stress responses." *Biochimica et Biophysica Acta* 1819 (2): 97–103.

Nambara, Eiji, and Annie Marion-Poll. 2003. "ABA action and interactions in seeds." *Trends in Plant Science* 8 (5): 213–17.

Nambara, Eiji, Masanori Okamoto, Kiyoshi Tatematsu, Ryoichi Yano, Mitsunori Seo, and Yuji Kamiya. 2010. "Abscisic acid and the control of seed dormancy and germination." *Seed Science Research* 20 (02). Cambridge University Press: 55.

Nguyen, H., R. C. Brown, and B. E. Lemmon. 2000. "The specialized chalazal endosperm in *Arabidopsis thaliana* and *Lepidium virginicum* (Brassicaceae)." *Protoplasma* 212 (1-2): 99–110.

Nguyen, H. 2001. "Patterns of cytoskeletal organization reflect distinct developmental domains in endosperm of *Coronopus didymus* (Brassicaceae)." *International Journal of Plant Sciences* 162 (1). The University of Chicago Press: 1–14.

Ni, Di An, Xiao Hong Yu, Ling Jian Wang, and Zhi Hong Xu. 2002. "Aberrant development of pollen in transgenic tobacco expressing bacterial iaaM gene driven by pollen- and tapetum-specific promoters." *Shi Yan Sheng Wu Xue Bao* 35 (1): 1–6.

Nikolaeva, M.G. 2004. "On criteria to use in studies of seed evolution." *Seed Science Research* 14 (04). Cambridge University Press: 315–20.

Nishimura, Noriyuki, Tomo Yoshida, Nobutaka Kitahata, Tadao Asami, Kazuo Shinozaki, and Takashi Hirayama. 2007. "ABA-Hypersensitive Germination1 encodes a protein phosphatase 2C, an essential component of abscisic acid signaling in Arabidopsis seed." *The Plant Journal : For Cell and Molecular Biology* 50 (6): 935–49.

Noguchi, T, S Fujioka, S Choe, S Takatsuto, S Yoshida, H Yuan, K A Feldmann, and F E Tax. 1999. "Brassinosteroid-insensitive dwarf mutants

of Arabidopsis accumulate brassinosteroids." *Plant Physiology* 121 (3): 743–52.

Nonogaki, H, O H Gee, and K J Bradford. 2000. "A germination-specific endo-beta-mannanase gene is expressed in the micropylar endosperm cap of tomato seeds." *Plant Physiology* 123 (4): 1235–46. h

Ogawa, Mikihiro, Atsushi Hanada, Yukika Yamauchi, Ayuko Kuwahara, Yuji Kamiya, and Shinjiro Yamaguchi. 2003. "Gibberellin biosynthesis and response during Arabidopsis seed germination." *The Plant Cell* 15 (7): 1591–1604.

Ogé, Laurent, Gildas Bourdais, Jérôme Bove, Boris Collet, Béatrice Godin, Fabienne Granier, Jean-Pierre Boutin, Dominique Job, Marc Jullien, and Philippe Grappin. 2008. "Protein repair L-isoaspartyl methyltransferase 1 is involved in both seed longevity and germination vigor in Arabidopsis." *The Plant Cell* 20 (11): 3022–37.

Oliver, W.C., and G.M. Pharr. 1992. "An improved technique for determining hardness and elastic modulus using load and displacement sensing indentation experiments." *Journal of Materials Research* 7 (06). Cambridge University Press: 1564–83.

Oliver, W.C., and G.M. Pharr. 2004. "Measurement of hardness and elastic modulus by instrumented indentation: advances in understanding and refinements to methodology." *Journal of Materials Research* 19 (01). Cambridge University Press: 3–20.

Pajor, R, A Fleming, C P Osborne, S A Rolfe, C J Sturrock, and S J Mooney. 2013. "Seeing space: visualization and quantification of plant leaf structure using x-ray micro-computed tomography." *Journal of Experimental Botany* 64 (2): 385–90.

Pan, Bing, Kemao Qian, Huimin Xie, and Anand Asundi. 2009. "Two-dimensional digital image correlation for in-plane displacement and strain measurement: a review." *Measurement Science and Technology* 20 (6). IOP Publishing: 062001.

Park, Sang-Youl, Pauline Fung, Noriyuki Nishimura, Davin R Jensen, Hiroaki Fujii, Yang Zhao, Shelley Lumba, et al. 2009. "Abscisic acid inhibits type 2c protein phosphatases via the PYR/PYL family of START proteins." *Science (New York, N.Y.)* 324 (5930): 1068–71.

Park, Yong Bum, and Daniel J Cosgrove. 2012. "Changes in cell wall biomechanical properties in the xyloglucan-deficient *xxt1/xxt2* mutant of Arabidopsis." *Plant Physiology* 158 (1). American Society of Plant Biologists: 465–75.

Peaucelle, Alexis, Romain Louvet, Jorunn N Johansen, Fabien Salsac, Halima Morin, Françoise Fournet, Katia Belcram, et al. 2011. "The transcription factor BELLRINGER modulates phyllotaxis by regulating the expression of a pectin methylesterase in Arabidopsis." *Development (Cambridge, England)* 138 (21): 4733–41.

Penfield, Steven, Yi Li, Alison D Gilday, Stuart Graham, and Ian A Graham. 2006a. "Arabidopsis ABA INSENSITIVE4 regulates lipid mobilization in the embryo and reveals repression of seed germination by the endosperm." *The Plant Cell* 18 (8): 1887–99.

Penfield, Steven, Elizabeth L Rylott, Alison D Gilday, Stuart Graham, Tony R Larson, and Ian A Graham. 2004. "Reserve mobilization in the arabidopsis endosperm fuels hypocotyl elongation in the dark, is independent of abscisic acid, and requires PHOSPHOENOLPYRUVATE CARBOXYKINASE1." *The Plant Cell* 16 (10): 2705–18.

Pennazio, S., and P. Roggero. 1991. "Effects of exogenous salicylate on basal and stressinduced ethylene formation in soybean." *Biologia Plantarum* 33 (3): 248–248.

Petruzzelli, L, I Coraggio, and G Leubner-Metzger. 2000. "Ethylene promotes ethylene biosynthesis during pea seed germination by positive feedback regulation of 1-aminocyclo-propane-1-carboxylic acid oxidase." *Planta* 211 (1): 144–49.

Petruzzelli, L., M. Sturaro, D. Mainieri, and G. Leubner-Metzger. 2003. "Calcium requirement for ethylene-dependent responses involving 1-aminocyclopropane-1-carboxylic acid oxidase in radicle tissues of germinated pea seeds." *Plant, Cell and Environment* 26 (5): 661–71.

Piskurewicz, Urszula, Yusuke Jikumaru, Natsuko Kinoshita, Eiji Nambara, Yuji Kamiya, and Luis Lopez-Molina. 2008. "The gibberellic acid signaling repressor RGL2 inhibits Arabidopsis seed germination by stimulating abscisic acid synthesis and ABI5 activity." *The Plant Cell* 20 (10): 2729–45.

Popko, J, R Hänsch, R-R Mendel, A Polle, and T Teichmann. 2010. "The role of abscisic acid and auxin in the response of poplar to abiotic stress." *Plant Biology (Stuttgart, Germany)* 12 (2): 242–58.

Rashotte, A M, S R Brady, R C Reed, S J Ante, and G K Muday. 2000. "Basipetal auxin transport is required for gravitropism in roots of Arabidopsis." *Plant Physiology* 122 (2): 481–90.

Rasmusson, D. C., and R. L. Phillips. 1997. "Plant breeding progress and genetic diversity from de novo variation and elevated epistasis." *Crop Science* 37 (2). Crop Science Society of America: 303.

Ray, Peter M., Paul B. Green, and Robert Cleland. 1972. “Role of turgor in plant cell growth.” *Nature* 239 (5368): 163–64.

Rayle, D L. 1973. “Auxin-induced hydrogen-ion secretion in avena coleoptiles and its implications.” *Planta* 114 (1): 63–73.

Richards, Donald E, Kathryn E King, Tahar Ait-Ali, and Nicholas P Harberd. 2001. “How gibberellin regulates plant growth and development: a molecular genetic analysis of gibberellin signaling.” *Annual Review of Plant Physiology and Plant Molecular Biology* 52 (June): 67–88.

Riefler, Michael, Ondrej Novak, Miroslav Strnad, and Thomas Schmülling. 2006. “Arabidopsis cytokinin receptor mutants reveal functions in shoot growth, leaf senescence, seed size, germination, root development, and cytokinin metabolism.” *The Plant Cell* 18 (1): 40–54.

Rodriguez, Pedro L, Gregor Benning, and Erwin Grill. 1998. “ABI2, a second protein phosphatase 2C involved in abscisic acid signal transduction in Arabidopsis.” *FEBS Letters* 421 (3): 185–90.

Rodríguez-Gacio, María del Carmen, Raquel Iglesias-Fernández, Pilar Carbonero, and Angel J Matilla. 2012. “Softening-up mannan-rich cell walls.” *Journal of Experimental Botany* 63 (11): 3976–88.

Routier-Kierzkowska, Anne-Lise, Alain Weber, Petra Kochova, Dimitris Felekis, Bradley J Nelson, Cris Kuhlemeier, and Richard S Smith. 2012. “Cellular force microscopy for in vivo measurements of plant tissue mechanics.” *Plant Physiology* 158 (4): 1514–22.

Ruiz-López, Noemí, Richard P Haslam, Mónica Venegas-Calerón, Tony R Larson, Ian A Graham, Johnathan A Napier, and Olga Sayanova. 2009. “The synthesis and accumulation of stearidonic acid in transgenic plants: a novel source of ‘heart-healthy’ omega-3 fatty acids.” *Plant Biotechnology Journal* 7 (7): 704–16.

Sachs, Julius. 1887. *Lectures on the Physiology of Plants / by Julius von Sachs, Translated by H. Marshall Ward.* Oxford :: The Clarendon Press.

Saez, Angela, Nadezda Apostolova, Miguel Gonzalez-Guzman, Mary Paz Gonzalez-Garcia, Carlos Nicolas, Oscar Lorenzo, and Pedro L Rodriguez. 2004. “Gain-of-function and loss-of-function phenotypes of the protein phosphatase 2C HAB1 reveal its role as a negative regulator of abscisic acid signalling.” *The Plant Journal : For Cell and Molecular Biology* 37 (3): 354–69.

Santner, Aaron, Luz Irina A Calderon-Villalobos, and Mark Estelle. 2009. “Plant hormones are versatile chemical regulators of plant growth.” *Nature Chemical Biology* 5 (5). Nature Publishing Group: 301–7.

Schaller, G. E., A. N. Ladd, M. B. Lanahan, J. M. Spanbauer, and A. B. Bleecker. 1995. "The ethylene response mediator ETR1 from Arabidopsis forms a disulfide-linked dimer." *Journal of Biological Chemistry* 270 (21): 12526–30.

Scheller, Henrik Vibe, and Peter Ulvskov. 2010. "Hemicelluloses." *Annual Review of Plant Biology* 61 (January): 263–89.

Schopfer, Peter. 2006. "Biomechanics of plant growth." *American Journal of Botany* 93 (10): 1415–25.

Sliwinska, Elwira, George W Bassel, and J Derek Bewley. 2009. "Germination of *Arabidopsis thaliana* seeds is not completed as a result of elongation of the radicle but of the adjacent transition zone and lower hypocotyl." *Journal of Experimental Botany* 60 (12): 3587–94.

Somerville, Chris. 2006. "Cellulose synthesis in higher plants." *Annual Review of Cell and Developmental Biology* 22 (January): 53–78.

Sorensen, M. B. 2002. "Cellularisation in the endosperm of *Arabidopsis thaliana* is coupled to mitosis and shares multiple components with cytokinesis." *Development* 129 (24): 5567–76.

Sørensen, Mikael Blom, Abdul M. Chaudhury, Hélène Robert, Estelle Bancharel, and Frédéric Berger. 2001. "Polycomb group genes control pattern formation in plant seed." *Current Biology* 11 (4): 277–81.

Steber, C M, and P McCourt. 2001. "A role for brassinosteroids in germination in Arabidopsis." *Plant Physiology* 125 (2): 763–69.

Stepanova, Anna N., and Jose M. Alonso. 2005. "Ethylene signalling and response pathway: a unique signalling cascade with a multitude of inputs and outputs." *Physiologia Plantarum* 123 (2): 195–206.

Sun, T P, and Y Kamiya. 1994. "The Arabidopsis GA1 locus encodes the cyclase ent-kaurene synthetase A of gibberellin biosynthesis." *The Plant Cell* 6 (10): 1509–18.

Sutton, M A, X Ke, S M Lessner, M Goldbach, M Yost, F Zhao, and H W Schreier. 2008. "Strain field measurements on mouse carotid arteries using microscopic three-dimensional digital image correlation." *Journal of Biomedical Materials Research. Part A* 84 (1): 178–90.

Sutton, Michael A. 2008. *Springer Handbook of Experimental Solid Mechanics*. Edited by William N. Sharpe. Boston, MA: Springer US.

Suzuki, Masaharu, Matthew G Ketterling, Qin-Bao Li, and Donald R McCarty. 2003. "Viviparous1 alters global gene expression patterns through regulation of abscisic acid signaling." *Plant Physiology* 132 (3): 1664–77.

Tracy, Saoirse R, Colin R Black, Jeremy A Roberts, Craig Sturrock, Stefan Mairhofer, Jim Craigon, and Sacha J Mooney. 2012. "Quantifying the impact of soil compaction on root system architecture in tomato (solanum lycopersicum) by x-ray micro-computed tomography." *Annals of Botany* 110 (2): 511–19.

Tyler, Ludmila, Stephen G Thomas, Jianhong Hu, Alyssa Dill, Jose M Alonso, Joseph R Ecker, and Tai-Ping Sun. 2004. "Della proteins and gibberellin-regulated seed germination and floral development in Arabidopsis." *Plant Physiology* 135 (2): 1008–19.

Van Sandt, Vicky S T, Dmitry Suslov, Jean-Pierre Verbelen, and Kris Vissenberg. 2007. "Xyloglucan endotransglucosylase activity loosens a plant cell wall." *Annals of Botany* 100 (7): 1467–73.

Voegele, Antje, Ada Linkies, Kerstin Müller, and Gerhard Leubner-Metzger. 2011. "Members of the gibberellin receptor gene family *GID1 (GIBBERELLIN INSENSITIVE DWARF1)* play distinct roles during *Lepidium sativum* and *Arabidopsis thaliana* seed germination." *Journal of Experimental Botany* 62 (14): 5131–47.

Wang, C X, L Wang, and C R Thomas. 2004. "Modelling the mechanical properties of single suspension-cultured tomato cells." *Annals of Botany* 93 (4): 443–53.

Wei, C. 2001. "An insight into cell elasticity and load-bearing ability. measurement and theory." *Plant Physiology* 126 (3): 1129–38.

Weitbrecht, Karin, Kerstin Müller, and Gerhard Leubner-Metzger. 2011. "First off the mark: early seed germination." *Journal of Experimental Botany* 62 (10): 3289–3309.

Wel, N. N., C. A. J. Putman, S. J. T. Noort, B. G. Grooth, and A. M. C. Emons. 1996. "Atomic force microscopy of pollen grains, cellulose microfibrils, and protoplasts." *Protoplasma* 194 (1-2): 29–39.

Wilhelm, C, F Gazeau, and J-C Bacri. 2003. "Rotational magnetic endosome microrheology: viscoelastic architecture inside living cells." *Physical Review. E, Statistical, Nonlinear, and Soft Matter Physics* 67 (6 Pt 1): 061908.

Winship, Lawrence J, Gerhard Obermeyer, Anja Geitmann, and Peter K Hepler. 2011. "Pollen tubes and the physical world." *Trends in Plant Science* 16 (7): 353–55.

Wolf, Sebastian, Kian Hématy, and Herman Höfte. 2012. "Growth control and cell wall signaling in plants." *Annual Review of Plant Biology* 63 (January): 381–407.

Wu, C T, G Leubner-Metzger, F Meins, and K J Bradford. 2001. “Class I beta-1,3-glucanase and chitinase are expressed in the micropylar endosperm of tomato seeds prior to radicle emergence.” *Plant Physiology* 126 (3): 1299–1313.

Wu, Yan, Siqun Wang, Dingguo Zhou, Cheng Xing, Yang Zhang, and Zhiyong Cai. 2010. “Evaluation of elastic modulus and hardness of crop stalks cell walls by nano-indentation.” *Bioresource Technology* 101 (8): 2867–71.

Wu, Ziheng, Tyler A Baker, Timothy C Ovaert, and Glen L Niebur. 2011. “The effect of holding time on nanoindentation measurements of creep in bone.” *Journal of Biomechanics* 44 (6): 1066–72.

Yamaguchi, S, and Y Kamiya. 2000. “Gibberellin biosynthesis: its regulation by endogenous and environmental signals.” *Plant & Cell Physiology* 41 (3): 251–57.

Yamaguchi, S, Y Kamiya, and T Sun. 2001. “Distinct cell-specific expression patterns of early and late gibberellin biosynthetic genes during Arabidopsis seed germination.” *The Plant Journal : For Cell and Molecular Biology* 28 (4): 443–53.

Yamaguchi, Shinjiro. 2008. “Gibberellin Metabolism and its regulation.” *Annual Review of Plant Biology* 59 (January): 225–51.

Yamauchi, Yukika, Mikihiro Ogawa, Ayuko Kuwahara, Atsushi Hanada, Yuji Kamiya, and Shinjiro Yamaguchi. 2004. “Activation of gibberellin biosynthesis and response pathways by low temperature during imbibition of *Arabidopsis thaliana* seeds.” *The Plant Cell* 16 (2): 367–78.

Yan, An, Minjie Wu, Limei Yan, Rui Hu, Imran Ali, and Yinbo Gan. 2014. “AtEXP2 is involved in seed germination and abiotic stress response in Arabidopsis.” Edited by John Schiefelbein. *PloS One* 9 (1). Public Library of Science: e85208.

Zamir, Evan A, and Larry A Taber. 2004. “On the effects of residual stress in microindentation tests of soft tissue structures.” *Journal of Biomechanical Engineering* 126 (2): 276–83.

Zentella, Rodolfo, Zhong-Lin Zhang, Mehea Park, Stephen G Thomas, Akira Endo, Kohji Murase, Christine M Fleet, et al. 2007. “Global analysis of della direct targets in early gibberellin signaling in Arabidopsis.” *The Plant Cell* 19 (10): 3037–57.